

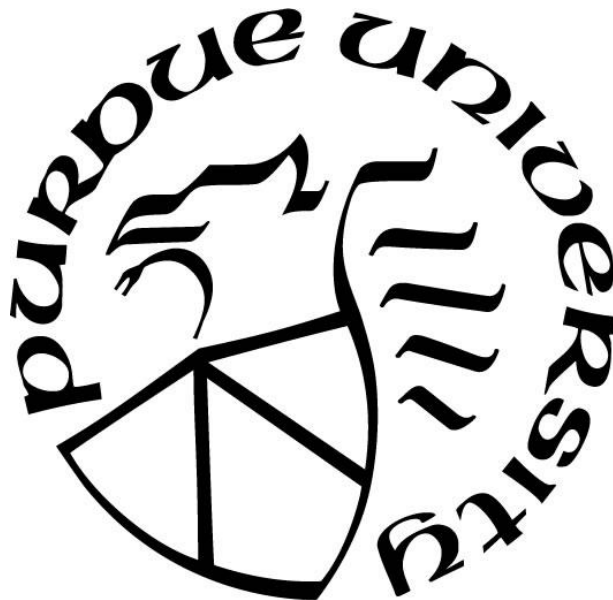
**AN ADAPTIVE PERSONALIZED DAYLIGHTING CONTROL
APPROACH FOR OPTIMAL VISUAL SATISFACTION AND LIGHTING
ENERGY USE IN OFFICES**

by
Jie Xiong

A Dissertation

*Submitted to the Faculty of Purdue University
In Partial Fulfillment of the Requirements for the degree of*

Doctor of Philosophy



Lyles School of Civil Engineering
West Lafayette, Indiana
December 2019

**THE PURDUE UNIVERSITY GRADUATE SCHOOL
STATEMENT OF COMMITTEE APPROVAL**

Dr. Athanasios Tzempelikos, Chair

Lyles School of Civil Engineering

Dr. Ilias Bilonis

School of Mechanical Engineering

Dr. Jianghai Hu

School of Electrical and Computer Engineering

Dr. Panagiota Karava

Lyles School of Civil Engineering

Approved by:

Dr. Dulcy M. Abraham

Chair, Burke Graduate Program, Lyles School of Civil Engineering

Dedicated to Ran & Rian

ACKNOWLEDGMENTS

I can still remember the first day I stepped into campus six years ago, and Purdue have become my home without my awareness for all these years. Yet all of a sudden, I have to pack myself up for the next stage of my life, despite my clinging to her. I would like to express my sincerest gratitude to all the people who shaped my colorful life in Purdue.

I'd like to thank my advisor, professor Thanos Tzempelikos, for his mentoring for my pursuit of knowledge and wisdom. I knew nothing about building technology when I started my graduate study here, and it is my advisor who has been leading my way, all the way to my current fulfillment. Thank my committee members, professor Ilias Bilonis, professor Jianghai Hu and professor Panagiota Karava, for their constant support. Many thanks to Jason, Claire, Seungjae, Michael and Nimish for their help during my research. Thank everyone I ever worked with in different departments, Herrick lab and Bowen lab. It's my honor to work with these excellent people.

I want to say thank you to my family for granting me a lot of "first time role playing" – a husband, and then a father. My life becomes full of happiness and responsibility with my wife and little son. I want to say thank you to my parents and the big family, for giving me the opportunity and supporting me to experience all these growing up and excitements. I want to thank all my friends for helping me and decorating every space of my life here.

TABLE OF CONTENTS

| | |
|---|----|
| LIST OF TABLES | 9 |
| LIST OF FIGURES | 10 |
| ABSTRACT | 13 |
| 1. INTRODUCTION | 15 |
| 1.1 Background and Motivation..... | 15 |
| 1.2 Objectives and Scope | 15 |
| 1.3 Document Overview | 16 |
| 2. LITERATURE REVIEW | 17 |
| 2.1 Shading System in Buildings | 17 |
| 2.1.1 Roller Shades | 18 |
| 2.1.2 Venetian Blinds..... | 19 |
| 2.1.3 Other shading devices..... | 20 |
| 2.2 Daylighting and Lighting Simulation | 20 |
| 2.2.1 Daylighting Simulation Methods | 20 |
| 2.2.1.1 Radiosity Method..... | 20 |
| 2.2.1.2 Ray Tracing Method | 21 |
| 2.2.1.3 Hybrid Ray-tracing and Radiosity Method..... | 22 |
| 2.2.2 Daylighting and Lighting Simulation Tools | 28 |
| 2.3 Visual Comfort, Preference, Satisfaction and Occupant Interactions with Shading and Lighting systems | 30 |
| 2.3.1 Variables | 30 |
| 2.3.1.1 Illuminance and Luminance..... | 30 |
| 2.3.1.2 Visual Discomfort (Glare) | 31 |
| 2.3.1.3 Building and façade Configuration..... | 35 |
| 2.3.1.4 Outdoor Conditions (Weather) | 35 |
| 2.3.1.5 Connection to Outside, View and Privacy | 36 |
| 2.3.1.6 Natural Light (Daylight) and Electric Light | 37 |
| 2.3.1.7 Other Factors..... | 37 |
| 2.3.2 Modeling Occupant Interactions with Shading and Lighting Systems | 38 |

| | | |
|---------|---|----|
| 2.3.3 | Modeling Visual Preferences and Satisfaction | 40 |
| 2.3.4 | Visual Preferences Learning..... | 42 |
| 2.4 | Shading and Lighting Controls | 43 |
| 2.4.1 | Shading Control | 43 |
| 2.4.2 | Electric Lighting Control | 45 |
| 2.4.3 | Model-based Control | 46 |
| 2.4.4 | Optimal Control | 47 |
| 2.5 | Research Gaps and Aims of Dissertation..... | 49 |
| 2.5.1 | Research Gaps..... | 49 |
| 2.5.1.1 | Variables affecting visual preference/satisfaction and Sensing Network..... | 49 |
| 2.5.1.2 | Learning and Modeling Visual Preference and Satisfaction | 52 |
| 2.5.1.3 | Optimal Shading and Lighting Control Considering Visual Preference and Energy Use | 56 |
| 2.5.2 | Aims of Dissertation..... | 59 |
| 3. | A BAYESIAN APPROACH FOR INFERRING PERSONALIZED VISUAL PREFERENCE AND SATISFACTION IN DAYLIT OFFICES | 60 |
| 3.1 | Overview..... | 60 |
| 3.2 | Experiment Design for Acquiring Comparative Visual Preference Data | 62 |
| 3.2.1 | Experiment Design and Setup..... | 62 |
| 3.2.2 | Experimental Data Analysis and Important Variables | 65 |
| 3.3 | Modeling Methodology..... | 68 |
| 3.3.1 | Problem Formulation..... | 68 |
| 3.3.2 | Probabilistic Utility-based Preference Model..... | 69 |
| 3.3.3 | Parameterizing the Utility Function..... | 69 |
| 3.4 | Results and Discussion..... | 72 |
| 3.4.1 | Posterior of (Mean) Visual Satisfaction Utility Function | 72 |
| 3.4.2 | Evaluation of Personalized Visual Satisfaction Models | 78 |
| 3.4.2.1 | Performance Metrics..... | 78 |
| 3.4.2.2 | Performance of Personalized Visual Satisfaction Models | 79 |
| 3.5 | Summary..... | 81 |
| 4. | AN ONLINE VISUAL PREFERENCE ELICITATION LEARNING FRAMEWORK | 83 |

| | | |
|---------|---|-----|
| 4.1 | Overview..... | 83 |
| 4.2 | Visual preference elicitation | 83 |
| 4.2.1 | Visual preference model and satisfaction utility learned from comparative preference data..... | 83 |
| 4.2.2 | Visual preference elicitation | 83 |
| 4.2.2.1 | Random exploration..... | 84 |
| 4.2.2.2 | Exploration..... | 85 |
| 4.2.2.3 | Exploitation..... | 85 |
| 4.2.2.4 | The exploration-exploitation dilemma: | 85 |
| 4.2.3 | Preference elicitation and passive learning with occupant override action | 87 |
| 4.2.4 | Evaluation metric and “stop” criterion | 87 |
| 4.3 | Experiment | 89 |
| 4.3.1 | Experiment design | 89 |
| 4.3.1.1 | Experiment setup | 89 |
| 4.3.1.2 | Experiment procedure..... | 90 |
| 4.3.2 | Experiment results | 94 |
| 4.3.2.1 | Data..... | 94 |
| 4.3.2.2 | Learning results..... | 95 |
| 4.3.2.3 | Learning efficiency..... | 99 |
| 4.4 | Summary and discussion..... | 101 |
| 5. | PERSONALIZED DAYLIGHTING CONTROLS – AN OPTIMIZATION FRAMEWORK TO DYNAMICALLY BALANCE VISUAL SATISFACTION AND LIGHTING ENERGY USE IN DAYLIT OFFICES..... | 103 |
| 5.1 | Overview..... | 103 |
| 5.2 | Methodology..... | 103 |
| 5.2.1 | Models | 105 |
| 5.2.1.1 | Integrated Daylighting and Lighting Energy Use Model | 105 |
| 5.2.1.2 | Personalized Visual Satisfaction Model | 105 |
| 5.2.2 | Optimization | 107 |
| 5.2.2.1 | Multi-Objective Optimization (MOO)..... | 107 |
| 5.2.2.2 | Single-Objective Optimization (SOO)..... | 108 |

| | |
|--|-----|
| 5.2.2.3 Optimization Algorithm..... | 109 |
| 5.3 Results and Discussion..... | 110 |
| 5.3.1 Representative optimization results – single point in time | 110 |
| 5.3.2 Time-varying Pareto fronts and optimal points | 111 |
| 5.3.3 MOO daily and annual results with different visual satisfaction profiles | 113 |
| 5.3.4 SOO daily and annual results with different visual satisfaction profiles..... | 114 |
| 5.3.5 Effects of occupant’s sensitivity (σ)..... | 117 |
| 5.4 Potential Application of Multi-Objective Optimization | 118 |
| 6. FUTURE WORK..... | 122 |
| 6.1 Improving the Personalized Visual Preference and Satisfaction Model | 122 |
| 6.2 Integration of Learning and Control | 122 |
| 6.3 Implementation and Evaluation of the Proposed Optimal Personalized Daylighting Controls..... | 125 |
| 6.4 Integrated Optimal Control for Coordinated Daylighting, Lighting and HVAC Systems Operation Considering Personalized Visual and Thermal Preferences and Energy Use | 125 |
| APPENDIX A. SURVEYS | 126 |
| APPENDIX B. Preferences and Utility Theory | 127 |
| APPENDIX C. Other Preference Elicitation Methods | 129 |
| REFERENCES | 130 |
| VITA..... | 160 |
| PUBLICATIONS | 161 |

LIST OF TABLES

| | |
|---|----|
| Table 1 Daylighting and lighting simulation software..... | 29 |
| Table 2 SMC settings used for sampling and posterior distribution approximation. | 71 |
| Table 3 Posterior median of σ for each model after normalization. | 77 |
| Table 4 Performance evaluation metrics for the three-variable models using 10-fold cross validation results. | 81 |
| Table 5 Representative data (Pref 1: preferring current; 2: preferring previous; 3: no preference). | 95 |

LIST OF FIGURES

| | |
|---|----|
| Figure 1 Flowchart of the hybrid ray-tracing and radiosity method. | 23 |
| Figure 2 Corresponding solar angles and directional vector of light rays. | 25 |
| Figure 3 The law of reflection on ideal specular surface. | 26 |
| Figure 4 Relationship between visual satisfaction and comparative visual preference. | 61 |
| Figure 5 Office space layout and part of instrumentation. | 64 |
| Figure 6 Distribution of vertical and horizontal illuminance across all shading positions and variable sky conditions. | 66 |
| Figure 7 Scatter plots between E_v , SP and LR experimental data. | 67 |
| Figure 8 Experimental pairwise comparisons of overall visual preferences displayed over the E_v -SP space for each of the subjects. | 68 |
| Figure 9 Posterior median of visual satisfaction utility functions of single-variable models (E_v and LR) for each subject. | 74 |
| Figure 10 Posterior median of visual satisfaction utility functions of two-variable models (E_v -SP and LR-SP) for each subject. | 75 |
| Figure 11 Posterior median of visual satisfaction utility functions of the three-variable model for each subject (top: sunny conditions; bottom: cloudy conditions). | 76 |
| Figure 12 ROC curves for the three-variable models and all subjects with 10-fold cross validation. | 80 |
| Figure 13 Model accuracy (HRAdist average and st. deviation) for all developed models (all subjects and variables). | 81 |
| Figure 14 Example PDF of criterion ($E_v * = 1000$ lux, $\sigma = 150$ lux). | 88 |
| Figure 15 System integration and communication flowchart. | 89 |
| Figure 16 Interfaces of survey (up), override enabled (bottom-left) and override disabled (bottom-right). | 90 |
| Figure 17 One-step learning flowchart. | 92 |
| Figure 18 Learning flowchart in each loop (T=8 min). | 93 |
| Figure 19 Data summary. | 94 |
| Figure 20 Representative results – utility samples plot (left) and PDF of maximum $E_v *$ (right). | 96 |
| Figure 21 Representative results – contour plot of mean preference probability $p(E_{v1} > E_{v2})$ | 96 |

| | |
|--|-----|
| Figure 22 Representative learning evolution in four steps (subject 5, sunny day). | 97 |
| Figure 23 Entropy evolution of maximum estimation. | 97 |
| Figure 24 Preference profiles of 13 subjects in the final step. | 98 |
| Figure 25 PDF of maximums of 13 subjects in the final step. | 99 |
| Figure 26 Learning curves of entropy evolution with steps (red dash line: “stop” criterion H=6.4). | 100 |
| Figure 27 Overall methodology flowchart. | 104 |
| Figure 28 Posterior median of two inferred satisfaction utilities (Ev-SP model). | 106 |
| Figure 29 Models and variables transfer flowchart in optimization. | 108 |
| Figure 30 A representative Pareto front with optimal points (satisfaction profile A, single time step). | 111 |
| Figure 31 Transition of MOO feasible region (dashed lines) and Pareto optimals (solid dots), as well as single-objective optimals (marked with X) during representative winter days for satisfaction profile A (top) and B (bottom). Different optimal points correspond to different shading positions and interior lighting conditions. | 112 |
| Figure 32 Daily range of optimal SP for the two visual satisfaction profiles under four different weather conditions. | 113 |
| Figure 33 Histogram of optimal solutions (top) and optimal SP range (bottom) during the year with the two visual satisfaction profiles. | 114 |
| Figure 34 SOO daily results for the two visual satisfaction profiles under four different weather conditions: optimal shading position (top) and range between optimal lighting power and power corresponding to maximum satisfaction (bottom). | 115 |
| Figure 35 SOO annual results for the two visual satisfaction profiles: optimal shading position (top), optimal vertical illuminance (middle) and range between optimal lighting power and power corresponding to maximum satisfaction (bottom). | 116 |
| Figure 36 Effect of sensitivity to the satisfaction utility function on optimal shading position and energy savings. | 117 |
| Figure 37 Example of a slider with hidden mapped optimal points within energy and satisfaction ends. | 119 |
| Figure 38 User-enabled application of MOO in personalized shading and lighting control. Example of mapped optimal conditions on the user interface for two different times, with the slider bar ends corresponding to maximum energy savings and maximum satisfaction respectively, at each time step. | 120 |
| Figure 39 Possible indicative information provided in the optimization application to study the influence of feedback on users. | 121 |

Figure 40 Integration of visual preference learning framework and optimal daylighting control framework. 124

ABSTRACT

In perimeter building zones with glass façades, controllable fenestration (daylighting/shading) and electric lighting systems are used as comfort delivery systems under dynamic weather conditions, and their operation affects daylight provision, outside view, lighting energy use, as well as overall occupant satisfaction with the visual environment. A well-designed daylighting and lighting control should be able to achieve high level of satisfaction while minimizing lighting energy consumption. Existing daylighting control studies focus on minimizing energy use with general visual comfort constraints, when adaptive and personalized controls are needed in high performance office buildings. Therefore, reliable and efficient models and methods for learning occupants' personalized visual preference or satisfaction are required, and the development of optimal daylighting controls requires integrated considerations of visual preference/satisfaction and energy use.

In this Dissertation, a novel method is presented first for developing personalized visual satisfaction profiles in daylit offices using Bayesian inference. Unlike previous studies based on action data, a set of experiments with human subjects was designed and conducted to collect comparative visual preference data (by changing visual conditions) in private offices. A probit model structure was adopted to connect the comparative preference with a latent satisfaction utility model, assumed in the form of a parametrized Gaussian bell function. The distinct visual satisfaction models were then inferred using Bayesian approach with preference data. The posterior estimations of model parameters, and inferred satisfaction utility functions were investigated and compared, with results reflecting the different overall visual preference characteristics discovered for each person.

Second, we present an online visual preference elicitation learning framework for efficiently learning and eliciting occupants' visual preference profiles and hidden satisfaction utilities. Another set of experiments with human subjects was conducted to implement the proposed learning algorithm in order to validate the feasibility of the method. A combination of Thompson sampling and pure exploration (uncertainty learning) methods was used to balance exploration and exploitation when targeting the near-maximum area of utility during the learning process. Distinctive visual preference profiles of 13 subjects were learned under different weather conditions, demonstrating the feasibility of the learning framework. Entropy of the distribution of

the most preferred visual condition is computed for each learned preference profile to quantify the certainty. Learning speed varies with subjects, but using a single variable model (vertical illuminance on the eye), most subjects could be learned to an acceptable certainty level within one day of stable weather, which shows the efficiency of the method (learning outcomes).

Finally, a personalized shading control framework is developed to maximize occupant satisfaction while minimizing lighting energy use in daylit offices with roller shades. An integrated lighting-daylighting simulation model is used to predict lighting energy use while it also provides inputs for computing personalized visual preference profiles, previously developed using Bayesian inference from comparative preference data. The satisfaction utility and the predicted lighting energy use are then used to form an optimization framework. We demonstrate the results of: (i) a single objective formulation, where the satisfaction utility is simply used as a constraint to when minimizing lighting energy use and (ii) a multi-objective optimization scheme, where the satisfaction utility and predicted lighting energy use are formulated as parallel objectives. Unlike previous studies, we present a novel way to apply the MOO without assigning arbitrary weights to objectives: allowing occupants to be the final decision makers in real-time balancing between their personalized visual satisfaction and energy use considerations, within dynamic hidden optimal bounds – through a simple interface.

In summary, we present the first method to incorporate personalized visual preferences in optimal daylighting control, with energy use considerations, without using generic occupant behavior models or discomfort-based assumptions.

1. INTRODUCTION

1.1 Background and Motivation

One of the main purposes of building design and control is to provide comfortable building environment to satisfy occupants. Meanwhile, building energy efficiency is a primary topic of interest with a great potential of energy and cost savings, as well as overall sustainability improvement. In perimeter building zones with glass façades, controllable fenestration (daylighting/shading) and electric lighting systems are used as comfort delivery systems under dynamic weather conditions, and their operation affects daylight provision, outside view, lighting energy use, as well as overall occupant satisfaction with the visual environment. A well-designed daylighting and lighting control system should ideally maximize occupant satisfaction while minimizing lighting energy consumption, and should be capable of adapting itself to controlled, dynamic visual conditions and learned occupant(s) preferences.

Toward the objectives, several studies have been conducted on daylight and lighting simulation algorithms, modeling and learning visual preference/satisfaction, as well as the development of control strategies. Automated shading controls aiming to reduce visual discomfort have been developed, while some studies focused on integrated shading and lighting control for minimizing energy use with visual comfort considerations. However, researchers have also recognized the research gaps with existing visual comfort models and control strategies, especially when smart control systems require self-tuning and personalization features in high performance buildings.

Therefore, reliable and efficient models and methods for learning occupants' visual preference or satisfaction profiles are needed, and the development of optimal daylighting and lighting control requires integrated considerations of visual preference/satisfaction and energy use.

1.2 Objectives and Scope

The objectives of this dissertation are:

- 1) To develop a modeling method for learning occupants' personalized visual preference and satisfaction profiles in daylit offices;

- 2) To develop and implement an online visual preference elicitation framework for efficiently learning occupants' visual preferences and satisfaction utility functions;
- 3) To develop a personalized daylighting control framework aiming at optimizing occupant satisfaction and lighting energy use in daylit offices.

1.3 Document Overview

Chapter 2 includes a literature review focusing on existing studies on building fenestration systems, daylighting and lighting simulation methods, conventional models of occupants' visual comfort, preference and satisfaction, as well as shading and lighting controls. It summarizes the current research gaps with respect to visual preference modeling, learning frameworks, optimization approaches and application frameworks.

Chapter 3 presents a Bayesian approach for inference of occupants' personalized visual preferences and satisfaction in daylit offices. A probit model structure is adopted to connect the comparative preference with a latent satisfaction utility model, in the form of a parametrized Gaussian bell function, and the satisfaction models are then inferred using Bayesian approach with preference data collected from experiments with human subjects.

Chapter 4 presents an online visual preference elicitation learning framework. To determine the (visual) condition "duels" for preference query with most information gain, a combination of Thompson sampling and pure exploration (uncertainty learning) methods was used. Distinctive visual preference profiles of 13 subjects were learned under different weather conditions, using data from experiments, demonstrating the feasibility and effectiveness of the proposed visual preference learning framework.

Chapter 5 presents a personalized shading control framework to maximize occupant visual satisfaction while minimizing lighting energy use in daylit offices. Two optimization schemes are developed and compared with single-objective and multi-objective formulations. A novel way to apply the multi-objective optimization based control is presented by allowing occupants to be the final decision makers in real-time balancing between their personalized visual satisfaction and energy use considerations.

Chapter 6 contains extensions of this Dissertation and recommendation for future work.

2. LITERATURE REVIEW

The building sector accounts for a significant portion (30%) of global energy consumption (IEA 2015) and lighting represents a major energy consumer in commercial buildings in U.S (DOE 2015), which indicates a great potential for energy savings. On the other hand, occupants play a significant role in energy use of buildings, while they have strong preferences for customized indoor environment. Their perception of a controlled indoor environment affects their satisfaction and productivity. In perimeter building zones with glass facades, controllable fenestration (daylighting/shading) and electric lighting systems are used as comfort delivery systems under dynamic weather conditions. Their operation affects daylight provision, outside view, lighting energy use, as well as overall occupant satisfaction with the visual environment. Researches on daylighting and energy, occupant comfort, as well as related building controls contribute towards energy conservation and improving occupant satisfaction.

2.1 Shading System in Buildings

Fenestration consists of glazing and shading systems, significantly affecting indoor environmental conditions, thermal and visual comfort, and building energy use. In perimeter zones of commercial buildings with large glass façades and high internal gains, reducing cooling and lighting requirements while maintaining good comfort conditions is often the major objective. Shading devices play a significant role in overall façade performance, providing privacy, blocking excessive solar heat gain and controlling natural light, as well as preventing glare. They are mainly categorized as fixed and movable, as well as interior and exterior.

Fixed shading devices include overhangs, louvers, vertical fins, awnings and light shelves, etc. Although they can block solar radiation in summer, when the solar altitude is high, fixed shading systems are inefficient for solar control and glare protection, especially with low-altitude sunlight. Furthermore, they are hardly adjustable according to occupants' preferences. Therefore, movable shading devices are more popular and widely employed in office buildings nowadays, as they are more flexible and efficient with changing conditions and can be centrally or locally controlled. Common movable shading devices include roller shades, venetian blinds, curtains and shutters.

2.1.1 Roller Shades

Roller shades are widely used in commercial buildings. They are pieces of fabric rolled around a roller that raises or lowers the fabric by spinning, either manually-operated, through chains/ropes, or motorized using electric motors.

Roller shades have various materials, colors and weave construction that result in different optical and thermal properties – openness factor, solar and visible transmission/reflection. Visible transmittance, openness factor and color have a direct impact on indoor daylighting and comfort conditions. Other factors, including reflectance and absorptance, are more related with their thermal performance. The amount of light transmitted through the fabrics depends on the fabric optical properties (Chan et al. 2014). Part of the direct light becomes diffuse, and part of it remains as direct, unobstructed sunlight.

Kotey et al. (2009) developed a semi-empirical model for direct-direct, direct-diffuse and angular properties of roller shades. The model was extracted from detailed integrated sphere measurements (Collins et al. 2012) of the spectral beam-beam and beam-diffuse transmittance, as well as beam-diffuse reflectance of different fabrics at incident angles ranging from 0° to 60°. The spectral data was converted to solar optical properties according to ASTM standards, and a cosine power function was fitted to the measured properties at different incident angles. The models were validated with integrated sphere measurements and full-scale experiments (Tzempelikos and Chan 2016) and errors were reported when using only normal incidence data by manufacturers. The calculation steps are described below.

The normalized beam-beam shade transmittance is calculated as:

$$\tau_{bb} = \cos^b \left(\frac{\theta}{\theta_{cutoff}} \frac{\pi}{2} \right) \quad \theta \leq \theta_{cutoff}, \quad (1)$$

where θ is the incident angle, and b is defined as:

$$b = 0.6 \cos^{0.3} \left(\tau_{bb}(\theta = 0) \frac{\pi}{2} \right), \quad (2)$$

And cut-off angle θ_{cutoff} is defined as:

$$\theta_{cutoff} = 65^\circ + (95^\circ - 65^\circ) \left(1 - \cos \left(\tau_{bb}(\theta = 0) \frac{\pi}{2} \right) \right). \quad (3)$$

The fabric beam-beam transmittance at normal incidence, $\tau_{bb}(\theta = 0)$ is assumed equal to the openness factor, provided by manufacturers.

The normalized beam-total shade transmittance is calculated as:

$$\tau_{bt} = \cos^d(\theta) \quad \theta \leq \theta_{cutoff}, \quad (4)$$

where d is defined as:

$$d = \begin{cases} 0.133(\tau^{str} + 0.003)^{-0.467} & 0 \leq \tau^{str} \leq 0.33 \\ 0.33(1 - \tau^{str}) & 0.33 \leq \tau^{str} \leq 1 \end{cases} \quad (5)$$

$$\tau^{str} = \frac{\tau_{bt}(\theta = 0) - \tau_{bb}(\theta = 0)}{1 - \tau_{bb}(\theta = 0)}. \quad (6)$$

Beam-total transmittance at normal incidence $\tau_{bt}(\theta = 0)$ is provided by manufacturers. The cut-off angle restriction is only applied to dark-colored fabrics.

The beam-diffuse transmittance is calculated by the beam-total minus the beam-beam respectively for every incident angle.

The diffuse-diffuse transmittance is calculated by integrating beam-total transmittance over the hemisphere:

$$\tau_{dd} = 2 \int_0^{\pi/2} \tau_{bt}(\theta) \cos(\theta) \sin(\theta) d\theta. \quad (7)$$

The above model is used to predict daylight transmission through roller shades in this Dissertation.

2.1.2 Venetian Blinds

Venetian blinds are popular both in commercial and residential buildings. They are sets of rotatable horizontal slats linked with pulling ropes for changing the slats angles, which make them able to control the amount and the direction of transmitted light rays. The transmittance and reflectance of venetian blinds depend on the solar incident angle, slat tilt angle and optical properties of slat surface.

Blinds with smooth slat surfaces will specularly reflect most of the light rays striking on it following the laws of reflection. However rough surfaces of slats reflect light anisotropically, and reflected lights result in diffuse or mixed patterns. Different blind properties could meet different application requirements. Case studies have shown that employing venetian blinds could bring significant energy profits (Chaiwiwatworakul et al. 2009; Kim et al. 2009).

2.1.3 Other shading devices

A light shelf is a horizontal or inclined overhang projecting over a view aperture with a reflective surface, usually in the upper window section (Rao 2011). It is able to reflect light to ceiling or outside to partly block solar radiation and to redirect light rays. Studies have showed that light shelves help to improve the uniformity of illuminance distribution in buildings (Claros and Soler 2002; Kim 2009).

2.2 Daylighting and Lighting Simulation

Simulation of daylighting and electric-lighting enables architectural engineers to evaluate the visual environment, visual comfort conditions in spaces and the energy performance related to lighting, cooling and heating brought by fenestration and lighting systems; it further helps for design and implementation of corresponding façade and lighting controls based on simulation results.

2.2.1 Daylighting Simulation Methods

Detailed simulation of daylight distribution (illuminances and luminances) in a space can lead to understanding of visual comfort and lighting energy consumption conditions, but it requires efficient algorithms and advanced, heavy computational models. Daylighting simulation usually requires large numbers of input information, among which some are hard to obtain or need expensive sensors, such as weather conditions, and the optical properties of all related materials and devices.

Radiosity and ray-tracing methods are two dominant methods applied in lighting simulation, as introduced in following sections.

2.2.1.1 Radiosity Method

The radiosity method was firstly developed in the engineering field of radiation heat transfer, and was later refined by Goral (1984) for application of computer graphics rendering and lighting simulation.

The radiosity method assumes that all considered surfaces in the environment are perfect (or Lambertian) diffusers, reflectors, or emitters, which reflect incident light hitting on them in all

directions with equal intensity. Observed from the surface, the amount of reflected light is proportional to the cosine of the angle θ between the observer's line of sight and the surface normal (Lambert's cosine law).

A formulation for the system is facilitated by dividing the environment into a set of areas (patches). The radiosity of a patch is defined as the total rate of energy leaving the surface and equal to the sum of the emitted and reflected energy. For each pair of patches, a view factor, the proportion of radiation that leaves one surface and directly strikes another, is computed and stored as a coefficient. The radiosity equation of patch i can be written as:

$$M_i = M_{0i} + \rho_i \sum_{j=1}^n M_j F_{i,j}, \quad (8)$$

where M_i is the final luminous exitance of patch i in lux, M_{0i} is the initial luminous exitance of patch i in lux, ρ_i is the reflectance of patch i , $F_{i,j}$ is the view factor from patch i to patch j , and n is the number of total patches.

Followed equation **Error! Reference source not found.** defines the system of equations in matrix form.

$$\begin{bmatrix} M_i \\ \vdots \\ M_i \end{bmatrix} = \begin{bmatrix} M_{0i} \\ \vdots \\ M_{0i} \end{bmatrix} \begin{bmatrix} 1 - \rho_1 F_{11} & \cdots & -\rho_1 F_{1n} \\ \vdots & \ddots & \vdots \\ -\rho_n F_{n1} & \cdots & -\rho_n F_{nn} \end{bmatrix}^{-1}. \quad (9)$$

A large inverse matrix in the equation creates computational problems when the dimension increases (e.g., separating interior surface into several sub-surfaces). To speed up the calculation process, iterative methods such as gathering and shooting algorithms can be implemented.

The most evident limitation of the radiosity method is its basic assumption – assuming all the surfaces are perfect diffusers in the calculation process. When using the radiosity method to solve surfaces with specular characteristics or non-uniform intensity reflections, the accuracy of results is questionable (Versluis 2005). Also, when the amount of patches increases, the required memory to store view factors and the required time to calculate view factors would increase exponentially.

2.2.1.2 Ray Tracing Method

Ray tracing is a technique capable of simulating complex light interactions including specular reflections. It is derived from the idea that light reflection can be modeled by recursively

following the path that a light ray takes as it bounces within an enclosed environment. Light rays can be traced from the light source to the object (forward ray-tracing), from the observer's eyes to the world (backward ray-tracing), or from both ways (hybrid ray-tracing). In forward ray tracing algorithms, each ray carries a certain amount of light intensity generated from the light source. When intersecting with a surface, a new ray is generated, resulting in a loss of intensity of the reflected light due to absorption by the surface. The trace process stops when the light intensity drops below a certain threshold. Forward ray tracing can accurately determine the luminance or illuminance of each object, but it is often inefficient as to limited target points since many rays from the light source never come through the reference point or through observer's eyes.

Backward ray tracing method was introduced to improve the efficiency of ray tracing, especially for computer graphics rendering purposes. However, there are disadvantages of the backward ray tracing method when applying it to daylighting simulation with complex fenestration systems. Several viewpoints need to be created which means several turns of tracing are required. Compared to backward ray tracing, forward ray tracing is independent of view and concentrates on producing numerical data rather than rendering a photo-realistic image. To combine the advantages of forward and backward ray tracing method, researchers also developed a hybrid ray tracing method that compromise speed and accuracy (Lafortune and Willems 1996; Chan and Tzempelikos 2012). The Monte-Carlo method, a sophisticated sampling method, was usually combined with ray-tracing calculations in ray sample generating process (Tsangrassoulis et al. 2002). Depending on the reflection characteristics of the surface, not all of the reflected light would follow the path of specular reflection. At each transition of ray direction caused by reflection or transmission, the new direction is calculated according to statistical probabilities defined by the optical properties of each surface (Tregenza 1983). However, even if combined with the sampling method, the computational efficiency is still a big issue in ray tracing simulation when dealing with diffuse surfaces, since a large number of samples is required.

2.2.1.3 Hybrid Ray-tracing and Radiosity Method

As discussed above, ray tracing and radiosity are two major algorithms used to simulate indoor daylighting distributions and they are suitable for different applications. Ray-tracing algorithms are better for specular surfaces and accurate direct light simulation, while radiosity methods are more efficient with Lambertian surfaces and diffuse light simulation. Therefore, Chan

and Tzempelikos (2012) developed a hybrid ray-tracing and radiosity daylighting model which combines the strengths of these two methods, for application in complex fenestration systems such as venetian blinds.

In the hybrid ray-tracing and radiosity method, the ray-tracing method is used to track the direct sunlight entering space and the radiosity method is used to simulate the diffuse inter-reflections between interior surfaces and the final lighting distribution. For daylight simulation model focusing on dynamic façades with controlled fenestration systems (glass and roller shades), the inputs are the transmitted direct and diffuse illuminance from glazing and shading respectively. Figure 1 presents a flowchart of the hybrid ray-tracing and radiosity method.

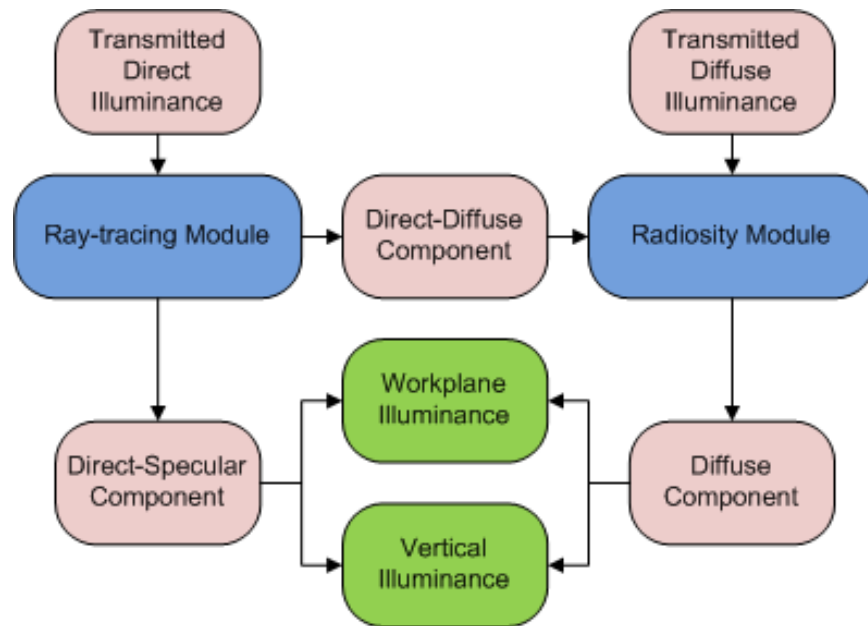


Figure 1 Flowchart of the hybrid ray-tracing and radiosity method.

Total illuminance transmitted through glazing could be measured by an illuminance sensor, and then it is separated into direct and diffuse parts with measured direct-diffuse ratio obtained from outside sensor, together with the known optical properties of glazing and shading layers. Calculation of glazing and shading transmittances for direct component and diffuse component are discussed in (Chan and Tzempelikos 2012; Xiong and Tzempelikos 2016).

Ray Tracing Module

For the direct sunlight, a ray tracing method is employed to track the daylight projection area after transmitted through façade (glazing-only part and glazing-shading part respectively). The one-bounce hybrid model assumes that all the interior walls, floors, and ceilings are perfect diffusers, which means all the direct components (rays) are reflected as diffuse component after they hit the surfaces once.

All the points, planes, and rays are defined in a three-dimensional Cartesian coordinate system before tracing the rays. A certain number of rays are generated with a uniform distribution representing direct lights transmitted through the window. The total rays number in the model affects the accuracy of simulation results as well as simulation load and speed – more rays require larger calculation memory and time but lead to more accurate simulation results. Chan and Tzempelikos (2012) selected 3000 rays per square meter for the façade area for compromising calculation speed and accuracy. Each of the rays carries a certain amount of direct luminous flux entering the space, based on following equations.

$$\text{luminance flux in each ray from glass} = \frac{E_{tr-dir}(1 - \kappa_{sh})}{Ray\#} \quad (10)$$

$$\text{luminance flux in each ray from shades} = \frac{\tau_{dir-dir}E_{tr-dir}\kappa_{sh}}{Ray\#} \quad (11)$$

where E_{tr-dir} is transmitted direct illuminance, κ_{sh} is the shaded window fraction, $\tau_{dir-dir}$ is the shades direct-direct transmittance, $Ray\#$ is the number of rays.

In the 3-D Cartesian coordinate system, the X-axis represents the north-south axis, the Y-axis represents the east-west axis, and the Z-axis represents the vertical (height) axis. Each of the rays is represented with a position vector and a directional vector, which indicate the position where the ray is generated (on the façade in this case) and the direction the ray is heading to. The position vector is a coordinate of the ray starting point on window. The direction vector of the ray is related to the simulated moment, the solar position and corresponding solar angles as expressed by:

$$\bar{T} = (\cos(\alpha) \cos(\phi), \cos(\alpha) \sin(\phi), -\sin(\alpha)) \quad (12)$$

where α is the solar altitude, and ϕ is the solar-surface azimuth as expressed in Figure 2.

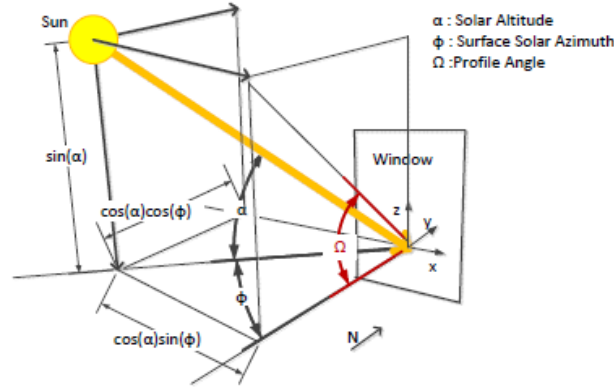


Figure 2 Corresponding solar angles and directional vector of light rays.

Some computational strategies are used to save computation time (Chan and Tzempelikos 2012). For example, if the solar incident angle indicates that the sun is under the horizon (less than 0 degrees) or not facing to the façade (greater than 90 degrees), or the sky has been classified as overcast (when measured incident radiation is below 100 W/m^2), it is assumed that no direct sunlight is transmitted through the façade and the ray-tracing step is skipped to save computation time.

After the rays are generated, they are traced to determine the location where the rays firstly strike on. Each of the interior surfaces is viewed as a plane and defined with a position vector which can be any point on the plane indicating the plane's position, and the normal vector of the plane which represents its direction. The travel distances from each ray's generated point to every plane are computed and then the plane with minimum travel distance is determined as the plane that the ray strikes on. Travel distances less than zero are eliminated as the plane is opposite to the ray's traveling direction.

The travel distance of a ray is computed by followed equation.

$$t = \frac{(\bar{P} - \bar{Q}) \cdot \bar{N}}{\bar{R} \cdot \bar{N}} \quad (13)$$

where \bar{P} is the position vector of plane, \bar{Q} is the position vector of the ray, \bar{N} is the normal vector of the plane, and \bar{R} is the directional vector of reflected ray.

The directional vector of reflected ray is calculated by the following equation, based on the reflection law that the incident angle is equal to the reflection angle, as shown in Figure 3.

$$\bar{R} = \bar{T} - 2(\bar{T} \cdot \bar{N})\bar{N} \quad (14)$$

where \vec{T} is the directional vector of incident ray.

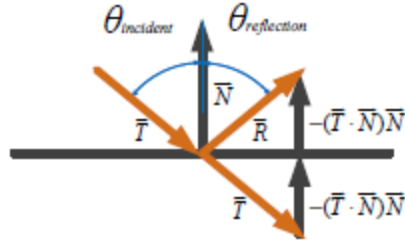


Figure 3 The law of reflection on ideal specular surface.

In the one-bounce ray-tracing model, reflected light from interior surfaces is assumed entirely diffuse and thus the initial exitance of each interior surface is used in the radiosity method described in the following section.

Virtual work plane (usually at 0.75-0.8 m height) and vertical reference point (usually at 1.1-1.3 m height) could be assumed for target light receiver (desk and eye). The same equations above are employed to determine whether and where the direct light will strike on the work plane or eye. It is assumed that the work plane will not interrupt the inter-reflection between other real existing interior surfaces – this assumption is realistic and does not affect the final results, except for cases with large desks/furniture.

Radiosity Module

After computing the direction and intensity of reflected rays, it is assumed that all the components become diffuse light sources (façade and projection on floor/walls). Then a 3-D radiosity method is employed to simulate the final illuminance distributions on all interior surfaces and the virtual work plane as well as on any vertical reference point. The luminance values of interior surfaces are also computed based on the results.

Each interior surface is usually evenly divided into small rectangular sub-surfaces for radiosity calculations. The final luminous exitance of each sub-surface can be expressed by:

$$M_m = M_{0-m} + \sum_k^t (1 - abs_m) F_{km} M_k \quad (15)$$

where M_m is the final luminous exitance of sub-surface m , M_{0-m} is the initial luminous exitance of sub-surface m , abs_m is the absorptivity of sub-surface m , t is the total number of surfaces except sub-surface m , F_{km} is a view factor between sub-surfaces k and m . View factor F_{ij} is defined as the ratio of flux emitted by surface i that falls on surface j .

The diffuse daylight coming from the sky is different from the diffuse daylight reflected from the ground, but to speed up the calculation, the sky and ground light are usually assumed uniform distributed respectively, which has a small impact on the accuracy of final results for most interior daylight simulations. Diffuse sky illuminance and ground reflected diffuse illuminance could be computed based on total horizontal illuminance measured by sensor and other simplified assumptions (Xiong and Tzempelikos 2016).

Except for sky and ground-reflected light incident on the window, the interior window luminance is also affected by the reflected illuminance from other room surfaces. These components are assumed to be isotropic, and should be added to window patch luminances. Following equations presents the final window patch luminance considering the diffuse light coming from sky and ground-reflected respectively.

$$L_{m-s} = \frac{\tau_d E_{sd}}{\pi/2} + \frac{M_m - M_{0-m}}{\pi} \quad (16)$$

$$L_{m-g} = \frac{\tau_d E_{gr}}{\pi/2} + \frac{M_m - M_{0-m}}{\pi} \quad (17)$$

where τ_d is diffuse transmittance of glass, E_{sd} and E_{gr} are sky diffuse illuminance and ground-reflected illuminance respectively.

Then the diffuse work plane illuminance on a point can be obtained by:

$$E_{wp-diff} = \sum_m^s L_m \cos \theta d\omega \quad (18)$$

where θ is the angle between the normal vector to the sub-surface m and the line connecting the work plane point and the sub-surface, and $d\omega$ is the solid angle of sub-surface m .

For horizontal work plane, any point on it is facing upward, so the light traveling from the point to the façade patch must contributed by the sky. Therefore, L_{m-s} values are assigned to all the window patches in the equation above in this case.

For a vertical point facing toward the façade, every façade patch is compared with the horizontal line of sight (perpendicular to the façade). If the façade patch is above the line, the light

is contributed by the sky. Otherwise, the light traveling direction would be extended to the ground, and L_{m-g} value will be assigned to the corresponding window patch.

The final step is to add the illuminance contribution from direct daylighting, which is calculated by the ray tracing method discussed in the previous section.

2.2.2 Daylighting and Lighting Simulation Tools

There are various software packages available nowadays for lighting and daylighting simulation for buildings, with different applications and different level of complexity and accuracy based on the simulation methods employed.

Radiance (Ward and Shakespeare 1998) is a sophisticated daylighting and lighting simulation tool, which is powerful to compute accurate and detailed illuminance and luminance distributions by employing backward ray-tracing algorithms. It is customizable so there are several programs developed based on Radiance, aiming at different application.

DAYSIM is one of the Radiance-based daylighting and lighting simulation tools (Reinhart and Herkel 2000) that is able to run annual dynamic simulation. It uses the daylight coefficients approach and the Perez sky luminance model to simulate indoor illuminances under various sky conditions. Reinhart and Walkenhorst (2001) compared six Radiance-based methods and validated the results for a test office with external venetian blinds, and showed that DAYSIM is a reliable and accurate tool for daylight simulation. In DAYSIM, the sub-model, Lightswitch, can predict the lighting energy performance of manually and automatically controlled electric lighting and blind systems (Reinhart 2004). Furthermore, to minimize the required time for dynamic simulation for complex glazing system, DAYSIM further employed the three-phase and five-phase methods based on Ray tracing method. In the three-phase method, flux transfer process is separated into the following three phases for independent simulation: 1) sky to exterior of fenestration with daylight coefficient method; 2) transmission through fenestration with BSDF function; 3) interior of fenestration into the simulated space with view matrix. Extended from three-phase method, the five-phase method handles the direct solar component separately from the sky and inter-reflected solar component to achieve better accuracy.

Evalglare (Wienold 2004) is another daylight simulation program based on Radiance but designed specifically for glare assessment. It determines and evaluates glare sources within a fisheye image, given in a RADIANCE image file. The program calculates the daylight glare

probability (DGP) as well as other glare indexes (DGI, DGI_MOD, UGR, UGR_EXP, VCP, CGI, UDP) to the standard output.

EnergyPlus is an integrated thermal and daylighting simulation tool. Simulated daylighting results are parameters to calculate internal heat gains involved in thermal modeling. EnergyPlus uses the daylight factor method in order to provide faster results. And it is capable of detailed daylight simulation only for representative days, with radiosity method in internally reflected calculations to achieve better accuracy.

Ecotect (Autodesk Ecotect Analysis) performs daylight simulation using the split flux method, which is based on daylight factors, combined with ray-tracing.

Relux (2013) is a commercial software widely used in Europe, which uses the daylight factor and ray tracing method to implement daylighting and artificial light simulation. DIALux (2013) is another commercial lighting simulation tool based on radiosity method.

Doulos et al. (2005) conducted a detailed review to introduce and compare Relux, SPOT and DAYSIM. In the study, they pointed out three challenges in current daylighting simulation tools: 1) the best position of the photosensor; 2) control optimization of various types of shading systems; 3) a database with control functions for voltage and lighting output ratio for a large number of ballasts.

The following table summarizes some of the most popular daylighting and lighting simulation software.

Table 1 Daylighting and lighting simulation software.

| Daylighting Simulation Software | Methods |
|---------------------------------|--|
| Radiance / Daysim / Evalglare | Ray tracing / Three phase method / Five phase method |
| EnergyPlus | Daylight factor / Radiosity |
| Ecotect | Daylight factor / Split flux |
| Relux | Daylight factor / Ray tracing |
| DIALux | Radiosity |

2.3 Visual Comfort, Preference, Satisfaction and Occupant Interactions with Shading and Lighting systems

2.3.1 Variables

In perimeter building zones, several physical or non-physical variables may affect occupants' visual perception and visual comfort/satisfaction, as well as the possible resulting actions. Many studies have been conducted to identify, decouple and investigate the main factors triggering the interactions between occupants and shading and lighting systems.

2.3.1.1 Illuminance and Luminance

One of the most commonly considered factors of visual environment is the amount of light on a certain surface, represented by illuminance - the total luminous flux incident on a surface, per unit area, which can be measured with a single photometric sensor. IES (Illuminating Engineering Society) Standard recommends 300-500 lux of illuminance on work plane in offices (IESNA 2000). Rea (1984) conducted an experiment in a large scale building and found that most occupants operate blinds when direct sunlight hitting on working plane and they rarely changed it for view contact with outside or for natural lighting. While Reinhart (2004) found the thresholds of exterior vertical illuminance to be 50 klux and 25 klux for blinds closings and openings respectively, other studies (Rea 1984; Reinhart and Voss 2003) attempted to find correlations between work plane illuminance and operation of window shades, and Haldi and Robinson (2010a) found the thresholds of 1200 lux and 200 lux work plane illuminance for blinds closing and opening, respectively. Overall, daylight work plane illuminance and vertical illuminance on screen have been found to be strongly related to occupant preference or interactions with shading devices (Hunt 1979; Love 1998; Sutter et al. 2006).

Luminance is another fundamental factor describing the amount of light - the luminous intensity per unit area of light travelling in a given direction, usually characterizing the emitted or reflected light from surfaces. Luminance can be measured with a luminance meter with specific direction and solid angle, or luminances in a certain field can be measured from processed image taken by digital camera, in a similar way to color images. The luminance image is useful as it could approximately represent the whole field of view of actual human and describe the distribution of lights on all the surfaces in the field, when using a fisheye lens in the camera. Inkarojrit (2005, 2008) concluded that luminances from window and background are proper indicators of blinds

operations. Most studies, on the other hand, further correlated the luminance with visual discomfort (glare). Escuyer and Fontoynt (2001) monitored occupant's behavior in three office buildings in France and stated that most people tended to close blinds when reflected lights affected computer work (disability glare problem) but they rarely or partially raised their blinds when there was no more glare. Glare is discussed in the following section.

Both illuminance and luminance represent the “brightness” concept in the visual environment, but from different aspects. Illuminance describes the brightness level of light falling on a specific point or surface (from all directions), and luminance represents the brightness level of light emitted or reflected from a specific point or surface in a given direction and solid angle. Illuminance is relatively easy to measure and gives a single value for brightness information, but the information is therefore limited as it is a point-measurement and independent of human. On the other hand, luminance image captured by a fish-eye-lens camera could replicate the perceived brightness information by human, but camera sensing applications involving occupants have many other issues, and a luminance image consists of a large number of outputs such as pixel-wise luminance values, positions (angles away from the line of eye sight) and solid angles which make it difficult to utilize in an efficient manner. Glare studies usually extract specific (part) information from luminance image such as glare source luminance identified with certain threshold, (average) background luminance, source solid angle and source positions.

2.3.1.2 Visual Discomfort (Glare)

Glare has been the focus of visual comfort studies in the past decades. Glare refers to the discomfort or difficulty of seeing as a result of bright light or contrast. A glare source can be direct or reflected daylight and artificial light, such as sun in the field of view and or headlamps. Glare can be generally divided into two types, discomfort glare and disability glare. Discomfort glare is usually caused by strong contrast of luminance between target seen and the glare source and it results in discomfort or difficulty in seeing, while disability glare does not necessarily cause discomfort (CIE). Our study is more related to discomfort glare caused by daylight.

Several discomfort glare indices have been studied in previous studies with human subjects involved, characterized by subjective feelings and physical factors such as glare source luminance L_s and source solid angle ω_s .

a. BRS glare index (BGI)

The earliest glare index published is BRS glare index (BGI), developed by Petherbridge and Hopkinson (1950) at the Building Research Station in England. The BRS glare equation is empirically developed as followed.

$$BGI = 10 \log_{10} 0.478 \sum_{i=1}^n \frac{L_s^{1.6} \omega_s^{0.8}}{L_b P^{1.6}} \quad (19)$$

where n is the number of glare sources; L_b is the background luminance (or general field of luminance) excluding the glare sources; Guth's position index P represents the change of glare sensed with source azimuth and altitude to observer's line of sight.

BGI is proved to be limited in application with large or wide glare sources (Chauvel et al. 1982; Iwata et al. 1991; Osterhaus 1996) since the intention of developing BGI is for glare characterization from point light source, with solid angle smaller than 0.027sr.

b. Visual Comfort Probability (VCP)

The Visual Comfort Probability (VCP) developed by S.K. Guth (1963, 1966) represents the percentage of people that consider the lighting conditions comfortable. It aims at electric lights as glare sources and requires complex calculations.

c. CIE glare index (CGI)

Einhorn (1969) proposed a unified glare assessment equation and it was adopted by the International Commission on Illumination (CIE).

$$CGI = 8 \log_{10} 2 \frac{1 + E_d/500}{E_d + E_i} \sum_{i=1}^n \frac{L_s^2 \omega_s}{P^2} \quad (20)$$

where E_d is the direct vertical illuminance at the eye from glare sources; E_i is the indirect (diffuse) illuminance at the eye from background.

CGI was developed to improve BGI for its mathematical inconsistency with multiple glare sources.

d. Daylight Glare Index (DGI)

Daylight glare index (DGI), or Cornell glare equation, is developed to modify BGI for large glare source by Hopkinson (1972).

$$DGI = 10 \log_{10} 0.48 \sum_{i=1}^n \frac{L_s^{1.6} \Omega_s^{0.8}}{L_b + 0.07 \omega_s^{0.5} L_s} \quad (21)$$

where Ω_s (sr) is the solid angle subtended by the glare source modified by the position of the source with respect to field of view and Guth's position index.

The equation was developed through experiments with glare from fluorescent lamps behind an opal-diffusing screen. Therefore its application is limited under real sky conditions and when the glare source is non-uniform or in the whole field of view (Fisekis et al. 2003; Osterhaus 2005; Bellia et al. 2008).

The new daylight glare index (DGI_N) was proposed by Nazzal (2001) to improve DGI equation, but its accuracy remains to be validated.

e. Unified Glare Rating (UGR)

Unified Glare Rating (UGR), proposed by Sorensen in 1987, was adopted by CIE (1992).

$$UGR = 8 \log_{10} \frac{0.25 \sum_{i=1}^n L_s^2 \omega_s}{L_b P^2} \quad (22)$$

UGR is a combination of CGI and BGI for glare prediction for artificial lighting system. It inherits BGI's application limitation to some extent with solid angle restriction from 3×10^{-4} sr to 10^{-1} sr.

f. Daylight Glare Probability (DGP)

The most recent glare index aiming at daylight discomfort glare assessment is daylight glare probability (DGP), introduced by Wienold and Christoffersen (2006).

$$DGP = 5.87 \times 10^{-5} E_v + 9.18 \times 10^{-2} \log_{10} \left(1 + \sum_{i=1}^n \frac{L_s^2 \omega_s}{E_v^{1.87} P^2} \right) + 0.16 \quad (23)$$

where E_v is the vertical illuminance at the eye.

The position index P used in DGP calculation is a combination of Guth's model (Guth 1966) and Inoue's model (Inoue et al. 1988). For the glare sources above the observer's line of sight (perpendicular to the façade), the Guth's position index is calculated by:

$$\ln P = (352 - 3.1889\tau - 12.2e^{-2\tau/9})10^{-4}\sigma + (21 + 0.26667\tau - 0.002963\tau^2)10^{-5}\sigma^2 \quad (24)$$

where τ is the angle between the normal of the plane where the glare source is on and the line of sight, and σ is the angle between the line from observer to source and the line of sight. For the glare sources below line of sight, the Inoue's model position index is calculated by:

$$P = 1 + 0.8 \times \frac{R}{D} \{R < 0.6D\}$$

$$P = 1 + 0.8 \times \frac{R}{D} \{R \geq 0.6D\} \quad (25)$$

$$R = \sqrt{H^2 + Y^2}$$

where D is the distance from eye to the plane of source, H is the vertical distance between source and view direction, and Y is the horizontal distance between source and view direction.

The solid angle ω is calculated by:

$$A_p = A \cos \theta \quad (26)$$

$$\omega = \frac{A_p}{D^2} \quad (27)$$

where A is the area of glare source, A_p is the projected area of glare source to observer, and θ is the angle between the normal vector of glare source plane and the line from observer to glare source, and D is the distance between the observer and the glare source.

DGP was evaluated by occupancy assessment experiments, initially showing better accord with occupant responses than any previous daylight glare index, such as CGI and DGI. The DGP limit for “unperceived” glare is 0.35 (Wienold 2009). Recent studies show that in some cases, DGP does not perform as well as expected (Suk and Schiller 2016).

The most eminent development of DGP is its strong linear relation with observer’s vertical eye illuminance, which performs well with large glare sources. Wienold (2007) then proposed simplified DGP (DGPs) for application with no direct sun within field of view.

$$DGPs = 6.22 \times 10^{-5} E_v + 0.184 \quad (28)$$

Recent studies (Konstantzos et al. 2015) showed that DGPs is appropriate to use for all cases except when direct light falls on the eye. Therefore, the use of DGPs is not recommended for shades with noticeable openness transmitting direct light.

Konstantzos and Tzempelikos (2017) conducted experiments with human subjects and developed two new metrics for cases when the sun is visible through roller shades. The first is a modified DGP equation, with coefficients that showed a better fit when the sun is within the field of view through shades:

$$DGP_{mod} = 8.4 \cdot 10^{-5} \cdot E_v + 11.97 \cdot 10^{-2} \cdot \log \left(1 + \sum_i \frac{L_{s,i}^2 \cdot \omega_{s,i}}{E_v^{2.12} \cdot p_i^2} \right) + 0.16 \quad (29)$$

The second metric is alternate glare discomfort index, based on direct and total-to-direct vertical illuminance on the eye, that captures the impact of sunlight as well as the interdependence between the fabric color, overall brightness, and the apparent intensity of the visible sun.

A collection of papers with recent discussion and findings on visual comfort and daylight discomfort glare can be summarized in Tzempelikos (2017).

2.3.1.3 Building and façade Configuration

Facade orientation affects the magnitude and distribution of daylight, and thus affecting visual comfort and preference. Studies focusing on human behaviors in buildings on northern hemisphere agree that the number of shading operations is lowest on north façade and highest on south façade (Foster and Oreszczyn 2001; Inkarojrit 2008; Eilers et al. 1996; Mahdavi et al. 2008; Rubin et al. 1978; Zhang and Barrett 2012), as the north façade receives the least daylight and south façade receives the most. The east and west façades, however, have most solar penetration depth in the morning and afternoon, respectively, and thus significant diurnal patterns were found in the human-shading interaction for those orientations (Inoue et al. 1988). Despite these correlations, studies suggested that the effects from façade orientation could be accounted for by the related interior factors such as solar angles or solar radiation (O'Brien et al. 2012; Haldi and Robinson 2010a; Rea 1984).

Office layout and interior design can have a profound influence over comfort (Day et al. 2012). Occupants' positions and view directions were found to be significant factors in glare studies (Jakubiec and Reinhart 2012; Heerwagen and Diamond 1992; Osterhaus 2005). Other studies (Galasiu and Veitch 2006) reported the importance of room dimensions and furniture positioning for preventing discomfort such as glare and draughts. The effects of glazing color on visual preference and human interaction with electric lights were studied by Arsenault et al. (2012) through simulation and experiment.

2.3.1.4 Outdoor Conditions (Weather)

Weather conditions outside are one of the early target of visual preference studies, but still the effects are ambiguous. While Rubin (1978) found that blind position seemed to be independent of sky conditions such as sunny, cloudy, and hazy, Rea (1984) showed that blind occlusion was significantly different with different sky conditions. Seasonal effects have been also studied by other researchers. Mahdavi et al. (2008) conducted a survey study on three office buildings, and found that cooling season resulted in 30% higher shade deployment than the heating season, due to higher solar radiation on the facade during cooling season. Zhang and Barrett (2012) found occupants inactive of operating shading even with substantial change in solar radiation and

illuminance. Haldi and Robinson (2010a) reported that the effects of seasonal changes are mixed with other physical variables, such as indoor temperature or daylight levels.

2.3.1.5 Connection to Outside, View and Privacy

Other factors directly associated with visual satisfaction are connection to the outdoors and the desire for privacy as one of the main design purposes of windows is to provide a clear view and physical connection to the outside (Reinhart and Wienold 2011), while shading devices could serve for privacy considerations but obstruct outside view.

The quality of view is one of the subjective factors associated with psychological sciences and mainly includes preferred outside scenes. Studies (Inoue et al. 1988; Aries et al. 2010) found that more attractive window views compromised discomfort, but this effect can be reversed for occupants close to unshaded windows. Tuaycharoen and Tregenza (2007) concluded that perceived discomfort glare was lower with satisfaction for “interesting” outside scenes. Similar findings, relating the type of view through the window with the perception of glare (Shin et al. 2012) or job stress and well-being (Leather et al. 1998) or health recovery (Raanaas et al. 2012), have been reported. Konis (2013) noted that despite the presence of visual discomfort, the occupants in the perimeter zones left a portion of the window unshaded for most of the time to maintain connection to the outdoor. Researchers (Inkarojrit 2005; Zhang and Barrett 2012; Mahdavi et al. 2008) have acknowledged that the view to the outside as a possible factor for triggering shading actions, but there is no conclusive finding because of the interferences from other variables. Wienold (2007) concluded that future studies should be focused on investigating occupants’ preferences towards connection to the outdoors.

Objective considerations such as the amount of view and view clarity are more important in urban areas, where there is limited flexibility in choosing the most desired outdoor scenery. Building rating systems (USGBC 2009) offer credits for outdoor views. The amount of view outside is usually quantified by the relative size of openings compared to opaque walls. Galasiu and Veitch (2006) suggested wider window with optimal height of 1.8 – 2.4 m, although window size will vary for different office settings. On the other hand, few studies focused on view clarity through windows with shading devices. Aston and Belichambers (1969) defined view clarity as a metric of sense of satisfaction, whereas Boyce (1977) defined it as the level of something being “visually distinct and clear”. Early studies associated clarity with distinctness of detail (Yonemura

and Kohayakawa 1976) or considered the visual clarity of an illuminated scene to be highly correlated with the specific spectral concentration of light sources (Thornton and Chen 1978). Tzempelikos (2008) presented a detailed method for calculating the projected outside view for venetian blinds as a function of rotation angle, taking into account edge effects and slat thickness. Konstantzos et al. (2015) first developed detailed metric View Clarity Index (VCI) quantifying view clarity with only shade openness factor and visible transmittance with experimental data.

Rubin, et al. (1978) first introduced the concept of privacy by stating that the view to the other office buildings can conflict with the preference to maintain a private indoor space. Later on, Inkarojrit (2005) reported that around 12% of occupants close blinds to maintain privacy. Similarly, Reinhart and Voss (2003) suggested that desire of privacy could be the main consideration if blinds were lowered at ambient horizontal illuminance less than 1000 lux.

2.3.1.6 Natural Light (Daylight) and Electric Light

Perception of daylight can also be another important factor influencing occupants' visual preference and the interactions with shading and electric lighting systems. Cuttle (1983) conducted a survey study with 471 subjects and 86% of the responses preferred daylighting as lighting source to electric lighting. Survey study by Heerwagen and Heerwagen (1986) revealed that occupants widely believe daylight is crucial for their general health and work environment. Veitch et al. (1993) confirmed that people prefer daylight to artificial lighting for working. Veitch and Gifford (1996) found similar results with a strong belief of the superiority of natural light. On the other hand, experimental study by Wells (1965) showed that people perceived considerable amount of daylight even when most of the illumination was provided by electric lighting, and he concluded that the perception of natural light is independent of the actual visual environment.

2.3.1.7 Other Factors

Although early studies focusing on occupant behavior modeling found that thermal perception (temperature, solar radiation, etc.) could be a substantial factor affecting interactions with shading systems (Lindsay and Littlefair 1992; Foster and Oreszczyn 2001; Mahdavi et al. 2008; Inoue et al. 1988; Inkarojrit 2005; Sutter et al. 2006; Zhang and Barrett 2012), it remains unclear if there is a link between thermal perception with visual preference.

The occupation dynamics was reported to be significant for visual preference in several studies (Haldi and Robinson 2010a; da Silva et al. 2013; O'Brien and Gunay 2014; Sadeghi et al. 2016), where occupants were found to be sensitive to arrival and intermediate occupation period, and different models were developed for different periods, respectively.

Additionally, in the last 3 years, focused research studies showed that perceived control, control access, interface and user preference with daylighting and electric lighting systems are inter-related and complex (Galasiu and Veitch 2006; Sadeghi et al. 2016). da Silva et al. (2013) found inconsistency between occupants' override patterns and existing behavioral models when shading and lighting control was deployed in experimental study. Field studies have shown general preference or improved satisfaction of occupants with the "sense" of controlled environment (Meerbeek et al. 2014; de Korte et al. 2015). Langevin et al. (2012) performed detailed statistical analysis and showed significant correlations between variables of thermal comfort and perceived control and stated that occupants' awareness and understanding of controls highly affect satisfaction and comfort. Several studies found that the type of control system, access to override and control frequency (Bakker et al. 2014), and the availability of expressive interface and feedback (Yılmaz et al. 2015; Meerbeek et al. 2016) are some of the parameters playing a significant role in occupants' preference and satisfaction, in offices equipped with automatic shading and lighting systems, but the detailed relationships remain to be investigated. O'Brien and Gunay in their review study (2014) summarized observational studies including contextual factors affecting occupant comfort and behavior, and most of the categorized factors are related to perception of control and control system design, which are availability and accessibility of personal control, complexity and transparency of automation systems, presence of alternate comfort delivering systems and visibility of energy use.

Finally, the physiological characteristics and psychological factors (e.g. mood) are important factors, but due to the difficulty of measuring or characterizing these states with existing techniques, there is no study that systematically considers them in learning visual preference/satisfaction.

2.3.2 Modeling Occupant Interactions with Shading and Lighting Systems

Conventionally, manual shading and lighting controls are applied in most buildings, either using ropes/chains or wall/remote switches. Even in buildings equipped with automatic shading

and lighting systems, occupant overrides on the automatic control are often observed and reported. Therefore, occupant interactions with shading and lighting systems were the main objectives for studies related to building simulation and operation. Occupant-shading and lighting interaction models have been developed with significant differences in the selection of variables and model formulation and structures.

Different environmental parameters were investigated with various duration of observations from several days to years to evaluate their impact on occupant behavior with respect to operating shades and their feasibility of prediction as discussed in previous sessions. Previous studies showed that manual shading could be driven by changes of work plane illuminance (Rea 1984; Reinhart and Voss 2003), luminance (Inkarojrit 2008), glare indices (Lee and Selkowitz 1994; Wienold et al. 2011), solar radiation (Foster and Oreszczyn 2001; Lindsay and Littlefair 1992; Zhang and Birru 2012), temperature (Nicol and Humphreys 2004), and other factors (Van den Wymelenberg 2012). In some studies (da Silva et al. 2013; Reinhart 2004), observations include both shading and lighting interactions.

Deterministic models are used in studies of early researchers (Newsham 1994; Lee and Selkowitz 1994; Goller et al. 1998) and most of current application to predict occupants' behaviors. Reinhart (2004) developed a dynamic model simulating manual blind operation based on the assumption that blinds are fully closed when direct solar radiation on façade is above 50 W/m^2 and solar projection falls on the work plane, and are fully re-opened at the beginning of working day. Several researchers in Japan and Germany (Inoue et al. 1988; Reinhart and Voss 2003) drew similar conclusion that shade position has strong relation with solar penetration depth when incident solar radiation on façade exceeds 50 W/m^2 . Several observational studies have shown that these models failed in predicting the observed occupant behaviors (Inkarojrit and Paliaga 2004; Inkarojrit 2005; Sutter et al. 2006; Zhang and Barrett 2012; da Silva 2013), as occupants' behaviors, although dependent on a set of physical features, are governed by a stochastic process instead of deterministic relationship (Nicol 2001).

Therefore, stochastic models have been developed to estimate human-building interactions by characterizing the randomness of occupant behaviors with probabilistic relationship (Haldi and Robinson 2010b; Fabi et al. 2015). Linear regression models were proposed by researchers (Foster and Oreszczyn 2001; Mahdavi et al. 2008; Van den Wymelenberg 2012), but linear models are not able to capture the upper and the lower bounds of the observations (Haldi and Robinson 2009;

Haldi and Robinson 2010a; Haldi and Robinson 2011) when distribution of variables are not Normal. Generalized linear models (e.g. logistic regression or probit), on the other hand, are more flexible in such cases. Most researchers (Inoue et al. 1988; Rea 1984; Nicol 2001; Clarke et al. 2006; Haldi and Robinson 2008; Inkarojrit 2008; Haldi and Robinson 2009; Haldi and Robinson 2010a; Zhang and Barrett 2012; da Silva 2013; Sadeghi et al. 2016; Gunay et al. 2017) suggested that logistic regression models are appropriate for estimating the probability of human-building interactions with respect to particular predictor variable(s). Different modeling formulation techniques such as Bernoulli process (Haldi and Robinson 2008), discrete-time Markov chain (Haldi and Robinson 2009), and survival analysis (Reinhart 2004; Haldi and Robinson 2008; Haldi and Robinson 2009) have been used in these studies. Modeling human behavior was also embedded in adaptive shading and/or lighting control in several studies (Guilemin and Molteni 2001; Gunay et al. 2014a; Gunay et al. 2017).

Most of these studies, however, are limited in terms of either input variables or prediction outcomes. Haldi et al. (2009) and Inkarojrit (2008) built models correlating multiple environmental variables with binary shading status (fully closed or fully open) although intermediate shading positions are important (Sadeghi et al. 2016). More models were developed (Haldi and Robinson 2010; Sutter et al. 2006) trying to explain the probability of shades movement with single variable. Recently, machine learning methods, statistical data-driven modeling methods such as maximum likelihood estimation, have been used to develop probabilistic models of interactions to overcome the limitations of traditional regression models (Inoue et al. 1988; Rea 1984; Haldi and Robinson 2010 A; da Silva 2013; Inkarojrit 2008; Zhang and Barrett 2012; Zarkadis et al. 2015), but it typically results in point estimates of the parameters without consideration of epistemic uncertainty induced by the limited data (epistemic uncertainty). Sadeghi et al. (2017) used Bayesian modeling approach, a novel probabilistic method capable of modeling epistemic uncertainty, to model occupant interaction with shading and lighting system with experimental data.

2.3.3 Modeling Visual Preferences and Satisfaction

Existing studies related to visual comfort have focused on predicting visual discomfort in daylight spaces by evaluating and suggesting visual discomfort metrics, mainly including daylight discomfort glare in perimeter offices with complex fenestration systems and variations in luminance patterns within the field of view (Van Den Wymelenberg and Inanici 2014; Karlsen et

al. 2015; Wienold and Christoffersen 2006; Van Den Wymelenberg 2014; Jakubiec and Reinhard 2016; Konstantzos et al. 2015; Hirning et al. 2014; Jakubiec and Reinhart 2012; Konis 2014; Borisuit et al. 2010; Suk et al. 2017; Kent et al. 2017). However, preventing occupants from glare does not necessarily lead to satisfaction with the visual environment or achievement of optimal visual conditions. As a matter of fact, dissatisfaction with the visual environment, especially in daylit offices, could still exist even if specific criteria are met (Reinhart and Voss 2003; Lee et al. 2013). Carter et al. (1999) reported that manually controllable lighting fixtures which do not even meet the lighting standards were perceived more satisfactory than the daylight linked automated lighting controls.

On the other hand, although modeling human-shading and lighting interactions is useful for applications in building simulation models, behavioral models could be unreliable or inapplicable for the purpose of discovering preference profiles with overall visual environment, since human actions could be the combined results of many uncertain factors other than discomfort or dissatisfaction (Gunay et al. 2014b; Wang et al. 2016; Yan et al. 2015). The key assumption of action-based preference models that an action or override is triggered by dissatisfaction or the condition after action is preferred than the condition before it might be untenable for many cases. Recent studies (Gunay et al. 2014a; Gunay et al. 2014b; Yan et al. 2015; Tahmasebi and Mahdavi 2017; Wang et al. 2016) reported general issues and limitations associated with the development of occupant behavior models in terms of their reliability, applicability and generalizability. Clevenger and Haymaker (2006) found the energy consumptions differed more than 150% considering the uncertainty of occupant behavior model. Gilani et al. (2016) highlighted the limitations of existing models predicting occupant-blinds interactions and associated impacts on occupant perception of view and connection to outdoors, by simulation study comparing conventional and stochastic modeling approaches.

In spite of intensive studies on visual discomfort (glare) and studies on modeling human interaction with shading and lighting systems, few studies directly aimed at visual preferences and satisfaction. Galasiu and Veitch (2006) in the literature review paper tried to summarize studies investigating occupant satisfaction and preference related to the visual environment, but all the reviewed studies were still focusing on glare indices or behavior-oriented. A few studies focused on occupant's preference toward electric lighting system, starting from simple statistical analysis on survey data (Hedge et al. 1995), to clustering and classification modeling with experimental

data (Despenic et al. 2017). Hua et al. (2011) investigated the daylighting design of a single building and the resulting occupant visual satisfaction, but the study outcome is still statistical analysis instead of modeling as the study aimed at evaluation of design. Sadeghi et al. (2018) firstly modeled occupant visual preference in daylit offices with experimental data using Bayesian approach, but the study focused on brightness preference only.

2.3.4 Visual Preferences Learning

In most studies on visual preferences learning mentioned in previous sections, actions are the most common feedback as monitoring human behavior or interactions with daylighting and lighting systems is straightforward and non-intrusive. However, there are two main issues with action-based visual preference learning. First, collecting enough action data usually requires more acquisition efforts as occupant actions are hardly predictable and controllable, and the frequency of actions varies among different occupants and with different environments (resulting in overall longer collection period), especially with manual shading and lighting systems or limited automatic control (Rea 1984; Inoue 1988; Lindsay and Littlefair 1993; Foster and Oreszczy 2001; Inkarojrit 2005 and 2008; Sutter et al. 2006; Haldi and Robinson 2010; Zhang and Barrett 2012; da Silva et al. 2014; Sadeghi et al. 2016). Second, actions are generally triggered by visual discomfort (glare) or comprehensive effects of multiple uncertain or random factors (Lindelof and Morel, 2008; Gunay et al., 2014; Wang et al., 2016; Yan et al., 2015), so the learned model based purely on actions would have overfitting or bias problems and high uncertainty beyond the boundary region of comfort and discomfort (especially in the standard comfort zone), and thus would fail to reflect the true preference. Visual preference learning based on actions easily results in behavioral modeling, which could not be directly used in control design and implementation as discussed previously.

Other studies tried to actively learn occupant preferences and utilize surveys to query ranking or scoring data for modeling the visual satisfaction utility function that motives preference (Sadeghi et al. 2016; Despenic et al. 2017; Konis and Annavaram 2017). User-friendly interfaces can be used as survey tools to extract some of the unknown information and rationale behind actions or dissatisfaction with visual conditions (Sadeghi et al. 2017; Sadeghi et al. 2018; Despenic et al. 2017; Konis and Annavaram 2017). However, asking humans to rate with a scale has some built-in problems (i) scales could vary with different individuals and (ii) human evaluation is

affected by drift, where the scale varies with time, and anchoring, where early experiences weigh higher (Payne et al. 1993; Siegel and Castellon 1981). Instead, studies have argued that relative (or comparative) preferences are often more accurate than absolute ratings (Kingsley 2006; Lockhead 2004; Conitzer 2007).

2.4 Shading and Lighting Controls

Researches, designs and products focusing on automated shading control attracted more and more attentions in recent years. While studies of manual shading control focus mainly on investigating occupant behavior, studies of automated shading control try to optimize energy performance or occupant comfort.

2.4.1 Shading Control

There are basically three types of automated shading control (closed loop, open loop and model-based). The first method utilizes feedback sensor signal (illuminance, radiation and/or temperature, etc.) to move shades based on certain threshold. The second control tracks the sun (solar angles – altitude, zenith and incident, etc.) according to a time-based solar model and controls shades position to avoid direct sunlight falling on the task area. The last control method takes sensor readings as model inputs, simulates desired parameters in model and adjust shading devices based on model outputs. The last type of control will be discussed in detail in section 2.4.3. Automatic shading control usually requires higher cost related to devices and control operation compared to manual shading control, while it has great potential of energy efficiency and comfort improvement. Several studies (Van Moeseke et al. 2007; Tzempelikos and Athienitis 2007; Nielsen et al. 2011; Shen and Tzempelikos 2012; Grynning 2014) have proved the effectiveness of automatic shading control strategies concerning energy efficiency or visual comfort.

Many studies have proposed control strategies for roller shades with threshold of certain variable, which could be modeled or measured by sensor. Measured incident or transmitted direct solar radiation were utilized by a few researchers (Shen and Tzempelikos 2012) and transmitted beam radiation of 94.5W/m^2 was selected by Lee and Selkowitz (2006) as the threshold to close shades completely. Other studies (Newsham 1994; Wilson et al. 2000; Van Moeseke et al. 2007; Wankanapona and Mistrickb 2011) chose incident total irradiation readings or indoor temperature measurement as the reference of actuating shades movement and there was no agreement of a

general threshold. Wankanapon and Mistrick (2011) performed comparative study on three different set points of incident solar radiation on façade (95 W/m^2 , 189 W/m^2 , and 400 W/m^2) for different orientations and climate zones with different shades. Tzempelikos and Shen (2013) compared control strategies based on different criteria and concluded that illuminance threshold is better than radiation and different strategies should be applied based on orientation and climate. In addition, they developed a control algorithm utilizing solar position as the first criterion and transmitted illuminance as the second one, and finally considering closing shades completely when solar heat gain is high in cooling season. Zhang and Lam (2011) used transmitted illuminance as the threshold with an outdoor temperature sensor distinguishing heating demand from cooling demand. For venetian blinds, solar angles are usually taken into account since blinds are controlled by rotating slats. “Cut-off” angle is introduced as the angle of slats at which direct lights are prevented, which can be calculated based by solar angles and blind geometry (Athienitis and Tzempelikos 2002), and Zhang and Birru (2012) employed it in open-loop blind control. Automated shading controls aiming to prevent glare using glare indices have been developed and studied in the last decade (Van Moeseke et al. 2007; Nielsen et al. 2011; Shen and Tzempelikos 2017; Chan and Tzempelikos 2013; Koo et al. 2010; Din and Kim 2014). In several cases, integrated shading and lighting control operation was studied to account for parallel energy use considerations (Park et al. 2011; Tzempelikos and Shen 2013; Wienold 2007; Yao 2014; Yun et al. 2014; Oh et al. 2012; Xiong and Tzempelikos 2016; Shen et al. 2014; Grynning et al. 2014; Inoue et al. 1988; Wienold et al. 2011), as summarized in a recent review (Jain and Garg 2018). Some previous studies considered only binary shading positions – fully open or fully closed, which limited the development of advanced control using complex algorithms developed in recent years. Modern control theories were combined in automated shading control allowing continuous shading operation (Shen and Tzempelikos 2013, 2017). Some studies presented shading control strategies based on genetic and fuzzy logic for both roller shades control (Lah 2006) and blinds control (Čongradac et al. 2012) to provide desired work plane illuminance from daylighting. The objective was achieved well but the conflict of better genetic rules and tuning difficulty remained a limitation. Hu and Olbina (2011) developed blind control algorithms based on an artificial neural network (ANN) daylighting model, which is trained offline by data from EnergyPlus simulation results. Due to ANN’s linear characteristic, the simulation speed of the model is fast. Guillemin and Molteni (2002) added occupant preferences as inputs into genetic algorithm (GA) to control blinds

providing user-defined daylighting. Control efficiency, application feasibility and other issues in latest automatic shading control still remain unresolved.

2.4.2 Electric Lighting Control

Electric lighting control can also be divided to two types – manual control and automatic control. Manual lighting control is proved to be ineffective in many studies concerning energy efficiency. Reinhart and Voss (2003) found that lights were switched on at the beginning of working hours and seldom turned off until the end of the day, even when indoor illuminance was very high.

Similar to automated shading control, electric lighting can also be controlled based on a sensor signal directly. The two main types of sensor-based lighting controls are occupancy sensor-based and photometer-based controls. Occupancy sensors save energy by automatically turning off lights when the occupant is absent and turn them on once detecting occupant presence. Nagy et al. (2015) applied adaptive control for variable occupancy sensor time delay for further energy savings. However, most studies of occupancy sensor-based control focus on sensor development. Photosensor-based control usually adopts closed-loop lighting control to adjust target illuminance levels which the sensor measures directly or reflects through model. Previous studies (Lee and Selkowitz 1994) have proved that photometer-based lighting control system could benefit in energy conservation. Significant work on this topic has been recently published by Shen et al. (2014).

Early studies of electric lighting control focused on on/off control due to the limit of devices, before dimmable lights allowed more complex continuous control. However, Galasiu et al. (2004) showed that both on/off and dimming control can reduce energy consumption by 50% - 60%. Other studies have also quantified and proved the energy benefits of on/off control and dimmable lighting systems (Lee and Selkowitz 1994; Vartiainen 2001; Tzempelikos and Athienitis 2005, 2007; Tzempelikos 2010; Shen and Tzempelikos 2012). Recent studies also consider separate control for every single lamp or even fixture to achieve even lighting distribution, but it requires accurate commissioning work.

2.4.3 Model-based Control

Model-based control (MBC) is a method of process control relying on the process model. It is widely used in motion control, aerospace, and automotive applications, and becomes an emerging technology in building automation. Model-based control takes input information from measurements, predictions or estimations, and manual settings, and processes them in a built-in real-time model with simulated control variables reflecting real environment and exports corresponding control actions or signals to achieve desired system behavior. It is well established in studies where model-based control technology has a great potential of application – in building automation regarding energy efficiency and indoor environment comfort. Most previous studies focused on model-based controls applied to HVAC system or IAQ control in office buildings and have showed the benefits of energy efficiency and comfort improvement (Lu et al. 2011; Morosan et al. 2010; Gruber et al. 2014a; Gruber et al. 2014b; Kolokotsa et al. 2005), as well as the flexibility in various applications from a single objective to large scale indoor environment in office buildings (Pr ívara et al. 2011).

Model predictive control (MPC) was derived from model-based control using prediction by optimizing a finite time-horizon. Hazyuk et al. (2012a; 2012b) combined occupancy schedule with MPC for temperature control in heating season and showed 30% -40% energy conservation. Goyal et al. (2013) and Oldewurtel et al. (2013) both compared model-based control with predicted and measured occupancy information in office HVAC system. They found that MBC with measurements inputs alone could provide 50% energy conservation, while predicted MPC could only provide small improvements compared to MBC.

However, few studies directly associated model-based control theory with shading and lighting controls. Fischer et al. (2012) utilized an accurate illumination model to control electric lights for different preferences at multiple locations. The model needs to be trained by measurements from light sensors located at every occupant seat. Although the model is trained offline and can be used for long term, it's not adaptive for any changes in electric lights or occupant locations. Mahdavi (2008) established a detailed daylight model to control blinds and lights. The daylight model takes inputs of outdoor daylight conditions measured by twelve illuminance sensors, and updates itself with furniture change via a location-sensing system. It outputs discrete dimming levels, blind angles and positions to optimize an objective function combining work plane illuminance, lighting energy consumption and cooling load with corresponding weights. The

model simulates real-time daylight conditions accurately but it requires an extensive sensor network and time-consuming calculations. Further, the objective function with simple weighting could not reflect real assessment concerning lighting task and energy conservation at the same time.

Le et al. (2014) applied machine learning algorithms with model-predictive control of shading devices to minimize cooling and lighting energy while providing daylight. Kim and Park (2012) employed model predictive control with an EnergyPlus model to determine the optimal blind slat angles within 24 hour concerning overall energy consumption using the Matlab optimization toolbox. The study compared developed MPC with static blinds and showed considerable energy savings. However, both the machine learning algorithm and the MPC optimization process increase the calculation load and lower the control response speed.

There are also studies utilizing model-based shading and lighting control aiming at both energy saving and improving visual comfort. Chaiwiwatworakul et al. (2009) developed a daylighting model (work plane illuminance) and glare model (DGI) for blinds and lighting control to minimize energy use while maintaining visual comfort. Annual simulation showed up to 80% energy savings compared to traditional control strategies. Oh et al. (2012) proposed a similar control strategy of optimizing energy performance with DGI below 22 and showed 24.6% energy saving. Xiong and Tzempelikos (2016) developed an integrated model-based shading and lighting control strategy to minimize lighting energy use while maintaining DGP below 0.35 with detailed daylighting, glare and lighting models, and validated the control with full-scale experiments. Shen and Tzempelikos (2017) developed simplified model-based shading control for reduced lighting energy use and satisfied visual comfort constraint, which could be generalized with different configurations of space, shading and glazing.

2.4.4 Optimal Control

Optimization algorithms are widely used in building studies, mainly in two directions – for building design and for building control. Optimal building design usually sets up an optimization problem to find the optimal set of design variables such as building orientation, construction materials and façade properties, etc. Various studies used optimization for façade design (Ouarghi and Krarti 2006; Tuhus-Dubrow and Krarti 2010; Bichiou and Krarti 2011; Chantrelle et al. 2011; Rapone and Saro 2012; Rakha and Nassar 2011; Asadi et al. 2012).

Optimal building control is the control method solving an optimization problem for optimal control decision for building components (HVAC system, shading and lighting system, etc.) with respect to the control objective(s) and constraints, such as energy consumption, thermal and/or visual comfort. Optimal shading and/or lighting controls aiming to minimize energy use with glare constraint have been studied and developed in recent years (Ochoa et al. 2012; Ferrara et al. 2018). Carlucci et al. (2015) reviewed potential visual comfort indices and their use in optimization, including aspects of light quantity, uniformity, quality and color. The study concluded that spatial and temporal indices are needed, flexible for use in design optimization, with adequate generality and longevity.

While traditionally comfort constraints were used when minimizing energy use in optimization efforts, previous studies have also considered comfort and energy use in multi-objective optimization (MOO) schemes, with different levels of complexity and formulation types. Multi-objective optimization is the optimization problem involving more than one objective function to be optimized simultaneously. MOO usually provides a set of non-dominated alternatives (Pareto front) instead of a deterministic solution.

Early related studies adopted MOO in optimal building design, especially for envelope design. Typical objectives combined with a measure of energy consumption and a measure related to human comfort were set in most studies (Wright 2002; Suga et al. 2010; Cassol et al. 2011; Ochoa et al. 2012; Han et al. 2013; Manzan and Padovan 2015; Futrell et al. 2015; Carlucci et al. 2015; Ferrara et al. 2018). Wang et al. (2005, 2006) presented a multi-objective optimization of life cycle cost and life cycle environmental impact, also using genetic algorithms, designing for the sets of optimal orientation, construction types, aspect ratio, window type, and window size. Feature of MOO that it provides multiple solutions suits well in optimal building design as it's natural to provide more than one design in real application.

Few studies, however, utilized MOO in optimal building control application, as control system requires deterministic decision. Hu and Cho (2014) used MOO as a support to device-scale operation for CCHP system, and decision was made with probabilistic model. These studies applying MOO tried to set weights for multiple objectives to reach unique optimal solution among Pareto front. However, one could argue that the rationale of constructing the optimization problem by choosing weights that arbitrarily connect energy and general comfort metrics is debatable (Nguyen et al. 2014). Villa and Labayrade (2013) applied MOO in real-time lighting control –

controlling the dimming levels of luminaires to minimize lighting power while maximizing the modeled satisfaction level, obtained from subjective data. In this way, relationships between visual preferences and energy impact can be identified, and constraints can be representative of actual preferred conditions. However, a single decision was still suggested among the Pareto front of MOO based on work plane illuminance standard. Ascione et al. (2016) developed a model-predictive temperature controller with MOO strategy targeting large-scale energy and thermal comfort control, and it is the first study allowing user as the final decision maker provided with the set of Pareto front.

2.5 Research Gaps and Aims of Dissertation

2.5.1 Research Gaps

In spite of the large amount of studies of visual environment in buildings, occupant visual comfort, and daylighting and lighting controls, the development of an ideal optimal shading and lighting control considering occupant visual satisfaction/preferences and energy use is a complex, challenging and long-term work. The challenges exist along with the compositions of designing a modern control system including variables and sensing, learning and modeling, as well as the control strategy and efficient implementation.

2.5.1.1 Variables affecting visual preference/satisfaction and Sensing Network

First, discovering and quantifying important variables affecting visual preference and satisfaction are challenging.

To date, limited and simple variables were usually considered when developing human interaction models with shading and lighting systems or visual preference/satisfaction models. For example, work plane illuminance is one of the most widely used variables (and the single variable considered for most cases) in existing models, which represents only part of the “brightness” information of occupant’s visual environment. As discussed in session 2.3.1, visual preferences depend on a variety of factors which could be environmental, contextual (e.g. illuminance, luminance, shading position and lighting level), psychological or subjective, and may be time-variant, especially when both work plane and vertical tasks (i.e., computer screens) are involved and daylighting systems can be dynamically controlled. Tasks of quantifying visual factors with variables, sensing and decoupling correlated variables are needed and difficult. Outside view, for

example, was verified as important visual factor by experimental or field studies with survey data, yet it is hard to quantify or represent outside view with simple variable as it includes both objective (amount of view and view clarity) and subjective (quality of view) effects. Only a few studies (Konstantzos et al. 2015; Sadeghi et al. 2017; Sadeghi et al. 2018) integrated outside view with quantitative variables in visual preference studies. Luminance images, on the other hand, have been widely used in glare studies but never utilized in visual preference researches despite their powerful ability of representing the whole visual field of occupant, mainly due to 1) lack of studies of advanced modeling approaches capable of processing all information of a luminance map for real-time control, 2) the limitation of camera measurement at or close to occupant's eye in practical applications. Also, most previous shading/lighting interaction or behavioral models were developed assuming manually-operated systems, which is different from automated operation. As discussed in the last part of section 2.3.1, the effects of “perceived” control of automatic shading and lighting systems and the characteristics of control system itself are potential factors affecting visual preference which need to be taken into account. Studies related to perceived visual environment are dominated by glare researches using partial information of luminance/illuminance and human behavioral model based on simple variable (illuminance), while quantitative modeling studies considering all possible factors affecting visual preference are needed.

In parallel, some of the visual factors are limited of accessibility in real application with sensing techniques. For example, photometric sensors are commonly used to measure illuminance on the work plane for closed-loop lighting control to achieve certain light set-point, but to deploy illuminance sensors directly on work plane is not realistic for several reasons – 1) any selection of sensor location is somehow arbitrary and debatable for representing the lighting condition of the whole work area; 2) at least one sensor is required for each point of interest (e.g. occupant or desk) in the control system; 3) measurement could be obstructed by items nearby; 4) the sensor itself could bring inconvenience or be disturbing to occupant, etc.. Existing applications of such lighting control requiring feedback of work plane illuminance usually deploy illuminance sensor above occupants (e.g. on the ceiling) and commission the sensor for corresponding work plane light measurement with regression model, which at the same time causes some other issues such as commissioning accuracy and extra maintenance effort. Luminance in the field of view of the occupant cannot be easily measured in a practical way (without disturbing the person) even with the newest, small-size HDR (High Dynamic Range) cameras.

In addition, sensing infrastructure related to visual environment has a large potential of improvement: the cost of sensing network is a practical consideration while most lighting-related sensors are expensive comparing to thermal sensing devices (e.g. temperature sensors); more operation efforts are also required such as high performance DAQ system and wireless communication capability. In fact, the development of an integrated and low-cost lighting and daylighting (wireless) sensing network based on different types of related sensors for measuring the perceived visual environment of occupants is an open research topic.

Another option to address some of the above sensing issues is to use advanced and detailed daylighting and lighting models and corresponding model-based control by simulating indoor illuminance or luminance distribution with less or no indoor sensors. However, there are also limitations using model-based control. First, compromise decisions between accuracy and efficiency must be carefully considered in terms of modeling structure, parameters and computational efforts. Most existing daylighting and lighting simulation tools employing daylight factor or radiosity methods might not be accurate enough when detailed prediction involving human occupants is needed. Radiance software, as introduced in section 2.2.2, is capable of detailed and accurate daylighting prediction with proper settings, but the backward ray-tracing simulation algorithm could be too computationally expensive to be used in real-time control with relatively short interval (e.g. 30 min), even much efforts were made for reducing the computation cost. The hybrid ray-tracing and radiosity method described in section 2.2.1.3 is a potential modeling algorithm that could be used in model-based control, and was validated in experimental study (Xiong and Tzempelikos 2016) using reduced number of exterior sensors as inputs, although the model is still limited in application as it requires comprehensive building information as model parameters and expert understanding for transferable use between different spaces. Other options of image-based simulation have been recently proposed (Zhao et al. 2018).

For the variables that are hardly accessible with either sensors or physical models by existing techniques, modeling approaches that are able to deal with hidden variables and the corresponding uncertainty could be effective solutions.

2.5.1.2 Learning and Modeling Visual Preference and Satisfaction

Visual discomfort vs. visual preference/satisfaction

Existing studies which claimed to aim at visual comfort have actually focused on visual discomfort (glare) or associating indoor light levels (mostly illuminance) with human behavior, and few studies directly aimed at occupant overall visual preferences or satisfaction, especially in the “standard” comfort range, considering not only brightness perception but also other essential factors. As discussed in section 2.3.3, achieving general visual comfort criterion does not necessarily result in high satisfaction level with the visual environment. Therefore, learning preference profiles with respect to overall visual conditions, without just considering discomfort scenarios, and implementing them in controls, is a better approach towards achieving optimal visual environments.

Personalized vs. generalized model

Occupant diversity in visual comfort and preferences has been observed and studied in experimental studies (Inkarojrit 2005; Haldi and Robinson 2010). However, similar to conventional thermal preference studies, most studies of visual comfort and preference focused on developing generalized model based on data from relatively large number of subjects (Sadeghi et al. 2017; Despenic et al. 2017; Sadeghi et al. 2018). Although generalized visual preference models might be useful for some cases, they are not suitable to be implemented in shading and lighting controls in either office buildings or residential buildings because of the following reasons: 1) generalized model might not be really “generalizable” when space configurations and controls are changed, 2) generalized model could not accurately predict the visual preferences of individual occupants even the data from the individual contribute to the model, especially for application in private offices and residential buildings, and 3) control based on generalized model built for open plan office with multiple occupants might not satisfy most of the occupants due to individual differences in visual preference and the nature of generalization – compromise, so other methods are required to predict the probability of conflict in user preferences (Chraibi et al. 2016; Despenic et al. 2017) or to “aggregate” multiple preferences. For private offices, personalized visual preference profiles related to shading/lighting operation are useful, considering a generic set of physical and human variables, as well as quantified implications on energy use.

Modeling approaches

Based on all above discussion, an ideal modeling approach for learning visual preference and satisfaction, should 1) be able to consider multiple variables and automatically identify and select the important ones from them, 2) have the flexibility of evolving according to any change in preference based on new data (data-driven), 3) be able to incorporate and quantify the effects of unmeasured/hidden variables, 4) be able to link and predict relative preference and satisfaction level, 5) be able to predict uncertainty due to hidden variables and/or limited data, etc.

Bayesian models serve these purposes well (Jaynes 2003; S. Guo et al. 2010). Furthermore, Bayesian approaches automatically incorporate epistemic uncertainty in an intuitive and natural way (Chu and Ghahramani 2005). These advantages allow for addressing decision-making problems in a principled manner: to combine existing knowledge (prior beliefs) with additional knowledge that is derived from new data at hand (likelihood function), resulting in our prior knowledge (beliefs) being updated to new knowledge (posterior beliefs), following Bayes rule. These posterior beliefs can then be used as priors in future analyses, providing learning chains in science (Eric et al. 2008; Kuikka et al. 2014). The spread associated with the inferred posterior distribution quantifies the uncertainty associated with the sampling distribution. Moreover, auto-selecting techniques such as automatic relevance determination (ARD) could be used for variable identification by introducing and tuning hyper-parameter along Bayesian inference. With these inherent advantages, we can develop flexible probabilistic models and investigate relationships between variables and models.

Three studies implemented Bayesian inference models in the visual preferences field to this date. Lindelöf and Morel (2008) applied a Bayesian formalism to infer the probability of occupants considering horizontal illuminance distributions as uncomfortable. Although still based on human interactions, this was the first study that used this approach, and the authors discuss the issues of including more variables, challenges related to implementation in adaptive controls, and balancing visual comfort and energy use. Sadeghi et al. (2017) developed a Bayesian model of human interaction with shading and lighting systems with multi-variables using experimental data. More recently, Sadeghi et al. (2018) predicted generalized occupant visual preferences in perimeter offices using a large data set, considering environmental and human variables, and determined the optimal number of clusters of occupants with similar visual preference characteristics. Mixtures of clustered models could then be used to derive personal preferences. A

new method for developing personal visual satisfaction profiles in daylit offices through Bayesian inference is presented in Chapter 3.

Online learning and model updating

Most previous modeling works on occupant preferences were developed based on occupant actions, which may not reflect actual occupant satisfaction, as discussed in section 2.3.3. As aptly stated by Lindelof and Morel (2008), “it makes sense for a controller to learn from the desired effects of the occupants’ actions, not necessarily from the actions themselves”. Also, the frequency of actions is unpredictable or low with specific control configuration, which could lead to inefficient learning. Asking for preference/satisfaction, on the other hand, is straight-forward with less uncertainty introduced during learning process, yet mostly adopted in studies of visual discomfort, acquired by survey. The main difference between these two learning objects is that behavior could be monitored through observing the changes of operative devices, while satisfaction level or preference vote needs to be asked or reported, which could be a concern of disturbing occupants in real settings. Moreover, asking for satisfaction ranking and preference vote are different, as discussed in section 2.3.4 – satisfaction rating introduces more uncertainty or bias than relative preference vote. To use occupant action for learning preference, proper discriminative data acquisition methods or advanced modeling approaches need to be utilized to (i) translate actions into true preference or (ii) to eliminate the effects of drives of action other than preference. Also, to directly query preference votes or satisfaction levels, the preference survey or other preference acquisition interface (also a part of the sensing network) should be carefully designed, and efficient learning techniques could be exploited to reduce the data requirement and the possible ensuing disturbances; integrating both means in the learning process with proper considerations of implementation would be ideal. Nevertheless, efficient methods for acquiring occupant’s true preference/satisfaction need further research.

Previous studies have shown the effectiveness and efficiency of building control strategies utilizing adaptive occupant preference models (Guillemin and Molteni 2002; Gunay et al. 2014; Gunay et al. 2017; Guillemin and Morel 2001; Haldi and Robinson 2010). Lee et al. (2019) proposed a novel HVAC control algorithm that enables self-tuning optimized temperature control with adaptive personalized thermal preference profile.

However, studies on occupant visual preferences are still isolated from incorporating preference learning into the real building operation process. There exist three major gaps. 1)

Developing the preference models in most researches requires intrusive and/or high-cost sensing network, which might not be practical in application. 2) Typical preference learning process demands sufficient and reliable data from occupant feedback either in a short period or from a long learning term. Short-term learning requires intensive interactions with occupants, which is disturbing. On the other hand, occupant dissatisfaction could arise if the learning process takes a long time, when an accurate and reliable preference model has not been developed or trained due to limited data, and the “optimal” control based on the model fails to achieve satisfying condition. 3) Human preference is dynamic so a robust preference model needs to be updated continuously to adapt itself to (possibly) changing preference (Jazizadeh et al. 2014; Daum et al. 2011; Zhao et al. 2014; Ghahramani et al. 2015).

Moreover, learning efficiency is a core concern when embedding model learning in a control system. For daylighting and lighting control systems, this is especially essential as many variables could be involved (ideally), and acquiring visual preference data is quite difficult so that learning data is limited. In preference learning, the idea of active learning, by choosing the compared pairs in order to learn preference with minimal preference queries, was proposed for improving learning efficiency. Specifically, for learning visual preference, active learning could be achieved by initiatively controlling the visual environment to form designed condition pairs to trigger preference. As pointed out in the last part of section 2.3.4, learning preferences by observing occupant actions or by asking preference both have limitations, but preference query suits the active learning framework better as it ensures preference data from each pair of compared visual conditions, while action is relatively a less-frequent event and may happen because of several reasons.

Therefore, an online visual preference learning method needs to be designed to actively acquire data efficiently in relatively short time with minimum disturbances to occupants. The concept of sequential learning in decision theory and utility theory, which uses the updated information after each learning step to determine the next step, could allow us to achieve this goal based on preference estimates or predictions. More specifically, (automated) preference elicitation in this field has brought increased interest and been applied to preference learning in recent years (Dyer 1972; White et al. 1984; Salo and Hamalainen 2001; Chajewska et al. 1998, 2000; Boutilier 2002; Birlutiu et al. 2013; Hernández-Lobato et al. 2014; Farrugia et al. 2015; Wang and Jegelka 2017; Gonzalez et al. 2017; Tee et al. 2017; Chapelle and Li 2011; Takahashi and Morimura 2015;

Radlinski and Joachims 2005), which aims at gaining sufficient preference information of a user through an appropriate sequence of queries or interactions to make a good or optimal decision.

The core design problem of the preference elicitation is to determine which preference query to ask during the learning process, and is dependent on the objectives of the decision making system. Three major criteria of query selection technique are the regret/cost (Wang and Boutilier 2003; Patrascu et al. 2005; Boutilier et al. 2004; Boutilier et al. 2003 and 2005), the uncertainty of preference or utility profile, and the expected value of information gain. More preference elicitation methods are reviewed in detail in Chapter 4.

The above learning strategy could be embedded in the control system operation as learning phase. Meanwhile, as discussed in previous sections, human preference is a dynamic and uncertain object to model due to human nature that tends to change and numerous hidden or uncertain factors, and thus any adaptive control system needs to integrate model updating and real-time learning within the control flow. That is, model updating is needed in the control phase. Practical considerations of model updating during control include: 1) update frequency/interval, 2) selection of data for model updating: usually the newest data with a fixed time horizon are selected to update the model so the length of the time horizon needs to be justified, 3) acquisition of new preference data and discrimination of valid data: passive observation of occupant action or initiative report from occupant might be more realistic for application than querying preference vote in the control phase, and preference-related action needs to be distinguished and translated into true preference.

2.5.1.3 Optimal Shading and Lighting Control Considering Visual Preference and Energy Use

Increasing visual satisfaction (or ensuring comfort) and reducing energy consumption (for lighting or lighting and HVAC) have been the general two objectives of daylighting and lighting control designs, and most studies constructed optimization problem for optimal control with the two objectives in different ways.

Optimal, personalized shading and lighting control

There are mainly two forms of optimal control integrating both satisfaction/comfort and energy objectives, both in a single-objective optimization scheme. The first one proposes or utilizes some kind of visual comfort threshold or range as constraint for optimizing the lighting energy use. The visual comfort threshold/range could be simply the standard light level (e.g. work plane illuminance) requirement, solar angle-related parameters (e.g. penetration length), limits of

developed visual comfort models or limits of glare indices (e.g. DGP) based on glare models. This formation of optimization treats visual comfort as the priority by setting it as constraint to satisfy before optimizing, which could be debatable for personalization consideration, and the limitation that satisfying visual comfort criterion does not equal to satisfaction still remains. The second formation tends to combine multiple objectives into one by constructing a “cost function” with weighted satisfaction and energy based on quantitative models. However, any fixed weighting between the two objectives is arbitrary and debatable as discussed in section 2.4.4.

Multi-objective optimization, on the other hand, could be an ideal algorithm for integrated both objectives in daylighting and lighting control, especially when personalized visual satisfaction/preference model takes the place of comfort constraint, and the relative relationships between visual preferences and energy impact should be identified and incorporated in the control process. MOO could provide multiple alternate “optimal” solutions (Pareto front) at each control step, which conflicts with conventional control application that requires deterministic control option. Therefore, most control-related studies adopting MOO picked one solution from Pareto front by setting fixed weight to avoid the conflict, which actually turned it back into single-objective optimization and did not take full advantage of MOO. In fact, the charm of MOO is exactly the multiple options it provides, and such decision of selecting could be handed over to user (occupant) since a controller can hardly deal with, which in turns fulfills another level of “personalized control” besides utilizing personalized visual satisfaction models. Utilizing MOO in this way will for sure require extra efforts in designing the control system (e.g. interface) as it involves distinctive interaction with occupants compared to existing control systems.

Realistically, to achieve optimal, personalized shading and lighting control we need to consider: (i) occupant satisfaction with the visual environment as one objective, adequately quantified, and (ii) energy minimization as another, provided that unique “optimal” solutions are not obtained by assigning arbitrary weights.

Shading and lighting control in multi-occupant spaces

In most buildings with automatic shading and lighting systems, spaces with multiple occupants (e.g. open plan offices) are usually controlled as groups. For the shading and lighting control system in such spaces, considering different preferences from multiple occupants is a difficult task to achieve high visual satisfaction of all occupants. Preference aggregation has been the topic aiming at such task, but mainly toward thermal comfort and HVAC control studies

(Jazizadeh et al. 2014; Sarkar et al. 2016; Li et al. 2017), proposing simple strategies such as summing and overlapping. More advanced preference aggregation methods are proposed in recent years for general algorithm development (Chen et al. 2013; Volkovs and Zemel 2012; Peters and Ketter 2013), but further studies related to application of advanced preference aggregation algorithm with shading and lighting control are required, and the rationale behind aggregating preferences should be carefully considered.

Applications

Although various application issues are discussed in previous sections, there are many other topics and issues related to applying optimal shading and lighting control considering visual preference and energy use.

First, the learning phase is necessary for personalized control to establish a personalized visual preference model for individual occupants; the learning efficiency needs to be validated with experiments when active sequential learning strategies are adopted to learn faster with less data, so that the learning phase is short and not disturbing to occupants. Also, during the learning, the variable and model structure selection are strongly dependent on the computational capability and the size of data that are available and accessible. More variables and more flexible model structure are always preferred when data is sufficiently large and controller is computationally powerful (e.g. cloud-based computing). With limited computing ability and data, modeling needs to sacrifice accuracy for efficiency. This trade-off exists and differs for different applications, buildings configurations, control and sensing systems, so it will be an enduring issue.

Next, human-machine interaction has become the emphasis of application studies or designs, especially when smart systems are involved. Traditional shading and lighting control systems have limited interaction with occupants except for switches or simple interfaces, while advanced control systems should have friendly, easy-to-use, well-designed user-interfaces (UI) which provide control (override) access for occupants, embedded sensing capability (e.g. preference query) and proper feedback to occupants such as energy consumption indication and suggestions, or even could enable AI-human interaction. All these are related to product development but still could start being tested in an experimental study.

Last but not least, shading and lighting control systems integrating sensing, learning, modeling, optimization, control and interface components would have different intervals for different components, which leads to integrating issues and needs consideration in actual

application. Learning, optimization and control intervals are the major parameters need to be determined, so that intervals of other components could be chosen accordingly – sensing to learning, modeling to optimization, and interface to control. Short learning interval is disturbing to occupants, while longer learning interval might lead to false preference vote due to ambiguous memory, especially for the cases when outdoor weather is fluctuating. Similarly, a short control interval is disturbing while the daylighting system might not be able to response to changing visual environment promptly with long control interval. Learning and control intervals, at the same time, should be consistent (not necessarily same) as preference is learned with controlled environment (although with a different strategy) if active learning is applied and the control is based on the learned preference to achieve satisfying visual condition. Optimization interval is more complex as it could involve different (daylighting and lighting, preference and satisfaction) models with different requirements for simulation interval, and the models might read inputs from sensing system with another interval. Decision on optimization interval should be made considering all the involved intervals (at least greater than or equal to the largest one), and also the intervals of learning and control. Setting all the intervals the same might not be a feasible solution due to possible conflicts of computing efficiency, hardware driving and communication issues in real application.

2.5.2 Aims of Dissertation

Based on above discussion, the aims of this Dissertation are:

- To develop a modeling method for learning occupants' personalized visual preference and satisfaction profiles in daylit offices using Bayesian approach;
- To develop and implement an adaptive online learning strategy for efficient visual preference learning;
- To develop a personalized daylighting (shading) control framework aiming at optimizing occupant satisfaction and lighting energy use in daylit offices.

3. A BAYESIAN APPROACH FOR INFERRING PERSONALIZED VISUAL PREFERENCE AND SATISFACTION IN DAYLIT OFFICES

3.1 Overview

This chapter presents a novel method for developing personalized visual satisfaction profiles in daylit offices using Bayesian inference. Unlike previous studies based on action data, a set of experiments with human subjects was designed and conducted to collect comparative visual preference data (by changing visual conditions) in identical, single-occupancy private offices. A probit model structure was adopted to connect the comparative preference with a latent satisfaction utility model, assumed in the form of a parametrized Gaussian bell function. The distinct visual satisfaction models were then inferred using Bayesian approach with preference data. The posterior estimations of model parameters, and inferred satisfaction utility functions were investigated and compared, with results reflecting the different overall visual preference characteristics discovered for each person.

In this dissertation, visual satisfaction and preference are two related but distinct concepts. Visual satisfaction is defined as the magnitude (or level) of satisfaction with the perceived visual environment for an individual; while visual preference refers to a relative attitude towards two (or more than two) different visual conditions by comparing them. Using this definition, the visual satisfaction level could be modeled as a utility function $u(\mathbf{x})$, where \mathbf{x} is a vector of variables describing the physical visual condition (state), and preference is a result of comparing the utility values corresponding to two (or more) conditions, which could be quantified by either deterministic or probabilistic link function. The relationship between these two concepts is illustrated in following figure.

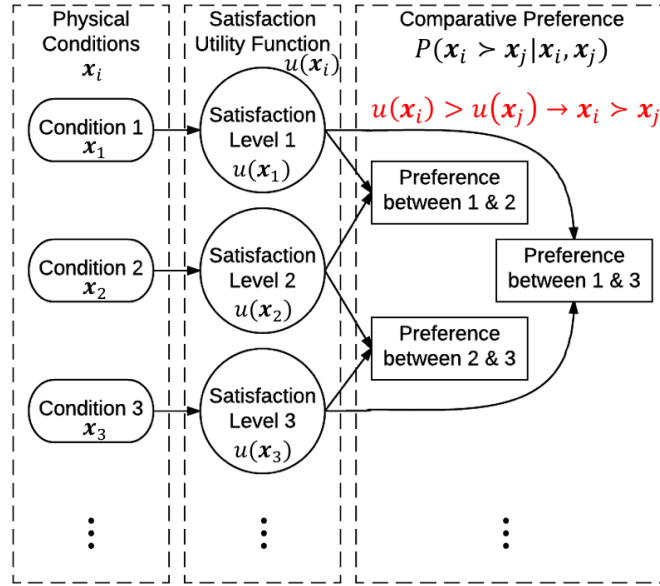


Figure 4 Relationship between visual satisfaction and comparative visual preference.

The statement that one visual condition is preferred to another can be expressed as an inequality relation $u(\mathbf{q}) > u(\mathbf{r})$, where \mathbf{q} and \mathbf{r} are two vectors of variables defining these two visual conditions (states), and $u(\cdot)$ defines the underlying (hidden) satisfaction utility function (Chu & Ghahramani 2005). This approach of defining a satisfaction utility function for preference learning is intuitive and easy to implement, but it is often very difficult to define a meaningful utility function (Keeney 1974; Marler and Arora 2004). One approach for creating the utility function is the algorithmic preference learning (Braziunas 2006). In our case, the preference learning process requires two parts: (i) acquiring comparative visual preference data from occupants and (ii) learning the response surface of the satisfaction utility function from the comparative preferences. For the first part, comparative visual preference data were obtained from specially designed experiments with human subjects. The preference data was then used to infer the visual satisfaction utility functions as posteriors through a Bayesian approach, and the inferred utility was sampled using a Sequential Monte Carlo algorithm.

3.2 Experiment Design for Acquiring Comparative Visual Preference Data

3.2.1 Experiment Design and Setup

Following the principles of preference learning, a set of experiments for studying personalized visual preference profiles was designed and conducted in identical private offices of the Center for High Performance Buildings at Purdue University in West Lafayette, Indiana. The offices are 3.3 m × 3.7m × 3.2 m high and have a south-facing curtain wall facade with 55% vision area (window-to-wall ratio) with high performance glazing units (normal visible transmittance=70%). The offices are equipped with motorized roller shades (openness factor=2.1%) and dimmable electric lights (32-W T5 fluorescent lamps), as well as with a comprehensive indoor environment sensing system, used in similar studies to investigating the impact of façade design and control strategies on occupant comfort and satisfaction. A Building Management System using the Niagara software framework is able to monitor and control the shading and electric lighting systems independently in each office using BACnet. In addition, the sensors measuring environmental variables are connected to data acquisition and control systems, which communicate wirelessly to the Niagara system through Modbus protocol. Figure 5 shows the office layout with respective instrumentation. Our experiment included continuous measurements of the following variables:

- Shade position (0-100%) and light dimming levels (0-100%), monitored and controlled through the main control system. The shades moved to different positions, as explained below, to acquire comparative preference data. Since our approach is focused on visual preferences, and not on inadequate light levels or potential glare conditions that may cause dissatisfaction for obvious reasons (and not of interest in this study), we made sure that both of these cases are excluded from the experiments as follows.
 - To avoid inadequate light levels, electric lights were automatically controlled to provide 300 lux on the work plane (IESNA 2012) in all cases when daylight was insufficient.
 - To avoid potential glare conditions:
 - The experiment was conducted with carefully adjusting scheduling to avoid having the sun in the field of view, even though the shades have a relatively low openness factor and recent metrics can quantify the perception of glare in such cases (Konstantzos and Tzempelikos 2017)

- All cases with vertical (eye) illuminance higher than 2760 lux were excluded from the analysis. This has been proved a sufficient discomfort glare criterion in the absence of sunlight and high contrast (Chan et al. 2015; Konstantzos et al. 2015; Wienold 2009), also based on recent experimental studies with human subjects (Konstantzos and Tzempelikos 2017)
- To ensure that the aforementioned restriction was adequate to eliminate all potential instances of glare, an additional validation check was obtained directly through surveys; perceptible glare was reported in very few instances and these were removed from the dataset.
- Work plane illuminance, vertical (eye) illuminance and transmitted illuminance through the window. Calibrated LI-COR 210 photometric sensors were used for illuminance measurements. The work plane illuminance sensor was placed in the working area facing upwards. The vertical illuminance sensor was mounted on a camera adjacent to the occupant's head (15 cm away) to capture representative values without obstructing the work area. The amount of transmitted light through the window was measured with a sensor vertically mounted on the inside of the glazing, facing outside.
- Luminance distribution in the field of view. A calibrated HDR camera, mounted next to the person's head, was used to measure the luminance field every 10 minutes (aligned with the survey response times), following the details described in Konstantzos and Tzempelikos (2017). These measurements were processed to obtain the luminance ratio of average screen luminance to average window luminance. More specifically, images were taken with nine exposures and were merged into HDR format using a calibrated response function with HDRgen (Ward 2017). The images were then processed in Radiance by creating mask files for the window area and the screen area, and finally used in Evalglare software (Wienold 2012) to compute average luminance of window and screen area, as well as DGP and average luminance of the visual field.

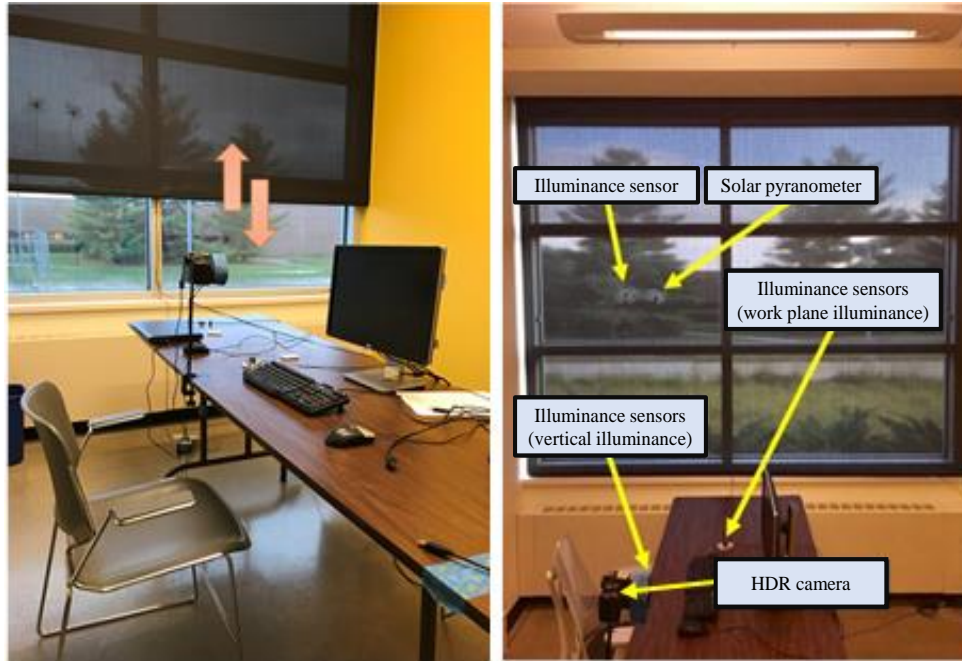


Figure 5 Office space layout and part of instrumentation.

The experiments were conducted from November 2016 - March 2017, under various sky conditions (sunny, cloudy and mixed). Four subjects participated in the experiment, spending 5 hours per day in the office (each subject was assigned to one office space) doing normal computer work (their own work). Note that this experiment was designed to obtain personalized preferences of studied individuals by comparing different visual conditions, and not to propose a “reference” general model. In that scope (*demonstration of the method and creating the personalized models*), the number of subjects did not need to be large, unlike studies that estimate general visual or thermal preferences (or actions) using a large number of subjects. The subjects were graduate students and staff (between 20 and 40 years old) not familiar with this research and were advised to avoid any direct contact with the monitoring instrumentation. Approval by the Institutional Review Board (IRB Protocol #: 1507016229) was obtained before conducting the experiments.

To obtain comparative preference data required for preference learning algorithms, shading positions were adjusted every 10 minutes during the experimental study (in different positions in each office, without following a specific pattern, but making sure that excessive illuminance levels and potential glare conditions are avoided as explained above); therefore, the indoor visual environment changed every 10 minutes. The 10-minute interval was selected to prevent memory fading, which was reported in a pilot study we conducted with time intervals equal or longer than

15 minutes. Five minutes after the change, allowing for adaptation, the subjects were asked to complete a short web survey (shown in Appendix A) while all required variables (illuminances, HDR images, shading and light dimming status) were simultaneously recorded and stored. The main question was about their overall visual preference between the two conditions, before and after the change (*prefer current condition; prefer previous condition; no preference*). These questions are pairwise comparison queries which are known to have low cognitive load (Chajewska et al. 2000), and in our case they provide an ideal data structure for formulating visual preference learning models that will lead to personalized preference profiles. Other questions were targeted at comparative illuminance levels or view preferences, as well as intended actions (moving shades or controlling electric lights), providing extra information and used as response reliability checks.

3.2.2 Experimental Data Analysis and Important Variables

Several variables (and their combinations) were considered to characterize the visual conditions in the room as perceived by the subjects: horizontal (work plane) illuminance, vertical (eye) illuminance, transmitted illuminance through the window, shading position and luminance ratio.

- Vertical illuminance (E_v) represents the amount of light perceived by the occupants, resulting from the luminance field, and is a critical variable. It also contains the combined effects of outside conditions and shading position. Since the subjects focused on vertical (computer) tasks, E_v is considered more important than horizontal illuminance, which could be an alternate variable. In addition, the horizontal illuminance distribution was not as uniform across its range as compared to E_v (Figure 6), and its value might change over the task area depending on the room/desk layout. Therefore, E_v was selected as a variable instead of horizontal illuminance.
- Transmitted illuminance (E_t) through the window is a useful variable since it provides information about the sky conditions. However, it cannot indicate the perception of visual environment from the occupants' point of view; therefore, it was used as an indicator variable (binary classifier) instead of a variable in the utility function. The E_t threshold can be inferred given a prior and a reasonable distribution, just like the other variables; in our study, a constant threshold (9000 lux) was selected to separate sunny and cloudy days since

it was in good agreement with observed conditions and can simplify the demonstration of the method.

- Shading position (SP) certainly affects the perception of the visual environment and is related to the amount of outside view (approximately proportional to the solid angle from the subject to the outside view), therefore it is one of the main variables.
- Finally, the luminance ratio (LR) –ratio of average window luminance to average screen luminance, extracted from HDR images- is an indicator of the brightness contrast between the daylight source and the target area in the field of view, so it was also considered as a variable.

All in all, based on the collected data from human subjects and their discovered effects on visual satisfaction, E_v , SP and LR were considered as significant variables (and used in the models) while E_t was used as a binary classifier to account for the impact of outside weather conditions. This framework proved to be sufficient for learning and predicting personalized visual preference profiles, as shown in the results and analysis sections.

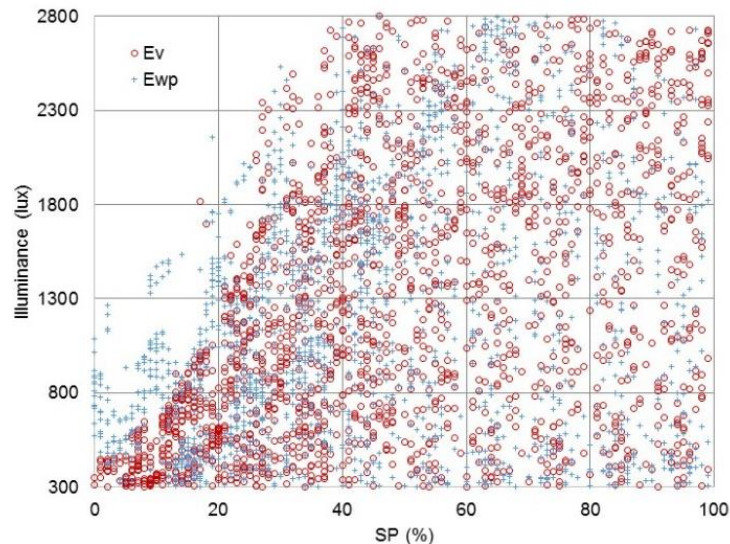


Figure 6 Distribution of vertical and horizontal illuminance across all shading positions and variable sky conditions.

Before the model training stage, the data was pre-processed and normalized to create homogeneous variable distributions (in terms of ranges and limits), convenient for efficiently facilitating the visual satisfaction inference process. The E_v data was transformed to $\log E_v$ to scatter

the data points more uniformly across its range – Figure 7 shows the respective scatter plots between variables. The data ($\text{Log}E_v$, SP , LR) were normalized in the range of $[-2, 2]$ by:

$$x_{norm} = -2 + 4 \cdot \frac{x - \min(x)}{\max(x) - \min(x)} \quad (30)$$

For visualization and analysis of the results, the data are converted back to the original scale (E_v , SP , LR) for easier evaluation.

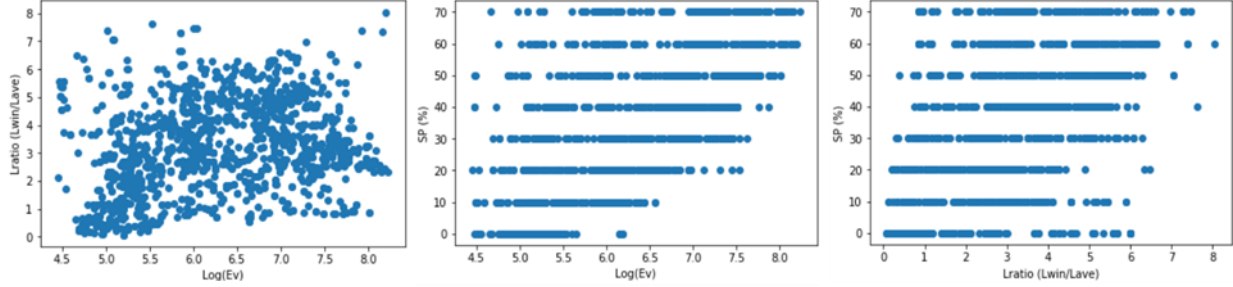


Figure 7 Scatter plots between E_v , SP and LR experimental data.

Let $\mathbf{q}, \mathbf{r} \in \mathbb{R}^d$ denote two visual conditions of the room, each of which is defined by d features (e.g. $\{E_v, SP, LR\}$, $d=3$). Assume that each subject (i) has experienced $N^{(i)}$ pairs of such conditions and reported the preferred ones. Then the data set consists of the ranked pairs (comparative preference):

$$\mathcal{D}^{(i)} = \{\mathbf{q}_k^{(i)} > \mathbf{r}_k^{(i)}; k = 1, \dots, N^{(i)}\}, i = 1, 2, 3, 4 \quad (31)$$

where $\mathbf{q}_k^{(i)} > \mathbf{r}_k^{(i)}$ denotes that the i^{th} subject prefers condition $\mathbf{q}_k^{(i)}$ over $\mathbf{r}_k^{(i)}$.

Figure 8 presents the experimental data from the four subjects in the $E_v - SP$ conditions space, as representative data visualization. The arrows start from the non-preferred conditions and point to the preferred conditions (“no preference” data were excluded from the graphs), while the different colors indicate different directions in that space. These vector plots essentially provide an intuitive visualization of the personalized satisfaction profile of each subject under variable conditions. For example, subjects 1 and 3 do not seem to prefer brighter conditions, while they prefer higher shading positions when E_v becomes quite low. Subject 4 prefers intermediate conditions in the $E_v - SP$ space, while subject 2 does not show any obvious pattern (and has less data displayed because of many “no preference” votes). Note that E_v and SP are correlated variables, and the slope of the arrows indicates the combined effects of these variables, as well as the *dominance* of one variable over the other as we move across the space. For example, the arrows tilt towards the vertical direction as E_v decreases, showing that SP becomes the dominant variable

at low vertical illuminance, and thus E_t can contribute as a binary classifier. Similar observations can be obtained from the data plotted in the $LR-E_v$ space.

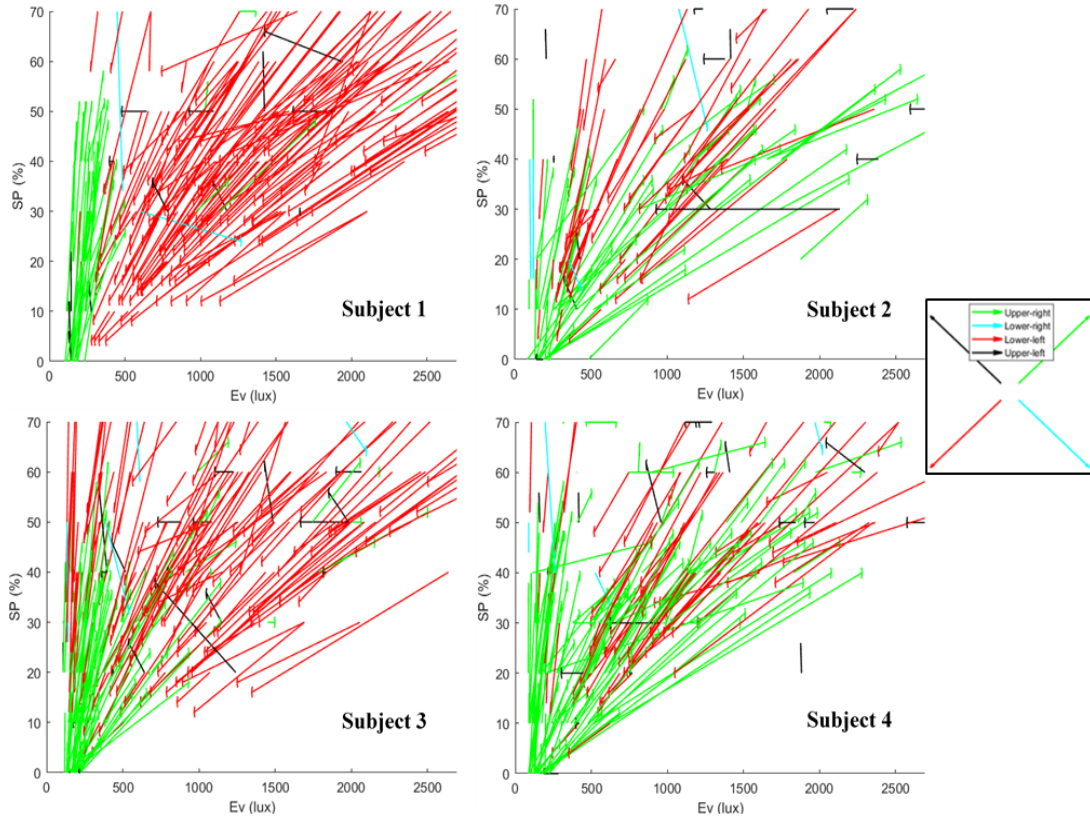


Figure 8 Experimental pairwise comparisons of overall visual preferences displayed over the Ev-SP space for each of the subjects.

3.3 Modeling Methodology

3.3.1 Problem Formulation

The scenario of learning personalized visual preferences is different from conventional supervised machine learning approaches in the sense that the training instances/features defining the state of the room are not assigned a single target (as in the case of regression or classification) (Chu and Ghahramani 2005). Instead, the training data consist of pairwise preferences between different visual conditions. The goal is to learn the underlying ordering over these states from the pairwise preferences. Bayesian parametric approaches are appropriate for preference learning due to their ability to encode prior beliefs; avoid overfitting; and explicitly capture uncertainty in occupants' latent satisfaction utility functions (Guo et al. 2010). This uncertainty is induced by the limited amount of data and can be exploited to sequentially design optimal experiments in the

future. The key hypothesis is that there is a latent (utility) function $u(\cdot)$ associated with each set of visual conditions, such that $\mathbf{q} > \mathbf{r}$ if $u(\mathbf{q}) > u(\mathbf{r})$ (that is, preserving the preference relations observed in the pairwise dataset (Chu and Ghahramani 2005)). Preferences and utility theory are briefly discussed in Appendix.

3.3.2 Probabilistic Utility-based Preference Model

In this problem of preference learning, the likelihood function is defined as the probability of observing one condition (state) being preferred over another, given that the utility function values for these two conditions are known. In other words, the likelihood models the deviation of an individual from the preference relation prescribed by $u(\cdot)$. Put simply, the probability of an occupant preferring visual condition \mathbf{q} over \mathbf{r} given their utility functions' values (Guo et al. 2010) is given as:

$$p(\mathbf{q} > \mathbf{r} | u(\mathbf{q}), u(\mathbf{r}), \sigma) = \Phi\left(\frac{u(\mathbf{q}) - u(\mathbf{r})}{\sqrt{2} \cdot \sigma}\right) \quad (32)$$

where $\Phi(\cdot)$ is the Normal cumulative distribution function (CDF), which serves the role of a sigmoid function: $\Phi(z) = \int_{-\infty}^z N(\gamma|0,1)d\gamma$, and σ is the variance of the normally distributed variable. The variance represents to what extent the preference is stochastic to the utility function if the scale of utility is fixed – the preference is more deterministic if σ is smaller, and vice versa. Therefore, the joint data-likelihood for occupant i over the ranked pairs data set $D^{(i)}$ is then given as:

$$p(D^{(i)} | u(\cdot)^{(i)}, \sigma^{(i)}) = \prod_{k=1}^{N^{(i)}} \Phi\left(\frac{u^{(i)}(\mathbf{q}_k) - u^{(i)}(\mathbf{r}_k)}{\sqrt{2} \cdot \sigma^{(i)}}\right) \quad (33)$$

In the next section, we discuss how we parameterize the utility function and how we learn the parameters using Bayesian inference.

3.3.3 Parameterizing the Utility Function

Based on the experimental findings and our intuitive understanding of the problem, we extracted the following assumptions about the utility function:

1. The utility function is continuous;
2. “Extreme” visual conditions (e.g., the corners of Figure 8 space) are not preferred by individuals;

3. There exists a single condition, or, more correctly, a set of neighboring conditions that are most preferred, which reflects that the utility function has an area of global maximum with a shape of a peak.

By the above assumptions, and given the fact that the utility corresponding to the underlying preference relations is not unique but it is arbitrary up to a monotonically increasing transformation, we adopted the following Gaussian bell form for the utility function:

$$u(\mathbf{x}; \boldsymbol{\mu}, \boldsymbol{\Sigma}) = \exp\left(-\frac{1}{2}(\mathbf{x} - \boldsymbol{\mu})^T \boldsymbol{\Sigma}^{-1}(\mathbf{x} - \boldsymbol{\mu})\right) \quad (34)$$

where \mathbf{x} are the model variables (d), $\boldsymbol{\mu}$ is a d -dimensional vector indicating the location of the peak (mostly preferred conditions), and $\boldsymbol{\Sigma}$ is a $d \times d$ positive definite matrix defining the shape of the function.

Based on the likelihood function and the assumed satisfaction utility function, we can obtain the posterior distribution (the learning objective) given the pairwise comparative training data \mathcal{D} by following Bayes' rule as:

$$p(\theta|\mathcal{D}) = \frac{p(\mathcal{D}|\theta)p(\theta)}{p(\mathcal{D})} \quad (35)$$

where parameters θ include $\boldsymbol{\mu}, \boldsymbol{\Sigma}$ and variance σ , $p(\theta)$ is the prior distribution of the parameters, and $p(\mathcal{D}|\theta)$ for each subject i , is essentially given as (u is determined by θ):

$$p(\mathcal{D}^{(i)}|\theta) = p(\mathcal{D}^{(i)}|u^{(i)}(\cdot, \theta), \sigma^{(i)}) \quad (36)$$

The prior on the mean vector $\boldsymbol{\mu}$ adopted is standard normal distribution for each element of $\boldsymbol{\mu}$, which is a weak prior assuming we have limited knowledge of the subjects. The priors on variance σ are selected as standard lognormal distribution to ensure positive estimation. The conjugate prior distribution for the matrix $\boldsymbol{\Sigma}$ is usually chosen as inverse-Wishart distribution (Kass and Natarajan 2006) for multivariate Gaussian-like functions, which means Wishart distribution for $\boldsymbol{\Sigma}^{-1}$, with degree of freedom equal to the dimension of variables d and identity scale matrix I_d , which again assumes lack of prior knowledge. The priors are summarized as followed:

$$\begin{aligned} p(\boldsymbol{\mu}) &\sim N(0, 1) \\ p(\boldsymbol{\Sigma}^{-1}) &\sim W_p(d, I_d) \\ p(\sigma) &\sim \text{Lognormal}(0, 1) \end{aligned}$$

Since the posterior of the parameters is not analytically available, sampling techniques, e.g. Markov Chain Monte Carlo (MCMC), must be used. Unfortunately, MCMC cannot estimate the

normalization constant $p(\mathcal{D}|\theta)$ robustly, which is essential for performing Bayesian model selection (Bishop 2006). To overcome this issue, the Sequential Monte Carlo (SMC) method is used. SMC defines one-parameter continuous family of probability densities that bridges the gap between the prior and the posterior. Then, it samples a set of weighted “particles” from the prior and adaptively propagates them to obtain a weighted particle approximation of the posterior. The intermediate weights can be used to obtain a robust estimate of the normalization constant of the posterior. Complete details on SMC methods are described in Doucet et al. (2001).

SMC implementation in pySMC (Bilionis 2014) requires specification of several parameters (number of particles, number of MCMC steps per SMC move, threshold below which sampling is triggered and reduction rate which controls how fast the family is traversed). Table 2 lists the SMC settings that provided consistent results in multiple tries with reasonable training times in our case.

Table 2 SMC settings used for sampling and posterior distribution approximation.

| Step method | Random Walk Metropolis algorithm |
|--|----------------------------------|
| Number of particles | 2000 |
| Number of MCMC steps | 50 |
| Effective sample size reduction rate | 0.9 |
| The threshold of the effective sample size | 0.5 |

Mathematically, SMC results in a weighted particle approximation $\{(\theta_j, w_j); j = 1, \dots, H\}$ of the posterior:

$$p(\theta|\mathcal{D}) \cong \sum_{j=1}^H w_j \cdot \delta(\theta - \theta_j) \quad (37)$$

where $\delta(\cdot)$ is Dirac’s delta function. Equation above should be interpreted in the sense that, for any smooth function $f(\theta)$, almost surely as $H \rightarrow \infty$, we have:

$$\sum_{j=1}^H w_j \cdot f(\theta_j) \rightarrow \int f(\theta) \cdot p(\theta|\mathcal{D}) d\theta \quad (38)$$

In particular, the predictive preference probability of our model can be approximated as:

$$p(\mathbf{q} > \mathbf{r}|\mathcal{D}) = \int p(\mathbf{q} > \mathbf{r}|\theta) \cdot p(\theta|\mathcal{D}) d\theta \cong \sum_{j=1}^H w_j \cdot p(\mathbf{q} > \mathbf{r}|\theta_j) \quad (39)$$

Above equation can be used to estimate the prediction accuracy of the models as discussed in section 3.4.2.

3.4 Results and Discussion

The SMC method approximates the posterior distributions of $\theta = (\boldsymbol{\mu}, \boldsymbol{\Sigma}, \sigma)$, with 2000 particles (samples). These results were used to compute the median of the posterior of $\boldsymbol{\mu}$ and $\boldsymbol{\Sigma}$, which define the posterior median of the satisfaction utility function for each of the subjects, as well as the median of the posterior of σ , which captures the random deviations from the preference relation encoded in the utility. The significant variables (E_v , SP and LR) and their combinations were investigated in this process, to evaluate how each model performs for each subject (the data indicate different personalized visual satisfaction profiles). Shading position (SP) was not considered as a single variable since it does not contain enough information about the visual environment. In addition, transmitted illuminance, E_t , was considered as a binary classifier to account for the effect of bright vs cloudy sky conditions, which plays an indirect but noticeable role in overall visual satisfaction.

From the experimental data (mixed arrow directions in Figure 8), it was clear that subject 2 did not show a preference towards any specific visual conditions, while most survey results indicated no preference among a variety of different conditions. Therefore, this subject was insensitive to changes in the visual environment, at least with the current dataset, and therefore it was not included in the following results (satisfaction utility plots are flat).

3.4.1 Posterior of (Mean) Visual Satisfaction Utility Function

The following figures present the personalized visual satisfaction utility functions. 10 final models were developed and trained for each subject. These include: (i) single-variable models (E_v and LR), models with two variables (E_v - SP and LR - SP) and a model with all three variables. Each model was developed for sunny and cloudy conditions separately as explained above.

To present consistent plots, the utility function and the σ were normalized by two steps, making the scale from 0 to 1:

$$\left\{ \begin{array}{l} u_i = \frac{u_i - \min u_i}{\max u_i - \min u_i}, \quad \sigma_i = \frac{\sigma_i}{\max u_i - \min u_i} \\ \tilde{u} = \text{median}(u_i), \quad \tilde{\sigma} = \text{median}(\sigma_i) \\ \tilde{u} = \frac{\tilde{u} - \min \tilde{u}}{\max \tilde{u} - \min \tilde{u}}, \quad \tilde{\sigma} = \frac{\tilde{\sigma}}{\max \tilde{u} - \min \tilde{u}} \end{array} \right\} \quad (40)$$

where $i = 1, \dots, 2000$ is the particle number. The first step of particle-wise normalization aims to eliminate the effect of floating values of utility inherited from the nature of learning from comparative preference – the scale of utility is arbitrarily changed without affecting the comparative results – so that taking the median of utility functions would be the true median over all the posterior particles. The scale from 0 to 1 of utility is then ensured by the second step of normalization. As a result, the randomness of preference to the utility could be comparable through comparing the normalized variance σ – the lower the value of $\tilde{\sigma}$ is, the more deterministic the subject is to the corresponding utility. Note that the variance does not determine the best model representing the subject's preference.

Figure 9 shows the posterior median of the satisfaction utility functions for the single variable models. All subjects have varying satisfaction with E_v while, in general, subject 1 seems to prefer darker conditions, subject 3 prefers medium brightness, and subject 4 prefers brighter conditions. Although Subject 4 shows preferences toward the bright range, these are all within visual comfort limits of 2760 lux in terms of E_v (Chan et al. 2015, Konstantzos et al. 2015, Wienold 2009) and 1:10 in terms of luminance between the visual task and near surfaces (Osterhaus 2008), as a result of the design of the experiment aiming at eliminating discomfort instances. Naturally, individuals have different tolerances and preferences towards brighter conditions. Similar patterns are observed for the *LR* utility functions. The effect of outside conditions is more pronounced for subject 4 with these models. The single-variable models cannot provide information on the combined effects of other variables on visual satisfaction (i.e., someone might be more sensitive to one variable versus another).

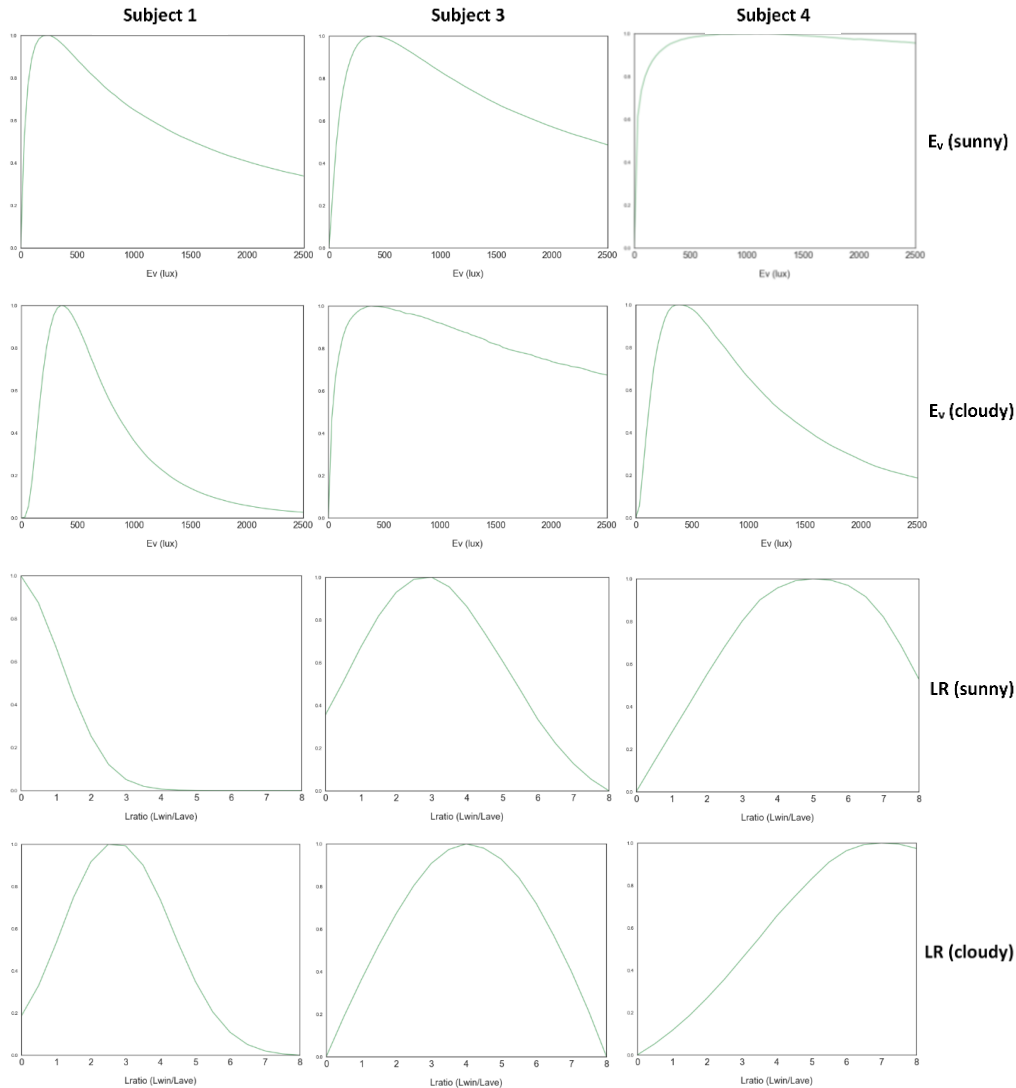


Figure 9 Posterior median of visual satisfaction utility functions of single-variable models (E_v and LR) for each subject.

Although the posterior medians of the utility functions are displayed over the entire conditions' space, the function values are meaningless where there are no data points –even if the inferred models discover low utility values in those regions. For example, there are no data for very low SP and very high E_v (it is physically impossible) as can be seen from Figure 8. To identify such cases in the utility plots, the actual data points are marked with red dots for the two and three-variable model functions.

The posterior median of satisfaction utility plots with the two-variable models are shown in Figure 10. In this case, the effects of outside conditions are clear and justify the development of

different models for bright and cloudy sky conditions. Lower E_v values are again preferred by subjects 1 and 3, while on cloudy days the effect of SP becomes more important (distinct preference for high or medium SP respectively). Subject 4 clearly prefers higher SP and also higher illuminance levels on sunny days. The LR - SP utility plots show the different preference profiles for sunny and cloudy days for each subject.

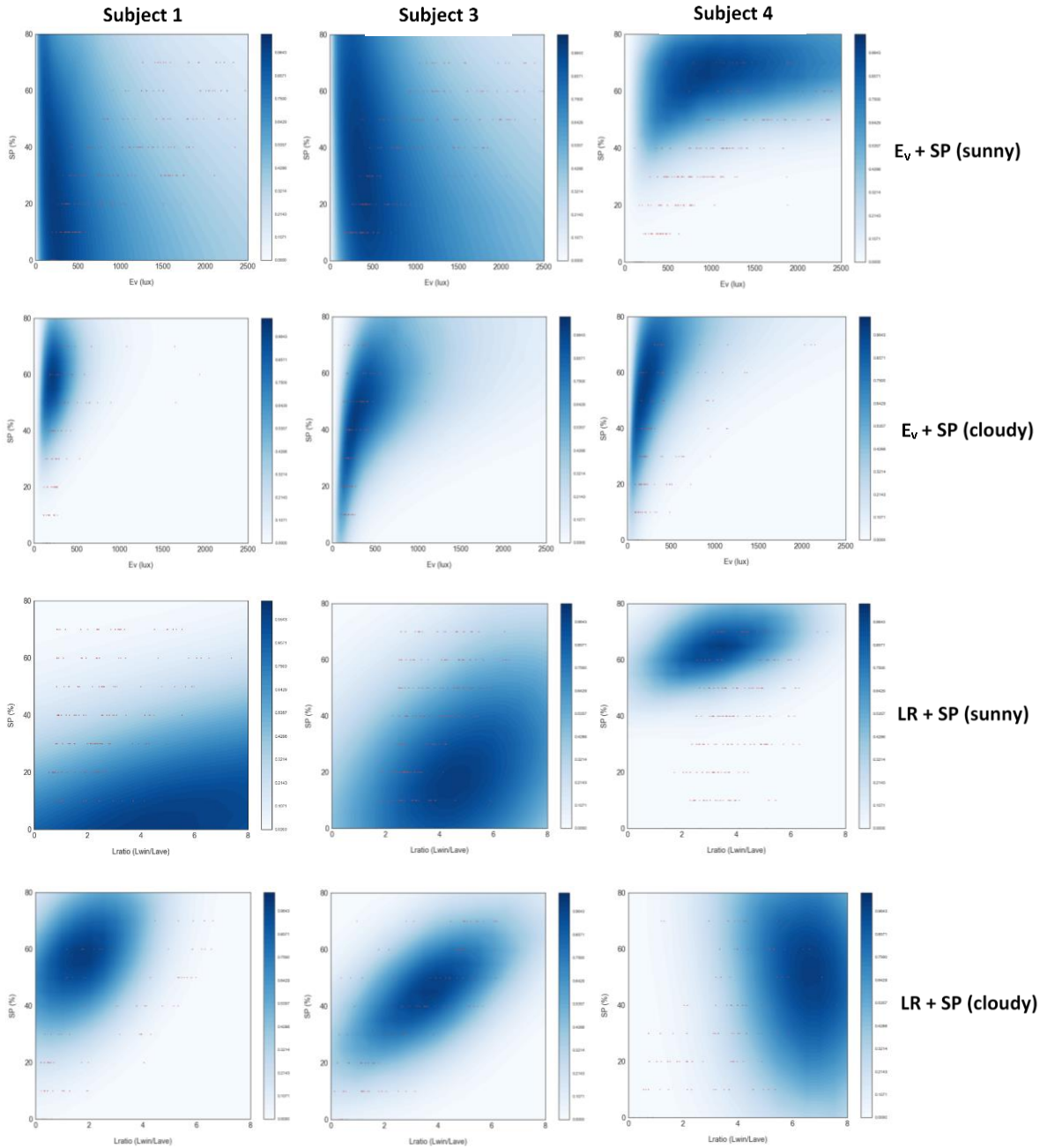


Figure 10 Posterior median of visual satisfaction utility functions of two-variable models (E_v - SP and LR - SP) for each subject.

Figure 11 shows the respective posterior median of satisfaction utility functions for the three-variable models. The graphs are displayed in the E_v - SP space with LR varying from 1 to 7 (top to bottom). These models combine the effects of all three variables. Subjects 1 and 3 are not sensitive to LR under sunny conditions using this model, while the effects of preferred E_v (and SP on cloudy days) are still there. The visual preference profile on subject 4, on the other hand, is affected by LR when all variables are considered, while higher SP is preferred on sunny days and lower E_v is preferred on cloudy days, in agreement with the two-variable model.

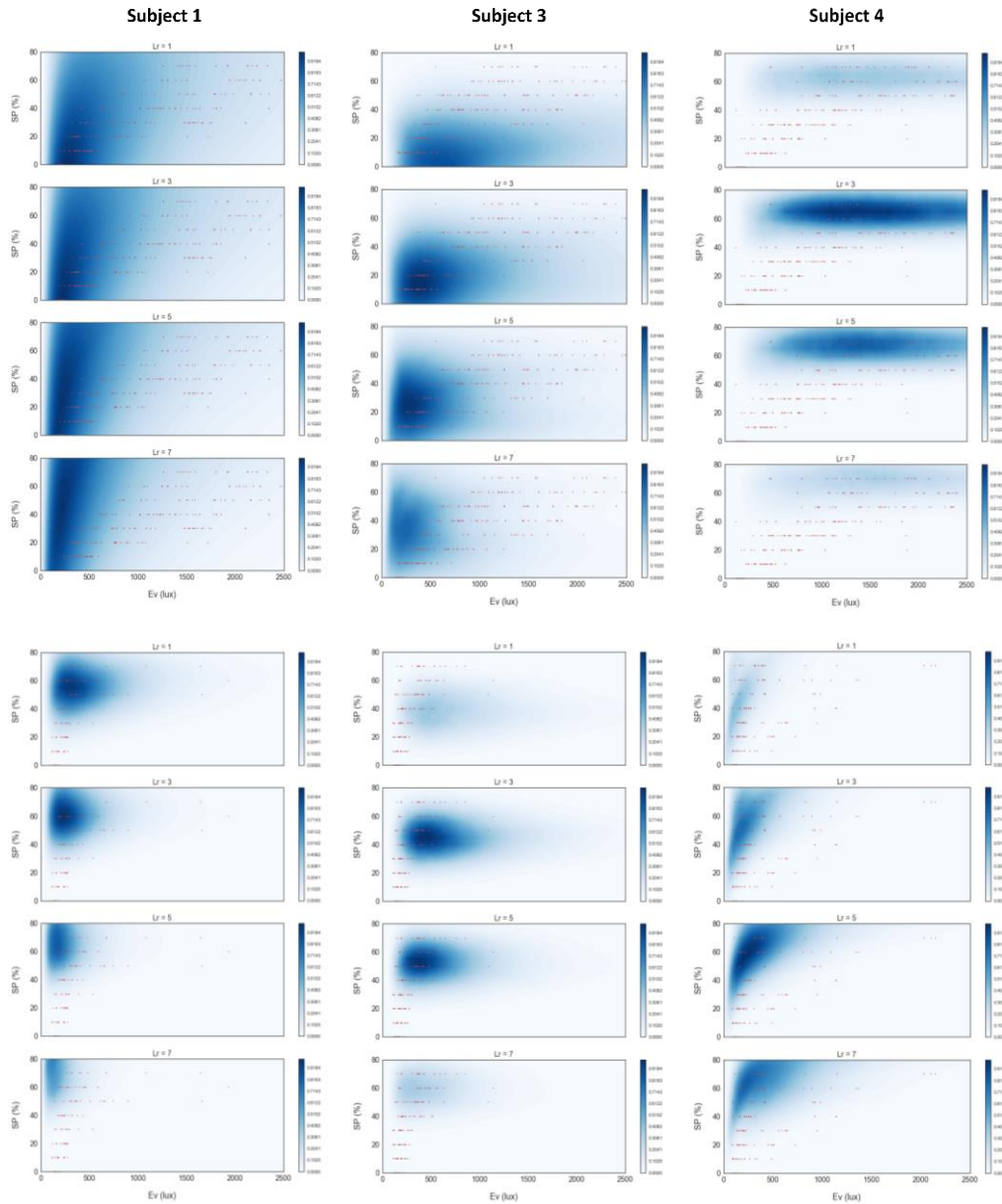


Figure 11 Posterior median of visual satisfaction utility functions of the three-variable model for each subject (top: sunny conditions; bottom: cloudy conditions).

Table 3 shows the posterior median of σ after normalization for each model for each subject. Lower values of σ indicate that the subject preference is more deterministic to the utility so that a smaller change in the condition could result in clear preference. Preferences of subjects 1 and 3 are less random to E_v during sunny conditions and models with SP during cloudy conditions, while subject 4 is more deterministic with models with SP on both sunny and cloudy conditions.

Table 3 Posterior median of σ for each model after normalization.

| Posterior median of σ | | Subject 1 | Subject 3 | Subject 4 |
|-------------------------------|--------|-----------|-----------|-----------|
| E_v | Sunny | 0.11 | 0.17 | 1.70 |
| | Cloudy | 0.22 | 1.12 | 0.44 |
| LR | Sunny | 0.20 | 0.98 | 1.50 |
| | Cloudy | 0.32 | 2.32 | 0.44 |
| E_v+SP | Sunny | 0.14 | 0.26 | 1.25 |
| | Cloudy | 0.15 | 0.78 | 0.37 |
| $LR+SP$ | Sunny | 0.15 | 0.30 | 1.23 |
| | Cloudy | 0.11 | 0.93 | 0.61 |
| $E_v+LR+SP$ | Sunny | 0.11 | 0.42 | 6.01 |
| | Cloudy | 0.24 | 2.56 | 0.45 |

The inferred visual satisfaction utility functions allow a schematic comparison of preferences between subjects and between models (different variables), but not on a relative scale. They show whether there is a pronounced area of maximum visual preference using the selected variables, and they reflect the fact that each person has different visual preferences. However, the utility plots cannot be compared directly since different variables are considered in each model – they all describe the personalized visual preference profiles based on the given data for each model. More importantly, the utility curves cannot be used to determine which model performs better. The prediction performance of each model should be evaluated separately as discussed in the next section.

3.4.2 Evaluation of Personalized Visual Satisfaction Models

3.4.2.1 Performance Metrics

In order to investigate the performance of different models, the data are divided into training (60% of data) and testing (40% of data) sets. Different split ratios from 90% -10% to 50%-50% were tested to demonstrate the best ratio for the given data and this split provides the most reliable results for our dataset (smallest standard deviation for the performance metrics). The models were constructed with the training set while their performance was evaluated on the testing set. The metrics used to evaluate the models' performance are the following:

- Hit Rate Accuracy (HRA) with condition distance threshold. HRA is defined as the average chance of correct prediction. That is, HRA is the proportion of true results (both true positives and true negatives) among the total cases examined. The predictive preference probability of our model is given in Eq. (39). We define our point predictions on the test data set as:

$$y_{pred}^{(k)} = \begin{cases} 1, & \text{if } p(\mathbf{q}_{test}^{(k)} > \mathbf{r}_{test}^{(k)} | D) \geq 0.5 \\ 0, & \text{otherwise} \end{cases} \quad (41)$$

where $k = 1, \dots, M$ represents each of the pairwise comparative data points in the test data set. The actual preference observations in the test data are given as:

$$y_{act}^{(k)} = \begin{cases} 1, & \text{if } \mathbf{q}_{test}^{(k)} > \mathbf{r}_{test}^{(k)}, \\ 0, & \text{otherwise} \end{cases} \quad (42)$$

The hit rate accuracy is then calculated as:

$$HRA = 1 - \frac{\sum_{k=1}^M |y_{pred}^{(k)} - y_{act}^{(k)}|}{M} \quad (43)$$

The problem with this commonly used metric is that it can give obscure results when the condition pairs are too close: for example, vertical illuminance equal to 500 lux or 520 lux will be the same to the occupant while the preference vote might be affected by other unmeasurable factors. To avoid such cases (very similar conditions), we introduce a minimum distance (ε) between visual conditions into the HRA calculation. The condition distance is defined as:

$$Dist(\mathbf{q}_{test}^{(k)}, \mathbf{r}_{test}^{(k)}) = \begin{cases} 1, & \text{if } \|\mathbf{q}_{test}^{(k)} - \mathbf{r}_{test}^{(k)}\|_2 \geq \varepsilon \\ 0, & \text{otherwise} \end{cases} \quad (44)$$

where $\|\cdot\|_2$ is the Euclidean norm (in our 3-dimensional space of normalized $\log E_v$, SP and LR) and the distance threshold ε is set equal to 0.2 with normalized variables (larger values would potentially exclude condition distances that should be considered). The hit rate accuracy with the distance threshold is then calculated as:

$$HRA_{dist} = 1 - \frac{\sum_{k=1}^M |Dist(\mathbf{q}_{test}^{(k)}, \mathbf{r}_{test}^{(k)}) \cdot (y_{pred}^{(k)} - y_{act}^{(k)})|}{M_{dist}} \quad (45)$$

where M_{dist} is the number of pairwise comparative points in the test data set which satisfy the condition distance requirement.

- Receiver Operating Characteristic (ROC) curve and Area Under Curve (AUC): ROC curve is a plot of the true positive rate against false positive rate for different possible cut points (Hanley and McNeil 1982), above which we define positive prediction. It depicts the tradeoff between sensitivity and specificity (any increase in sensitivity (true positive rate) will be accompanied by a decrease in specificity (1 - false positive rate)). AUC is a metric of accuracy by computing the area under the ROC curve. An area of 1 represents perfect performance, while an area of 0.5 indicates baseline performance.

3.4.2.2 Performance of Personalized Visual Satisfaction Models

The model evaluation results, together with the inferred visual satisfaction utility functions reflect the ability of the developed models to discover personalized visual preference characteristics. The performance metrics were computed using 10-fold Monte Carlo cross-validation (random seeds from 1 to 10). The ROC curves of all cross-validation folds and the corresponding mean ROC curves for the three variable models are shown in Figure 12. The closer the curve follows the left and top edges of the plot, the better the performance is, and the diagonal line represents the baseline performance.

Table 4 lists the performance metrics (AUC values and HRAdist) of the predicted probability distribution for each model with the average value and standard deviation. The results show that different performance is observed for different sky conditions for each subject and across subjects, indicating that this classification is indeed meaningful. The models for subject 1 show excellent performance for both sunny and cloudy cases; for subject 3, the model for sunny conditions performs well while for cloudy conditions the performance is fair; and vice versa for subject 4. The two metrics are consistent for all cases. The model evaluation results, together with the inferred visual satisfaction utility functions reflect the ability of the developed models to discover personalized visual preference characteristics.

Finally, model performance results are presented in Figure 13 for all models, including single and dual variable models. Although multivariable models contain the effects of single variables and are safer to use, simpler models can be useful and computationally efficient,

especially for implementation in control applications – although the prediction performance might decrease. For example, models using only vertical illuminance and shade position are relatively easy to implement, since vertical illuminance can be predicted using advanced lighting models and shading position can be easily monitored.

Due to the personalized nature of visual preferences, the performance of each model varies between subjects. For instance, the single E_v model works very well for subject 1 and subject 3 during sunny days, while the E_v -SP model performs well for subjects 1 and 3 overall. Subject 4 has different visual preferences, as shown in the experimental data and in the inferred utility functions. This person prefers brighter conditions and higher shading positions in most cases, and the LR model shows good performance in this case. The multivariate model performance is either better or within the standard deviation limits of the best performing model for all cases. For different and/or larger data sets, it is expected that multivariable models will always perform better.

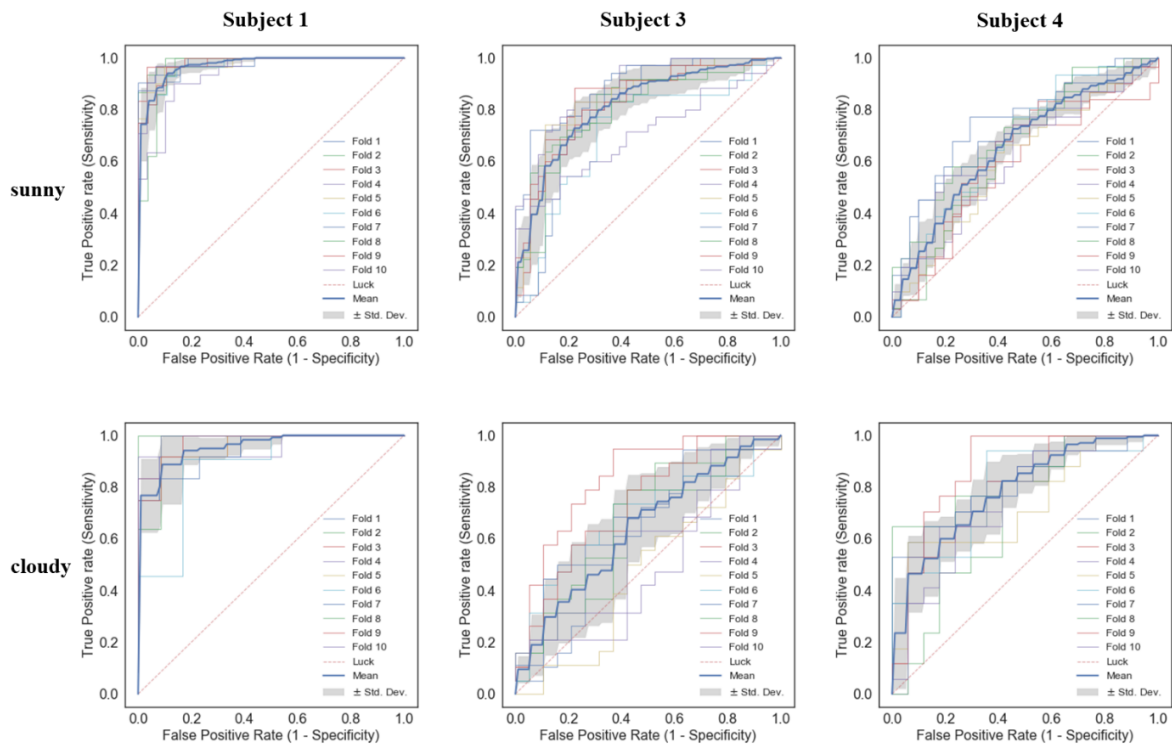


Figure 12 ROC curves for the three-variable models and all subjects with 10-fold cross validation.

Table 4 Performance evaluation metrics for the three-variable models using 10-fold cross validation results.

| Subject# | Sky conditions | HRA _{dist} (Average ± St. dev.) | AUC (Average ± St. dev.) |
|-----------|----------------|--|--------------------------|
| Subject 1 | Sunny | 0.92 ± 0.04 | 0.97 ± 0.01 |
| | Cloudy | 0.91 ± 0.05 | 0.95 ± 0.03 |
| Subject 3 | Sunny | 0.78 ± 0.05 | 0.81 ± 0.06 |
| | Cloudy | 0.62 ± 0.07 | 0.64 ± 0.10 |
| Subject 4 | Sunny | 0.68 ± 0.03 | 0.66 ± 0.05 |
| | Cloudy | 0.75 ± 0.07 | 0.78 ± 0.05 |

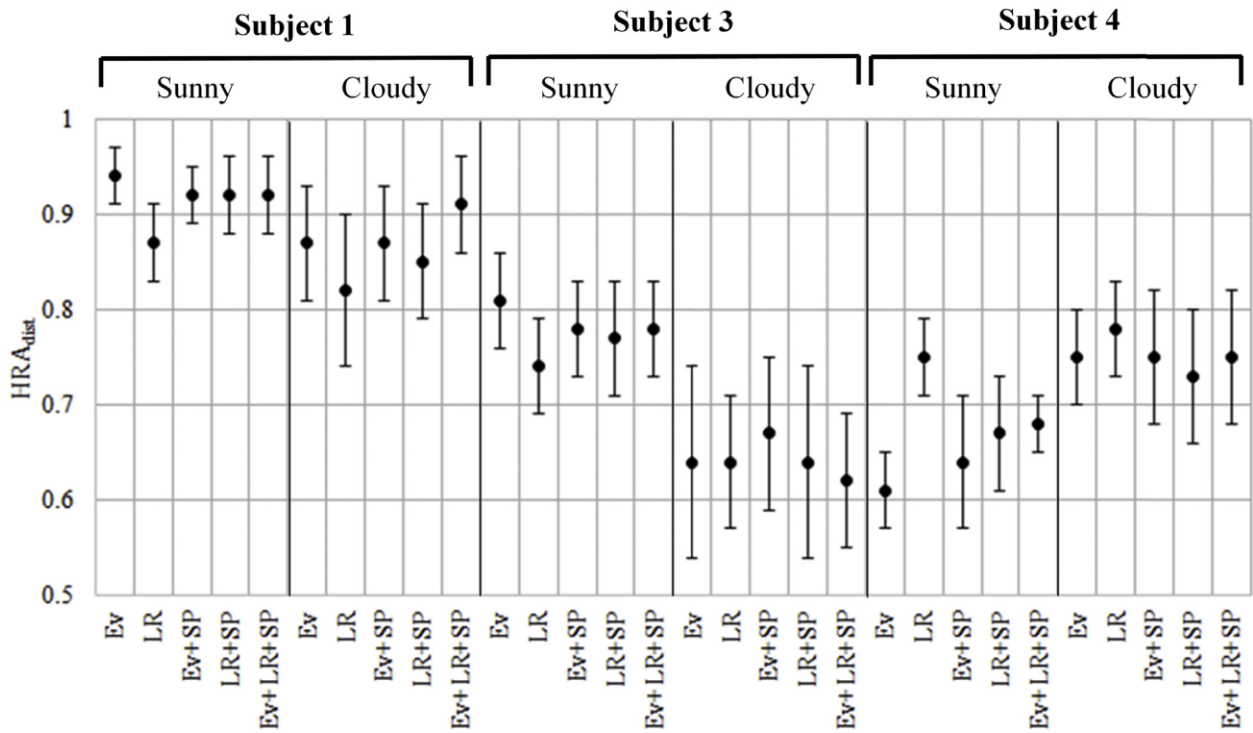


Figure 13 Model accuracy (HRA_{dist} average and st. deviation) for all developed models (all subjects and variables).

3.5 Summary

This chapter presents a method for developing personalized visual preference and satisfaction profiles in private daylit offices. Comparative visual preference data were collected from sets of experiments with human subjects in private offices with changing visual conditions, and visual satisfaction profiles were inferred using a Bayesian approach. The preference data were used to infer the visual satisfaction utility functions as posteriors, adopting a parametrized

Gaussian bell function for the latent utility models. Personalized visual satisfaction models were trained with a Sequential Monte Carlo algorithm using the experimental data. The inferred visual satisfaction utility functions and model evaluation results show the ability of the models to discover different personalized visual satisfaction profiles – therefore, it can be potentially used in personalized indoor environment controls.

The inferred satisfaction utility functions and developed visual preference models presented in this study are not generalizable. They were not developed as a reference general model, but as individual, personalized visual satisfaction profiles for the studied human subjects. Therefore, the subject population did not need to be large. At the same time, other daylighting systems would result in different illuminance and luminance distributions under the same external conditions, and therefore visual preferences would be different even for the same occupants (brightness, view and contrast perception would be different). Therefore, diverse preference profiles are expected depending on the systems used, and potentially other variables might play a significant role. Nevertheless, the method presented in this chapter can be adopted to account for other factors.

4. AN ONLINE VISUAL PREFERENCE ELICITATION LEARNING FRAMEWORK

4.1 Overview

This chapter presents the development of an online visual preference learning method using preference elicitation framework, for efficiently learning occupants' visual preference profiles with the modeling approach developed in Chapter 3. To determine the visual condition duels for preference query with most information gain, a combination of Thompson sampling method and pure exploration (uncertainty learning) method was used, addressing the balance of exploration and exploitation when targeting the near-maximum area of utility during the learning process. A set of experiments were designed and conducted to implement the proposed learning framework with human subjects and the experimental results demonstrated the feasibility and efficiency of the method.

4.2 Visual preference elicitation

4.2.1 Visual preference model and satisfaction utility learned from comparative preference data

The developed personalized visual satisfaction profiles described in Chapter 3 were adopted. For demonstration purposes, the single-variable model using only vertical illuminance (E_v) is used: $\mathbf{x} = E_v$, to reduce the order of the models and the optimization problem (into one dimension).

4.2.2 Visual preference elicitation

Preference elicitation is a learning task involving preference modeling and decision making. Assuming that the occupant is experiencing the current visual condition \mathbf{x}_1 , designing a preference elicitation learning method is to choose and achieve the next visual condition \mathbf{x}_2 to query the preference vote comparing the two conditions from the occupant, and then learn the visual preference profile of the occupant from the feedback. An optimal elicitation framework is to design sequentially and iteratively the condition duels $\{\mathbf{x}_1, \mathbf{x}_2\}, \{\mathbf{x}_3, \mathbf{x}_4\}, \dots$ or $\{\mathbf{x}_1, \mathbf{x}_2\}, \{\mathbf{x}_2, \mathbf{x}_3\}, \{\mathbf{x}_3, \mathbf{x}_4\}, \dots$ in a (limited) feasible region such that we learn the preference model and satisfaction utility efficiently, essentially a two-armed bandit sequential decision problem (Robbins 1952;

Fürnkranz et al. 2012; Agrawal and Goyal 2012; May et al. 2012). There exist different elicitation learning methods targeting different objectives of what aspect and how well one wishes to learn the utility. When the objective could be stated as an optimization problem for tuning the hyperparameters θ of the target satisfaction utility, the preference learning problem could then be solved with machine learning optimization techniques (e.g., Bayesian optimization). In this study, we construct the optimization problem as selecting next visual condition \mathbf{x}_{t+1} in step t such that:

$$\mathbf{x}_{t+1} = \underset{\mathbf{x}}{\operatorname{argmax}} a(\mathbf{x}, \mathbf{x}_t | \mathcal{D}_t) \quad (46)$$

where $a(\mathbf{x}, \mathbf{x}_t | \mathcal{D}_t)$ is an information acquisition function of duel $(\mathbf{x}_t, \mathbf{x})$, given all the data at and before current step \mathcal{D}_t . And the formulation of the acquisition function determines the objective (what and how) of learning.

Specifically, visual preference elicitation serves as a decision support system for optimized visual environment control for the occupants. For most optimal control strategies optimizing a utility function, either the whole utility or the location of the maximum of the utility (and maybe a range around it) is of most interest. Several methods with different acquisition functions are discussed in the following sections.

4.2.2.1 *Random exploration*

Random exploration is a simple but effective method utilized in global optimization (Brochu et al. 2010; Fürnkranz and Hüllermeier 2010; Bergstra and Bengio 2012). In this study, when we want to learn the whole utility function over the feasible space (under all achievable visual conditions), random exploration is the first candidate technique as it simplifies the learning process with respect to system design and control implementation. The selection of the next condition duel in each learning step is random, so it could be achieved by changing the visual environment randomly. In practical applications, however, feasible visual conditions are dynamically limited by changing outdoor weather, which results in higher randomness and decreased efficiency – it might take more steps with more repeated and redundant preference data and is dependent on weather condition.

4.2.2.2 Exploration

Pure exploration method, or uncertainty learning (UL), aims at discovering the whole utility more efficiently by exploring the most uncertain point of the model in every step. That is, in step t , the acquisition function is the variance of the predictive preference probability :

$$a_{var}(\mathbf{x}, \mathbf{x}_t | \mathcal{D}_t) = \text{Var}(p(\mathbf{x}_t < \mathbf{x} | \mathcal{D}_t)). \quad (47)$$

4.2.2.3 Exploitation

Exploitation methods aims at finding maximum fast. In Bayesian optimization studies, an acquisition function characterizing the potential or predicted higher objective function value is defined; and as a result, maximizing the acquisition function translates to discovering the maximum of utility (Brochu et al. 2010). The probability of improvement (PI) is a representative acquisition function in early work (Kushner 1964):

$$PI(\mathbf{x}) := p(\mathbf{x}_t < \mathbf{x}), \quad (48)$$

So, the next condition selection \mathbf{x}_{t+1} is made by maximizing the expectation of PI over posterior samples:

$$a_E(\mathbf{x}, \mathbf{x}_t | \mathcal{D}_t) = \mathbb{E}(p(\mathbf{x}_t < \mathbf{x} | \mathcal{D}_t)), \quad (49)$$

Pure exploitation (maximizing PI repeatedly at every step for selecting both arms of the duel) could easily fall into the trap of false maximum before exploring enough possibilities.

4.2.2.4 The exploration-exploitation dilemma:

Exploitation is more efficient than exploration when an optimal control system focuses on satisfying occupants (by achieving maximum utility). However, learning only the maximum could be insufficient or risky depending on the application. There are two major concerns in the practical application of visual preference model in daylighting and lighting control: 1) sometimes the most satisfying visual condition corresponding to the maximum utility is not achievable, due to the limitation in outdoor conditions; 2) even when the maximum of utility is achievable, the control system might need to satisfy another conflicting objective such as energy saving. An example could be the daylighting control using multi-objective optimization for parallel visual satisfaction and energy use developed by Xiong et al. (2019). Both cases are equal to optimal control with a constrained utility objective, and the final realized visual condition is usually near but not at the exact maximum of the utility (in the feasible space); in other word, satisfying but not the most satisfying condition. Therefore, the “exploration-exploitation dilemma” should be addressed when

learning visual preference for practical applications, and the learning target becomes a certain area near the maximum other than a single maximum. Modified PI has certain drawbacks although it is capable of tuning the trade-off between exploration and exploitation, as described in the previous section. Thompson sampling (TS) method (Thompson 1933) is an heuristic method dating back to 1930s and a promising solution to addressing the “exploration-exploitation” in multi-armed bandit problems that draws back researcher’s interest in recent years (Graepel et al. 2010; Granmo 2010; May et al. 2012; May and Leslie 2011; Scott 2010). Chapelle and Li (2011) showed the effectiveness of the Thompson sampling method with empirical results and comparison with popular algorithms with simulation on real data, and emphasized its competitiveness of efficient implementation, which is an essential factor for system design. Agrawal and Navin (2012) guaranteed the efficiency of Thompson sampling method theoretically by proving its regret bound for two-armed and N-armed bandit problem.

In this study, we adopt the Thompson sampling method to deal with the exploration-exploitation trade-off in discovering a range of satisfying visual conditions. In an exploitation step t , instead of using all the samples of model posterior (mean or variance), the Thompson sampling method randomly adopts one sample $\theta_t^{(1)}$ from posterior θ_t and selects the next condition \mathbf{x}_{t+1} following the PI principle for that sample:

$$a(\mathbf{x}, \mathbf{x}_t | \mathcal{D}_t) = p(\mathbf{x}_t < \mathbf{x} | \theta_t^{(1)}, \mathcal{D}_t), \quad (50)$$

$$\mathbf{x}_{t+1} = \underset{\mathbf{x}}{\operatorname{argmax}} p(\mathbf{x}_t < \mathbf{x} | \theta_t^{(1)}, \mathcal{D}_t). \quad (51)$$

This randomized selection step embeds an exploring element in Thompson sampling method by testing different possibilities of maximum of utility. This results in a search inside a wider region enclosing the most satisfying visual condition, without sacrificing much the efficiency of pure exploitation (Agrawal and Navin 2012). On the other hand, the randomness of TS suffers from the same problems as pure exploitation, i.e., it can get trapped in local maxima. We address it by combining uncertainty learning (pure exploration) and TS iteratively to enforce stable exploration – when selecting the two conditions (arms) of a duel in two consecutive steps, one arm is selected with maximum uncertainty and the other one with Thompson sampling. And to increase data collection efficiency, each condition is shared in two duels with previous condition and next condition respectively. That is, the combined TS and uncertainty learning algorithm (TS+UL) follows the iterative learning sequence:

$$\begin{aligned}
\mathbf{x}_1 &= \underset{x}{\operatorname{argmax}} p(\mathbf{x}_0 < \mathbf{x} | \theta_0^{(1)}, \mathcal{D}_0), & (\text{TS}) \\
\mathbf{x}_2 &= \underset{x}{\operatorname{argmax}} \operatorname{Var}(p(\mathbf{x}_1 < \mathbf{x} | \mathcal{D}_1)), & (\text{UL}) \\
\mathbf{x}_3 &= \underset{x}{\operatorname{argmax}} p(\mathbf{x}_2 < \mathbf{x} | \theta_2^{(1)}, \mathcal{D}_2), & (\text{TS}) \\
\mathbf{x}_4 &= \underset{x}{\operatorname{argmax}} \operatorname{Var}(p(\mathbf{x}_3 < \mathbf{x} | \mathcal{D}_3)), & (\text{UL}) \\
& \vdots &
\end{aligned} \tag{52}$$

where $\theta_0^{(1)}, \theta_2^{(1)}, \dots$ are randomly selected single-samples from posterior $\theta_0, \theta_2, \dots$ at step 0, 2, ... respectively; and $\mathcal{D}_1, \mathcal{D}_3, \dots$ are the data at and before step 1, 3, ... respectively.

4.2.3 Preference elicitation and passive learning with occupant override action

In a well-designed building control system, override should always be granted to the occupant(s) even in the learning process, especially for daylighting control with changing weather. In the meantime, occupant actions could be used in passive preference learning. Therefore, a method of integrating passive learning into the preference elicitation learning framework is proposed as follows. Assuming a rational occupant who takes override actions to adjust the visual condition towards the maximum of his or her utility (even if the utility is hidden to himself/herself), the action could be equivalent to a combination of a preference vote (that the condition after action is preferred) and a selection of the next visual condition, which is a complete exploitation step. Thus, an action during the learning process could take the place a TS step; the next learning step would be UL step; and the learning sequence in Equation 52 continues until another occupant override occurs.

4.2.4 Evaluation metric and “stop” criterion

To evaluate the performance of the proposed visual preference learning strategy, a metric is needed to quantify how well the learning outcome (the satisfaction utility or preference model) is at each step. Typically, a model is tested or validated by accuracy metrics, given a set of test or validation data. For an online learning system, however, obtaining such data for validating the updated preference model in each step is unrealistic as they are “future” data – all the current data has to be used for training the current model. Alternatively, considering that the objective of the learning framework is to find out the (most) satisfying visual condition, which is to discover the location of the maximum satisfaction utility, we could translate the goodness of learning results to

quantifying how sure we are about the maximum by obtaining the probability density function (PDF) of the posterior of maximum for each step:

$$\text{PDF}(\mathbf{x}_t^*) = p(\mathbf{x}_t^*|\theta_t, \mathcal{D}_t), \quad (53)$$

where \mathbf{x}_t^* is the posterior of maximum of utility in step t :

$$\mathbf{x}_t^* = \underset{\mathbf{x}}{\text{argmax}} u(\mathbf{x}|\theta_t, \mathcal{D}_t). \quad (54)$$

Given the samples of posterior, the PDF is estimated by taking the histogram of the posterior of maximum:

$$p(\mathbf{x}_t^*|\theta_t, \mathcal{D}_t) \approx \sum_{i=1}^N 1_{B_i}(\mathbf{x}_t^*) f_i, \quad (55)$$

where B_i and f_i is the i^{th} histogram bin and the corresponding sampling frequency. The function $1_A(x)$ is the indicator function of the set A . Then, we could quantify the certainty level by calculating the information entropy (or Shannon entropy, H) of the PDF (Shannon 1948):

$$H_b[p(\mathbf{x}_t^*|\theta_t, \mathcal{D}_t)] \approx - \sum_{i=1}^N f_i \log_b f_i, \quad (56)$$

where b is the base of the logarithm, and is 10 in this study.

Entropy measures the unpredictability of the variable \mathbf{x}_t^* , so lower entropy reflects higher certainty of the maximum. Note that entropy is a relative value that is meaningful only when comparing two or more entropy values. In this study, the evolution (ideally reducing) of entropy of the maximum as the number of steps increases could provide intuitive insights on the learning trend, and a “stop” criterion is defined as a benchmark of a usable preference profile. The “stop” criterion is not a threshold to stop the learning process, but a sign of when the learned preference profile starts to be usable for control purpose. The criterion is computed as the entropy of a Gaussian distribution of a maximum (some arbitrary E_v^*) with a standard deviation of 150 lux (Figure 14):

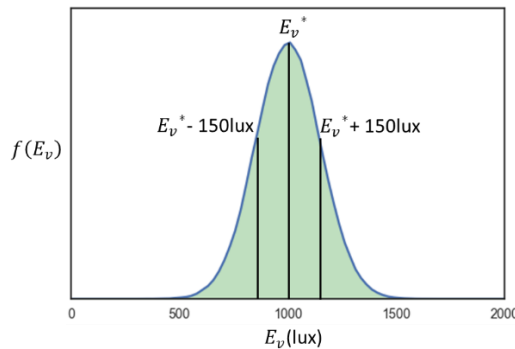


Figure 14 Example PDF of criterion ($E_v^* = 1000$ lux, $\sigma = 150$ lux).

$$H_{stop} = H(E_v \sim N(E_v^*, 150 \text{ lux})) = 6.43. \quad (57)$$

If the calculated entropy at a specific step is larger 6.43, it means that the location of the maximum is more uncertain than a Gaussian distribution with 150 lux standard deviation. This criterion is set with considerations that 150 lux difference of vertical illuminance could be around the boundary that transit from insignificant to noticeable to typical occupants.

4.3 Experiment

4.3.1 Experiment design

To demonstrate and evaluate the proposed visual preference elicitation learning framework, a set of experiments was designed and conducted with human subjects in the same experimental facility described in Chapter 3.

4.3.1.1 Experiment setup

Figure 15 is a flowchart illustrating the connections between systems (platforms), sensing, programming, controls and the communication flow in each step. Sensor measurements, override interface (Figure 16) and action monitoring, as well as control implementation (shading control) are realized in Niagara framework; Online preference survey is obtained through MySQL database management system with a simple web interface (Figure 16); preference modeling and learning are implemented in a Python program, communicating with all other platforms through Modbus protocol (Niagara) and MySQL client/server protocol (MySQL).

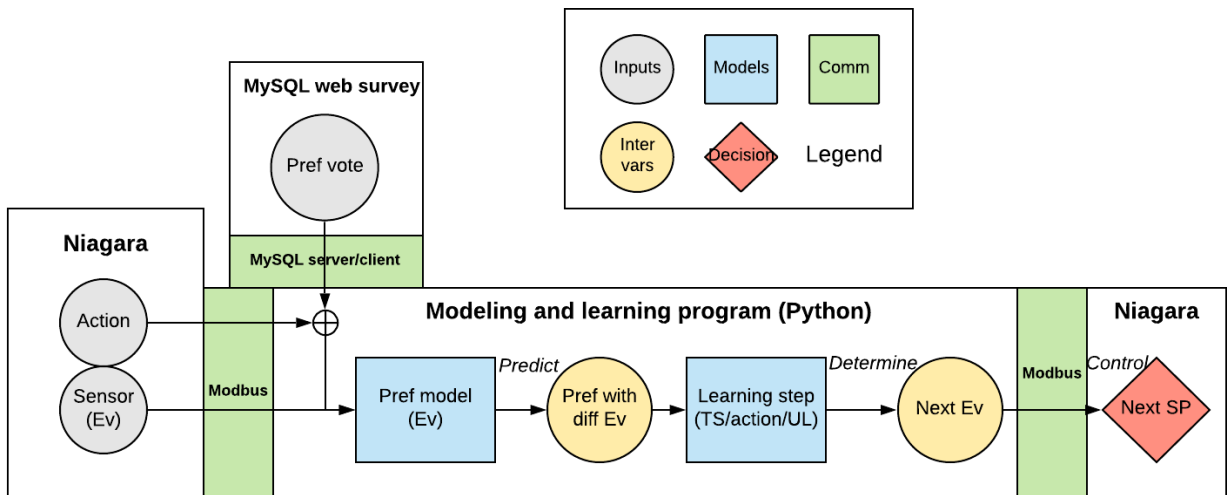


Figure 15 System integration and communication flowchart.

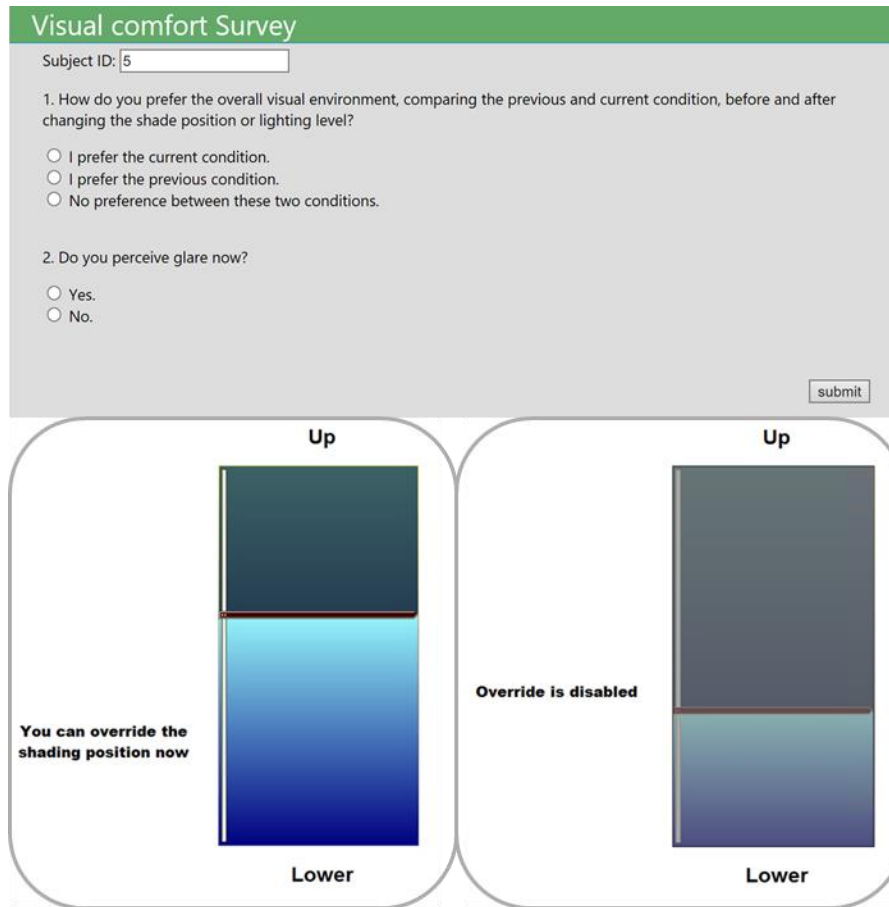


Figure 16 Interfaces of survey (up), override enabled (bottom-left) and override disabled (bottom-right).

4.3.1.2 Experiment procedure

The experiments were conducted from May – June, 2019 with 13 subjects. Each subject participated in the experiment for two days (or four half-days depending on weather conditions) to experience one complete sunny day and one complete cloudy day, in order to learn their visual preference profiles under different sky conditions. Subjects were asked to spend 7 hours per day (or two half-days) in the office doing normal computer work. The subjects were graduate students and staff (between 20 and 40 years old) not familiar with this research and were advised to avoid any direct contact with the sensing instrumentation. Approval by the Institutional Review Board (IRB Protocol #: 1507016229) was obtained before conducting the experiments.

During the experiment, the visual condition (E_v) was changed by operating the roller shade position (SP) (see Figure 15) with a simple feedback control – adjusting SP according to the difference of measured and target vertical illuminance – together with an automatic lighting control

to achieve the minimum work plane illuminance requirement (300 lux). Note that the simple shading control was adopted to simplify control implementation under stable weather conditions. When the preference model becomes more complicated (with more variables), model-based control that utilizes advanced daylighting and lighting model is more competent and robust with fluctuating weather. Subjects would be asked to complete a short web survey (Figure 16) for preference vote after the condition change and adaptation while variables for visual preference modeling were collected at the same time, and override of SP was enabled for a limited period after answering the survey.

Figure 17 shows the learning procedure in one learning step during the experiment. Learning interval is determined as 8 min in a step (when one learning decision is made) to accelerate the learning process, referring to the 10-min interval selected in Chapter 3. At the beginning of one step (4 minutes after the last change of visual condition by changing SP, and override is disabled), the occupant is asked to vote for the preference between the current condition E_{v_t} and the previous condition $E_{v_{t-1}}$ before the last change (when the last survey is completed), and the sensor measurements of the current visual condition are taken at the same time of the survey. The model is trained and updated with the collected preference vote and measurement data (including the measurement of the previous condition). The occupant is allowed to override the shading position once finishing the survey.

If there is no action taken in half interval (4 minutes), override is disabled temporally when learning framework starts working – a set of feasible E_v values are predicted according to the weather conditions and the elicitation method will select the next condition $E_{v_{t+1}}$ based on the elicitation framework principle and the decision of last step (whether it is TS step or UL step). The control system then communicates with the device (roller shades) to achieve the determined condition $E_{v_{t+1}}$ with feedback control. The occupant will have 4 minutes to adapt to the new visual condition $E_{v_{t+1}}$ until the next step starting with the preference survey comparing E_{v_t} and $E_{v_{t+1}}$.

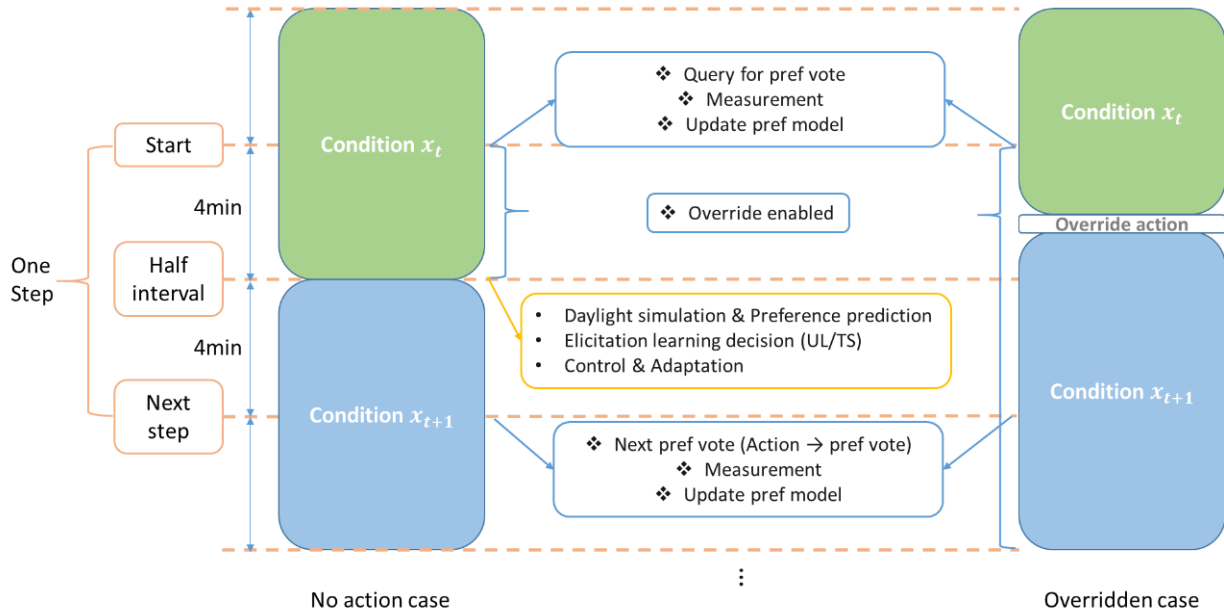


Figure 17 One-step learning flowchart.

If the occupant takes an action when override is enabled, on the other hand, the learning framework will not determine the condition but translate the action into a preference vote at the end of the step (8 minutes since last survey): $E_{v_t} < E_{v_{t+1}}$.

Figure 18 shows the overall flowchart of the experiment procedure in each loop. During the iteration, whether an override action is taken or not is the judgement criterion to activate elicitation learning framework. A detected action will bypass the learning framework to serve as a passive exploitation step and reset the choice of next elicitation learning step into UL. Learning framework starts working when no action is detected in the previous interval, by selecting TS or UL step depending on the last learning step or action and disabling override. The next visual condition is determined by the selected learning algorithm and achieved through the shading and lighting control system as shown in Figure 15. Then the framework queries preference after adaptation and enables override once preference data is collected.

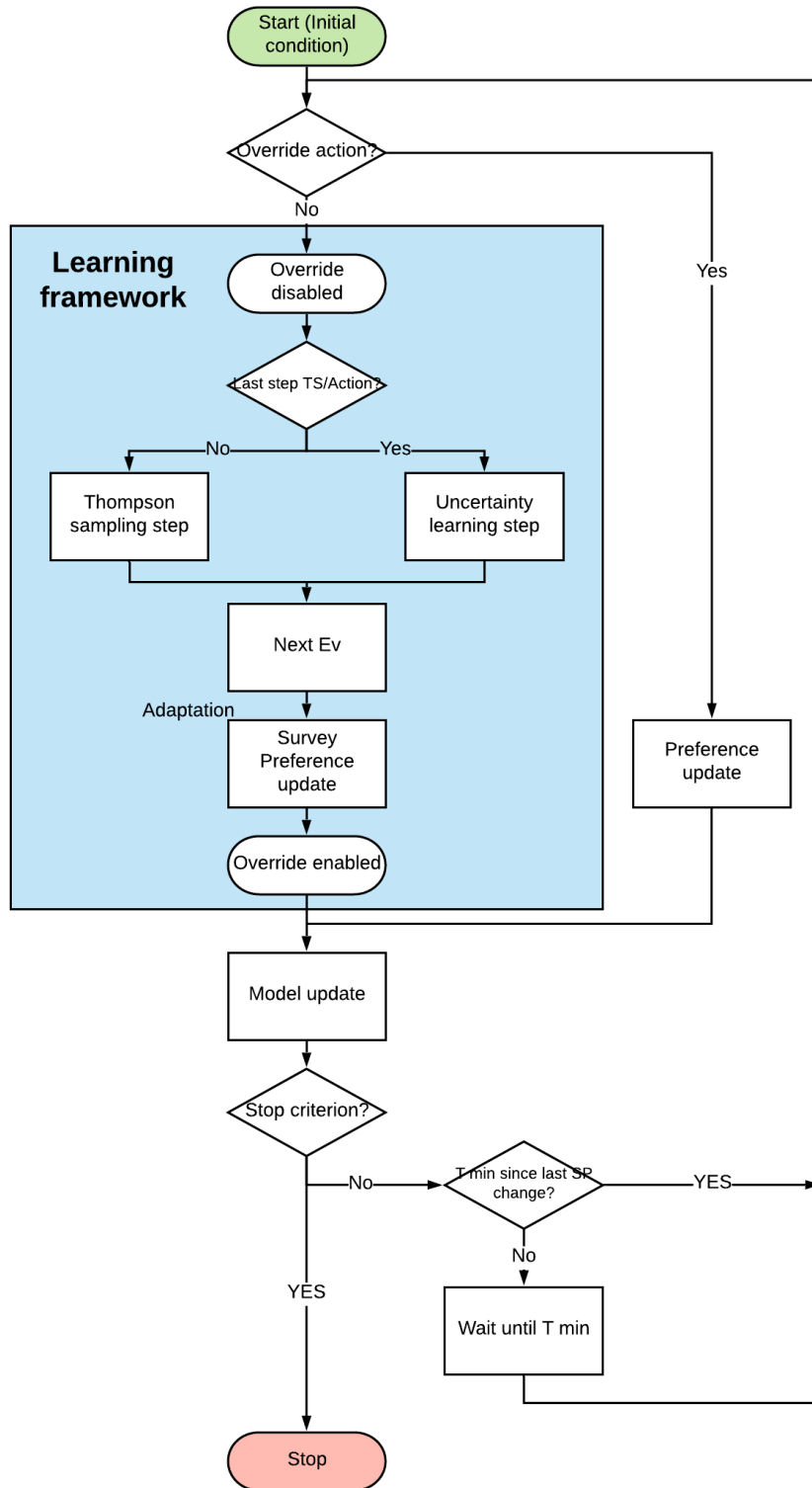


Figure 18 Learning flowchart in each loop (T=8 min).

4.3.2 Experiment results

4.3.2.1 Data

Figure 19 summarizes the number of data collected for all 13 subjects under different weather conditions. Assuming active occupants with the ratio of action data to total data larger than 10%, most subjects were active and interacted with shades in both sunny and cloudy days (subject 2, 4, 5, 6, 8, 9, 11) -mainly for the reason that UL step tends to explore visual conditions away from the satisfying ones as the uncertainty of maximum of the utility becomes smaller, as learning goes on. A few subjects were willing to interact even when the conditions are satisfying. Subject 1 was active in sunny days but inactive in cloudy days as the subject was more sensitive to bright conditions. Other subjects (subject 3, 7, 10, 12, 13) were inactive in both days for different reasons – some subjects were insensitive to any change in visual environment; some subjects were mostly satisfied or very tolerable with unsatisfied conditions; some subjects were unwilling to interact with the system.

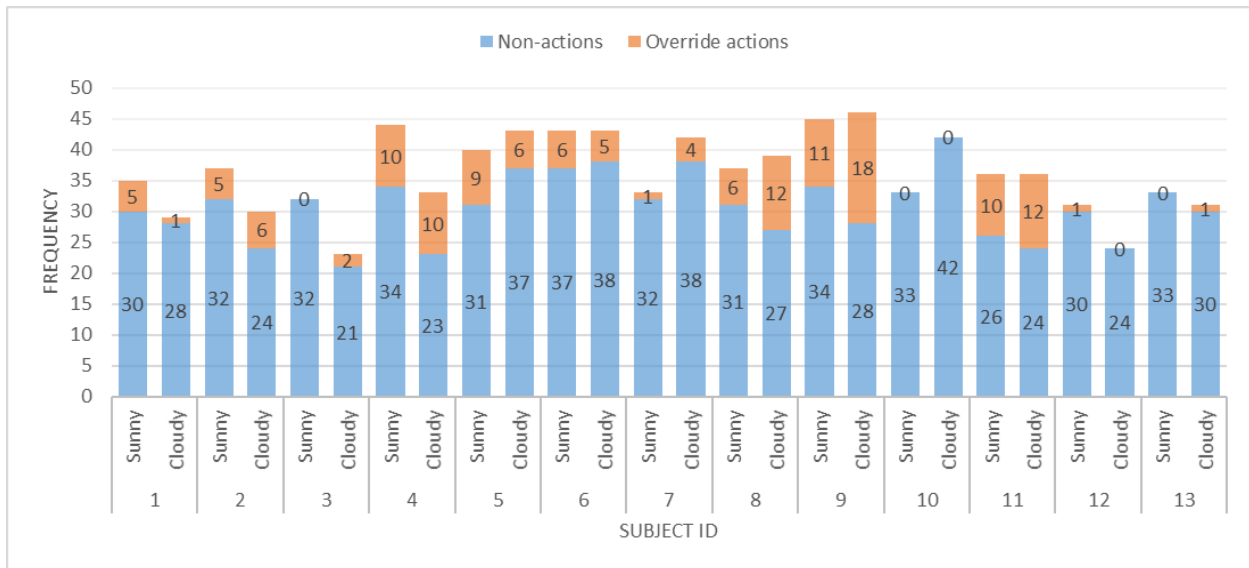


Figure 19 Data summary.

Table 5 shows the data of first 10 learning steps for subject 5 in a sunny day. The first duel conditions were generated with a fixed (initial 20%) and a random SP. This subject was mostly consistent in his/her own visual preference in these steps (with a maximum satisfaction in a range of 600-1000 lux). Two actions were taken following a UL step to lower E_v and a TS step to increase brightness respectively. The decisions of TS steps adapting and exploiting on the

preference votes in previous steps could be observed in step 2 and 4. The exploring ability of TS endured from randomness is reflected in step 8, where TS decision moves opposite from the dominating estimation of maximum, which results from a distinctive (minority) utility sample with maximum around 300 lux, possibly capturing the preference uncertainty inherited from step 4. And this uncertainty was “corrected” right away in the next step by the subject’s override (step 9). The UL steps explored over the feasible E_v space and tended to search the tails of utility because the center part is more and more certain as TS steps hovered around the maximum.

Table 5 Representative data (Pref 1: preferring current; 2: preferring previous; 3: no preference).

| Step | Time | Learning step / Action | E_v (lux) | $E_{v_{pre}}$ (lux) | Pref | SP (ShadeOpen %) |
|------|-------|---------------------------|-------------|---------------------|------|---------------------|
| 0 | 13:35 | | 630 | | | 20 |
| 1 | 13:39 | Random | 285 | 630 | 2 | 0 |
| 2 | 13:45 | TS | 1495 | 285 | 1 | 52 |
| 3 | 13:53 | UL | 410 | 1495 | 2 | 10 |
| 4 | 14:01 | TS | 438 | 410 | 2 | 6 |
| 5 | 14:09 | UL | 1428 | 438 | 1 | 58 |
| 6 | 14:13 | Action | 794 | 1428 | 1 | 45 |
| 7 | 14:23 | UL | 284 | 794 | 2 | 0 |
| 8 | 14:31 | TS | 272 | 284 | 2 | 0 |
| 9 | 14:35 | Action | 692 | 272 | 1 | 42 |
| 10 | 14:51 | UL | 276 | 692 | 2 | 0 |

4.3.2.2 Learning results

Figure 20 and Figure 21 show the example visualization of the learning results.

For the learned satisfaction utility, the first 100 estimation samples (out of 2000) are plotted to reveal the distribution of maximums and the overall uncertainty as shown on the left of Figure 8, and the distribution of maximum of all the samples form the probability density function (PDF) as shown on right of Figure 20, which illustrates how certain the model is of where the most satisfying E_v is – wider and flatter PDF indicates uncertain maximum – and is used to calculate the entropy of maximum distribution (number displayed in the plot).

The preference profile is visualized using a contour plot (Figure 21) in the condition duels space (E_{v_1} - E_{v_2} space), where the mean probability of the subject preferring E_{v_1} to E_{v_2} is indicated by color, and the red dots on the plot represent all the condition duels used for the model ($E_{v_1} =$

$E_{v_t}, E_{v_2} = E_{v_{t-1}}$). The preference contour plot is linked with the utility plot in the way that the intersection part of the X-shape color pattern corresponds to the maximum of utility.

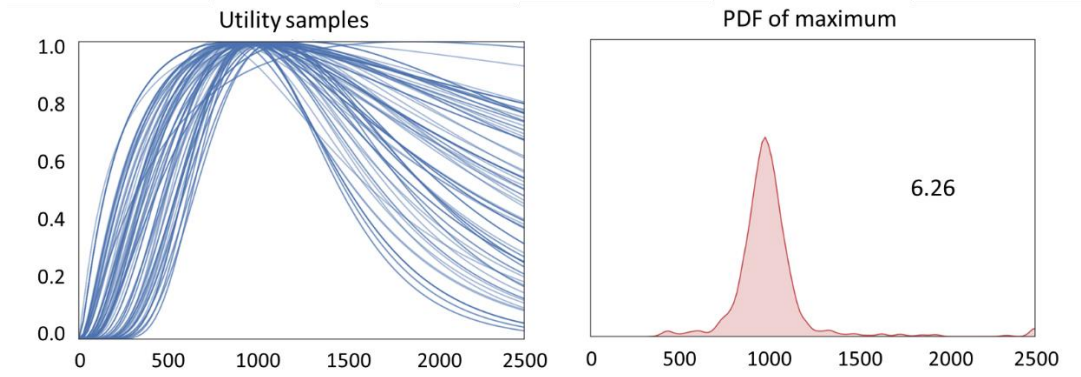


Figure 20 Representative results – utility samples plot (left) and PDF of maximum E_v^* (right).

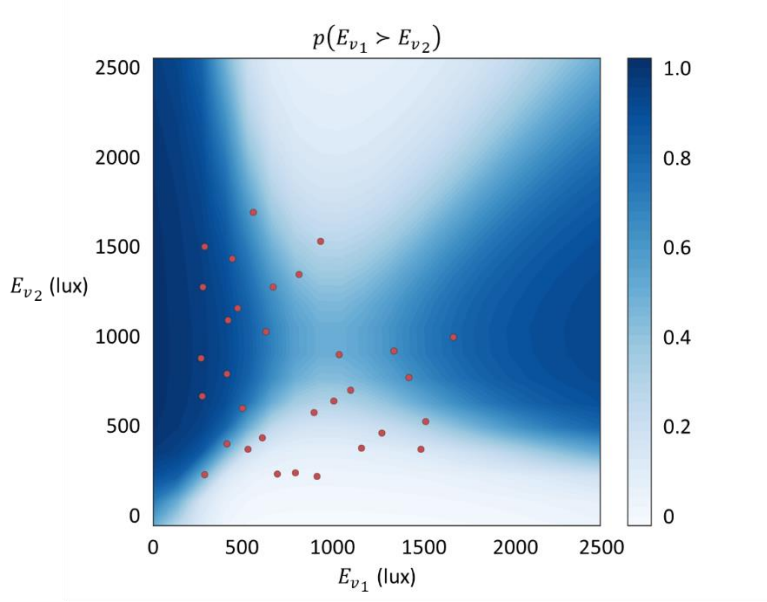


Figure 21 Representative results – contour plot of mean preference probability $p(E_{v_1} > E_{v_2})$.

Given the plots above, the learning progress could be investigated by visualizing the pattern of evolution of the learning results by steps. Figure 23 is an example of the learning progress of subject 5 in sunny day, with utility sample plot and PDF of maximum plot in four selected steps. As can be seen, utility samples in early steps have different shapes and maximums, which looks

messy, but gradually transitions to unifying shapes and converging maximums in a narrower and more certain range, and the uncertainty is higher with the utility going away from the near-maximum area due to the exploiting efficacy. Correspondingly, the PDF of maximum changes from flat bumps to a sharp peak and the calculated entropy (Figure 23) becomes lower than the “stop” criterion ($H=6.4$ indicated with the horizontal red dash-line).

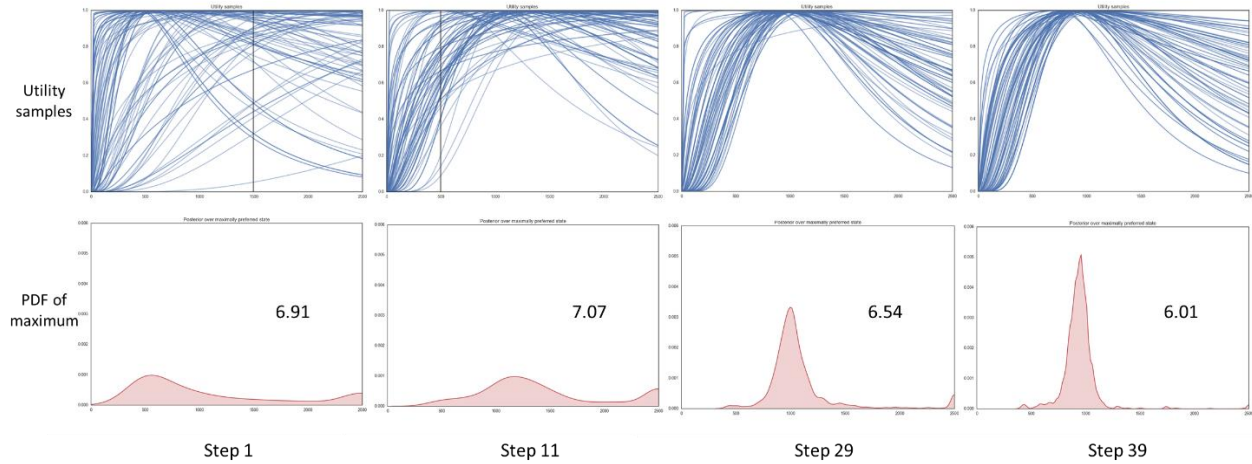


Figure 22 Representative learning evolution in four steps (subject 5, sunny day).

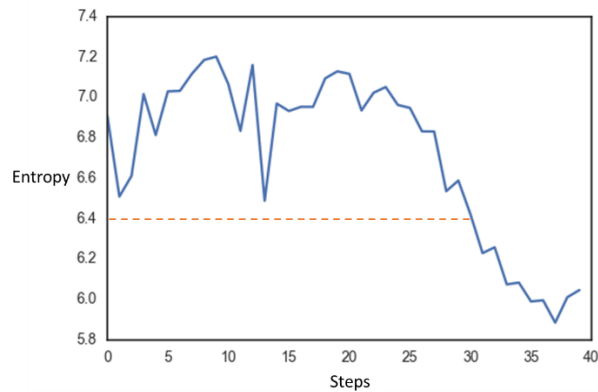


Figure 23 Entropy evolution of maximum estimation.

Figure 24 shows the final preference models learned in the experiments for all the subjects. Similar and distinct profiles could be observed among different subjects. Some subjects have consistent preference patterns for sunny and cloudy days (subject 1, 2, 3, 4, 6, 11, 12, 13), while others have different preferences with changing weather. Similar conclusions could be drawn from Figure 25, which shows the distribution of estimated maximums of all the subjects in the final step.

Moreover, the uncertainty of final estimation could be observed intuitively – flat PDFs such as the ones of subject 2 and 7 for both sunny and cloudy days indicate that the most satisfying E_v remains uncertain. The axis labels of these figures are omitted as all the axes are consistent with the example ones in Figure 21.

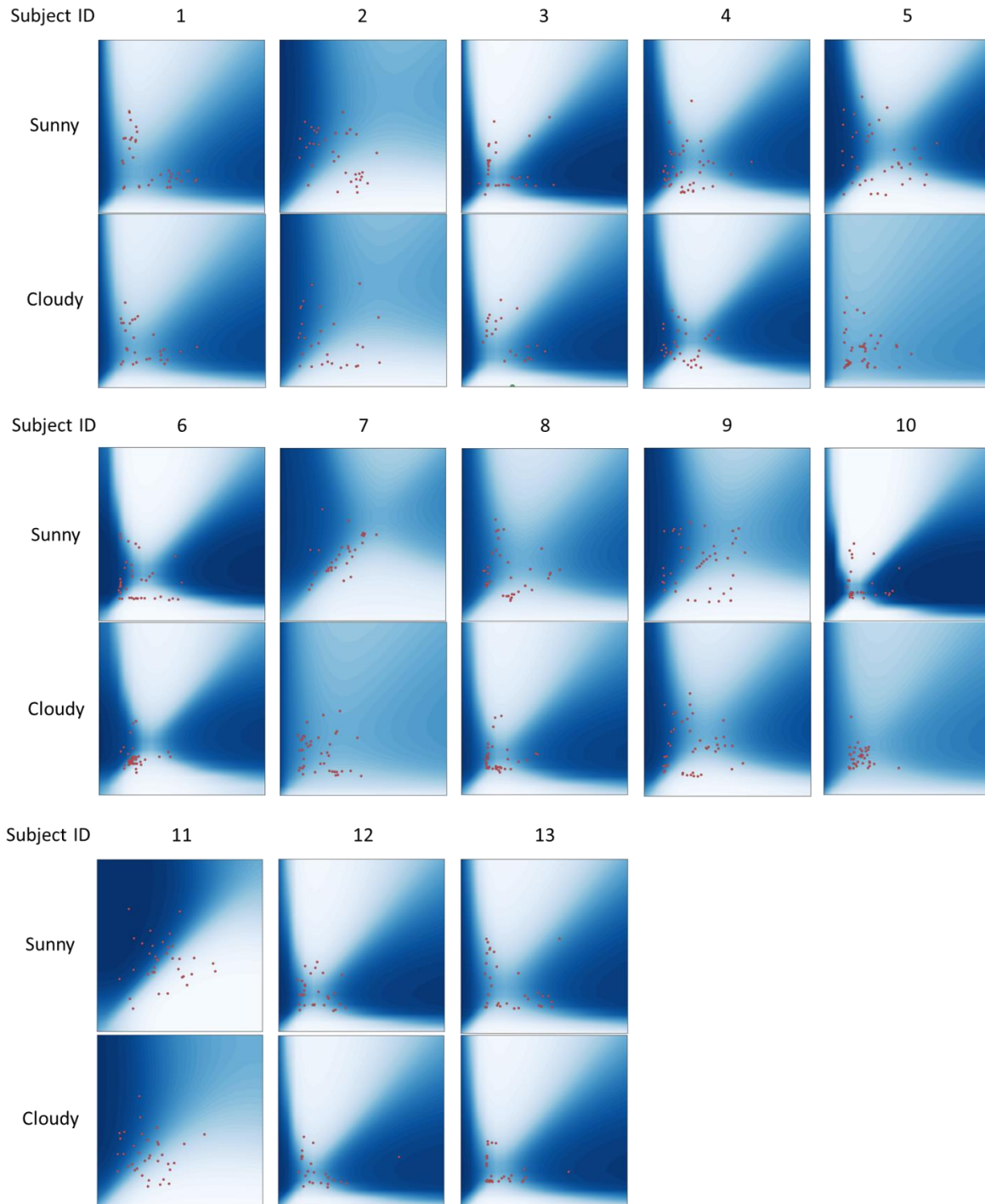


Figure 24 Preference profiles of 13 subjects in the final step.

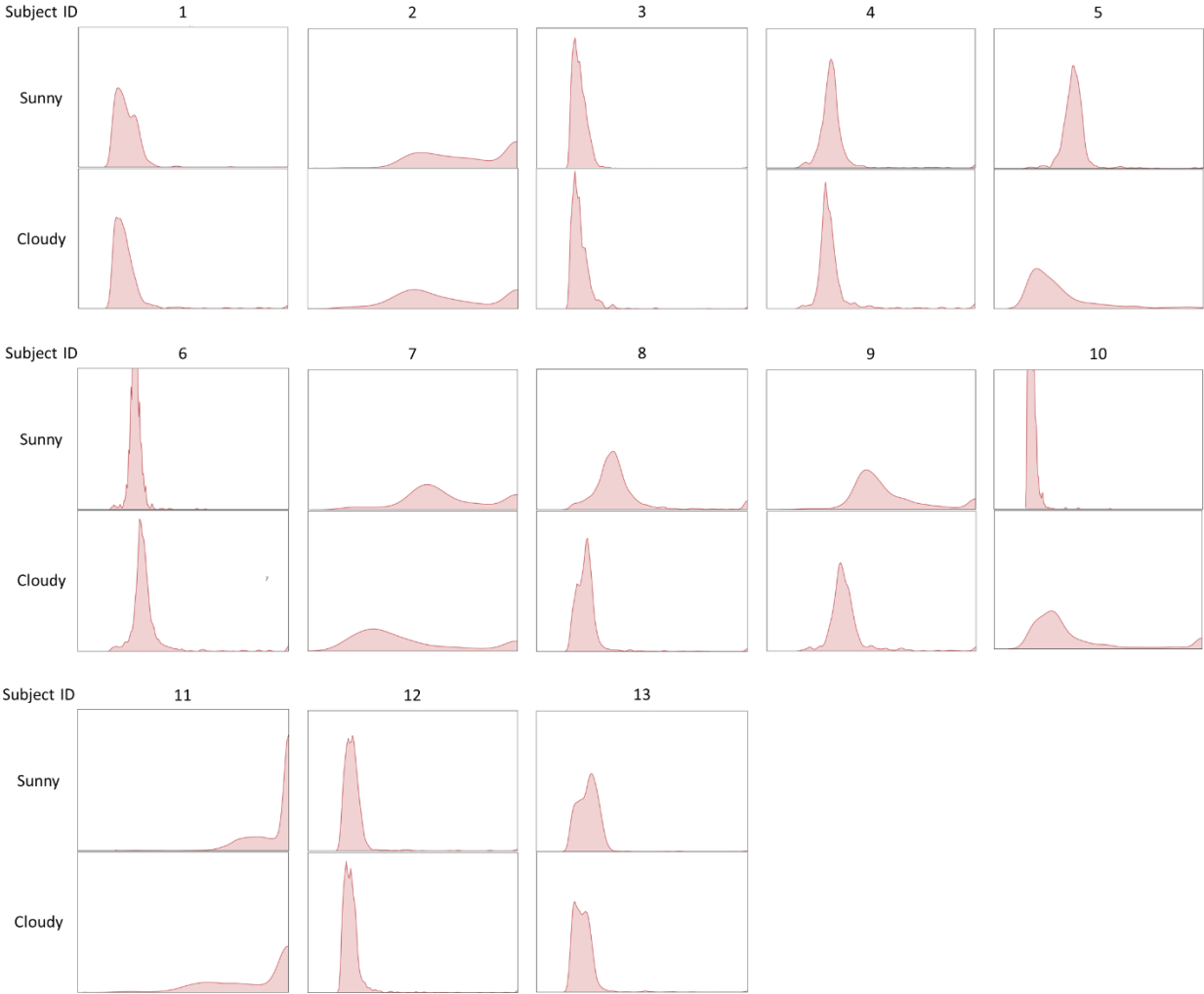


Figure 25 PDF of maximums of 13 subjects in the final step.

4.3.2.3 Learning efficiency

By investigating the evolution of entropy of maximum distribution, we could evaluate the learning efficiency of the preference elicitation framework for each subject, as shown in Figure 26. The axis labels are omitted to make the plots clear, and all the axes are consistent in range and scale (x-axis: 1 – 45 step; y-axis: 4.5 – 7.5 entropy). Most of the (Figure 26) models are converging below the criterion of $H=6.4$ except for subject 2 both sunny and cloudy models, subject 5 cloudy, subject 7 both sunny and cloudy models, subject 9 sunny model, subject 10 cloudy model and subject 11 cloudy model. There are several possible reasons. First, some subjects have complicated preference with other significant environmental factors not related to the brightness preference. For example, desire of outside view might have a conflict with darker preference. Second,

variations or change of preference of some subjects took place in the middle of learning process and the learning framework needed to re-adjust model for more steps. For example, subject 5 participated in two cloudy half-day session, and at the first few steps of the second session the learning curve had a deep turning-back (middle part of the curve) due to preference changes in two different days, which could be related to other factors (the first reason). Actually, similar phenomenon appeared in a few subjects' learning curves (subject 1 cloudy, subject 4 cloudy, subject 13 sunny), but the learning process re-adapted the model fast enough to again achieve converging results before the final step. Third, some subjects were insensitive to brightness, and answered preference survey randomly, especially with cloudy weather. Last but not least, some subjects had emotion-driven preference driven by the psychological effects brought from the controlled environment –these cannot be measured or observed easily.

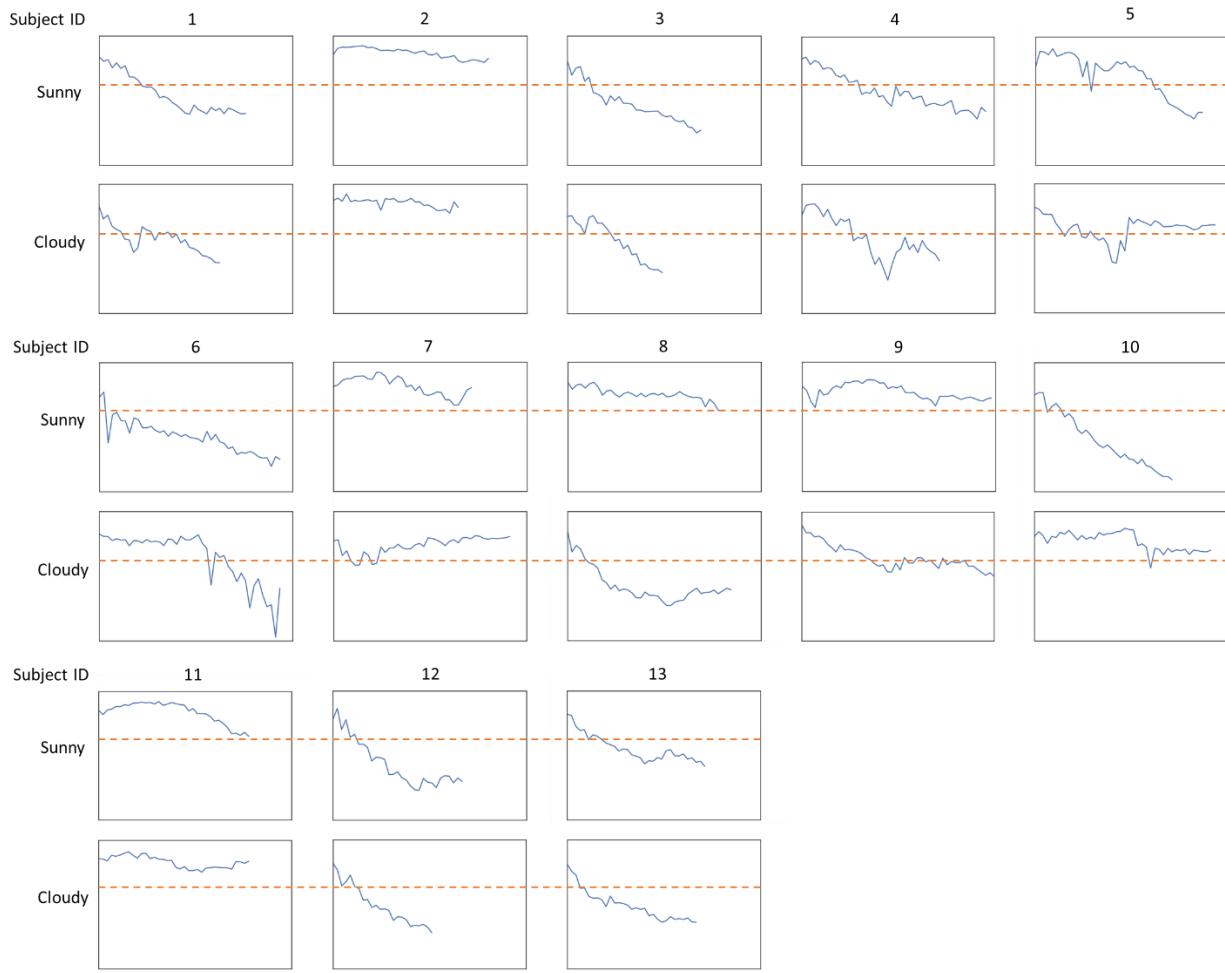


Figure 26 Learning curves of entropy evolution with steps (red dash line: “stop” criterion $H=6.4$).

Figure 26 also illustrates the learning speed and robustness for the proposed learning framework with different subjects. For those that learned model that has reached the “stop” criterion (and kept below), the fastest learning took less than 10 steps while the slowest took more than 30 steps. Nevertheless, these results demonstrate that the developed learning framework is able to learn a one-variable preference profile within one day (less than 45 steps) for most of the subjects. Note that these results are only applicable for this specific model (with one variable E_v) – when more variables are considered, more learning steps are required to collect enough data for higher-dimensional model, and the criterion will change according to the desire distribution of maximum in higher dimension space.

4.4 Summary and discussion

This chapter presents the design of an online visual preference elicitation learning framework for efficiently learning and eliciting occupants’ visual preference profiles and hidden satisfaction utilities. A set of experiments were designed and conducted to implement the proposed learning algorithm with human subjects in order to validate the feasibility and evaluate the performance. To determine the visual condition duel for preference query with most information gain, a combination of Thompson sampling method and pure exploration (uncertainty learning) method was used, addressing the balance of exploration and exploitation when targeting the near-maximum area of utility during the learning process. The experimental results demonstrated the feasibility and efficiency of the proposed visual preference learning framework. Distinctive visual preference profiles of 13 subjects were learned and studied under different weather conditions. Entropy of the distribution of the most preferred visual condition is computed for each learned preference profile to quantify the certainty, and used to evaluate the learning outcomes. Most of the subjects could be learned to an acceptable certainty level within one day with stable weather for visual preference model using E_v , and the preference profiles and learning speeds vary with different subjects.

Although the developed learning framework could be generalized with any visual preference model using sampling modeling methods, it is sensitive and dependent on selected visual environment variables and the performance of the visual preference model. In this study, specifically, vertical illuminance is the only variable used for demonstration purpose, and some of the learning results are limited by the one-variable model because other factors play more important roles in the subjects’ visual preference. Similarly, due to limitations of the modeling

approach, this study requires stable weather conditions, either sunny or cloudy, but could easily fail to learn visual preferences that are affected by weather (e.g. subject 5, 7, 8, 9, 10) with mixed or fluctuating weather conditions (when sunny model is intruded by cloudy model and vice versa), indicating that weather should be quantified by variable(s) (e.g. sky luminance distribution) and included in the visual preference model other than being a binary classifier for different modes of model. On the other hand, for practical considerations, including more variables to describe all possible environmental factors would increase the complexity of the visual preference model and thus the cost of learning, in terms of different aspects of implementation – computational efforts, time efficiency, large data requirement and advanced and non-intrusive sensing instruments. Some variables are even not quantifiable with current research or sensing techniques. Therefore, in real application, a proper visual preference model should be selected carefully considering the trade-off of accuracy and efficiency, as well as practical limitations.

5. PERSONALIZED DAYLIGHTING CONTROLS – AN OPTIMIZATION FRAMEWORK TO DYNAMICALLY BALANCE VISUAL SATISFACTION AND LIGHTING ENERGY USE IN DAYLIT OFFICES

5.1 Overview

In this chapter, a personalized shading control framework is developed to maximize occupant satisfaction while minimizing lighting energy use in daylit offices with roller shades. An integrated lighting-daylighting simulation model is used to predict lighting energy use while it also provides inputs for computing personalized visual preference profiles, previously developed using Bayesian inference from comparative preference data. The satisfaction utility and the predicted lighting energy use are then used to form an optimization framework. We demonstrate the results of: (i) a single objective formulation, where the satisfaction utility is simply used as a constraint to when minimizing lighting energy use and (ii) a multi-objective optimization scheme, where the satisfaction utility and predicted lighting energy use are formulated as parallel objectives. Unlike previous studies, we present a novel way to apply the MOO without assigning arbitrary weights to objectives: allowing occupants to be the final decision makers in real-time balancing between their personalized visual satisfaction and energy use considerations, within dynamic hidden optimal bounds. Essentially, we present the first method to incorporate personalized visual preferences in optimal daylighting control, with energy use considerations, without using generic occupant behavior models or discomfort-based assumptions.

5.2 Methodology

Figure 27 shows the overall flowchart of the methodology. The framework is based on a combination of model-based control and optimization schemes. First, models are required to compute the control objectives: lighting energy use (f) is predicted by an integrated daylight-electric lighting model, while the personalized satisfaction level is quantified by a satisfaction utility function (u) inferred from preference data. In our case, u was determined from comparative preference experiments (Xiong et al. 2018) described in Chapter 3. Both functions are multivariate and x in the figure refers to a vector of variables affecting energy use and/or satisfaction utility.

The modeling results then formulate the objectives towards optimal personalized daylighting (shading) control, following two application paths. In the single-objective optimization (SOO) path, the satisfaction objective is converted into a constraint when minimizing lighting energy use, resulting in a unique optimal set of conditions, x^* , achieved through shading operation, at each time step. In the multi-objective optimization (MOO) path, both objectives are used to provide a set of optimal solutions on a Pareto front at each time step. The optimal points are used to provide a pool of options to the users, who are then the decision makers in the final balancing between their personalized satisfaction limits and energy use. The entire process is discussed in the following sections.

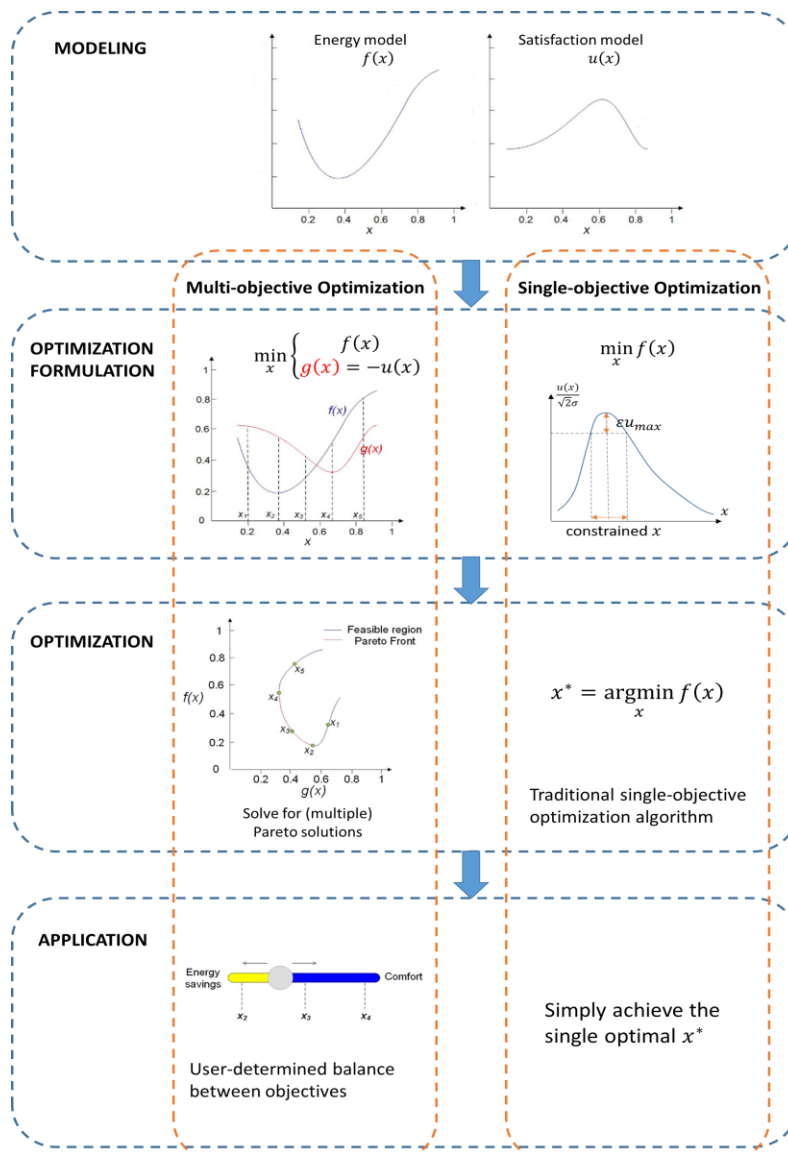


Figure 27 Overall methodology flowchart.

5.2.1 Models

5.2.1.1 *Integrated Daylighting and Lighting Energy Use Model*

A validated hybrid ray-tracing and radiosity daylight model (Chan and Tzempelikos 2012) was used for daylight simulation. The model combines the accuracy of forward ray tracing for direct light with the computational efficiency of radiosity for diffuse light entering the space and interior reflections. Angular direct-direct and direct-diffuse light transmission through windows and complex fenestration systems is enabled; for roller shades, an expanded semi-empirical model by Kotey et al. (2009) is employed, which has been repeatedly validated using integrated sphere measurements and full-scale experiments (Chan et al. 2015).

At each time step, incident beam and diffuse illuminance on the window (calculated or measured with sensors for real-time control, or using processed TMY3 data for an annual analysis) are used to compute transmitted beam and diffuse daylight. For real-time control, readings of transmitted illuminance and direct-diffuse portions of incident or horizontal solar radiation are needed as inputs. Xiong and Tzempelikos (2016) showed how this approach can be used for real-time, model-based shading control, which is used in this work. Interior daylight distributions are calculated along with vertical illuminance on the eye of the observer and dynamic glare metrics such as DGP (Wienold and Christoffersen 2006) as required. Note that vertical illuminance is an input to the visual preference models, described in the next section. Electric lighting is controlled based on work plane illuminance levels, using a set point (e.g., 300 lux based on IESNA recommendations (ref standard)), and mapping between horizontal (and vertical) illuminance and light dimming levels. Lighting energy use is then directly computed from light dimming levels at each time step.

For a given set of exterior conditions, the integrated daylighting and lighting energy model at each calculation step can be mathematically expressed as:

$$[P, E_v] = f(SP) \quad (58)$$

where P is the predicted lighting power (in W or W/m^2 of floor area); E_v is the vertical illuminance and SP is the roller shade position. Therefore, SP becomes the control variable.

5.2.1.2 *Personalized Visual Satisfaction Model*

The developed personalized visual satisfaction profiles described in Chapter 3 was adopted. Two inferred personalized satisfaction utility functions from previous results, reflecting different

overall visual preference characteristics discovered for each person, are used in this study. To demonstrate optimization results considering both reliability and efficiency, the two variable function with E_v and SP are selected, and sky condition is also used as a binary variable (cloudy vs sunny).

The normalized posterior medians of the two inferred satisfaction utilities (subject 1 and 4 from previous chapter, namely profiles A and B from now on), plotted as a function of E_v and SP in 3D space, are shown in Figure 28.

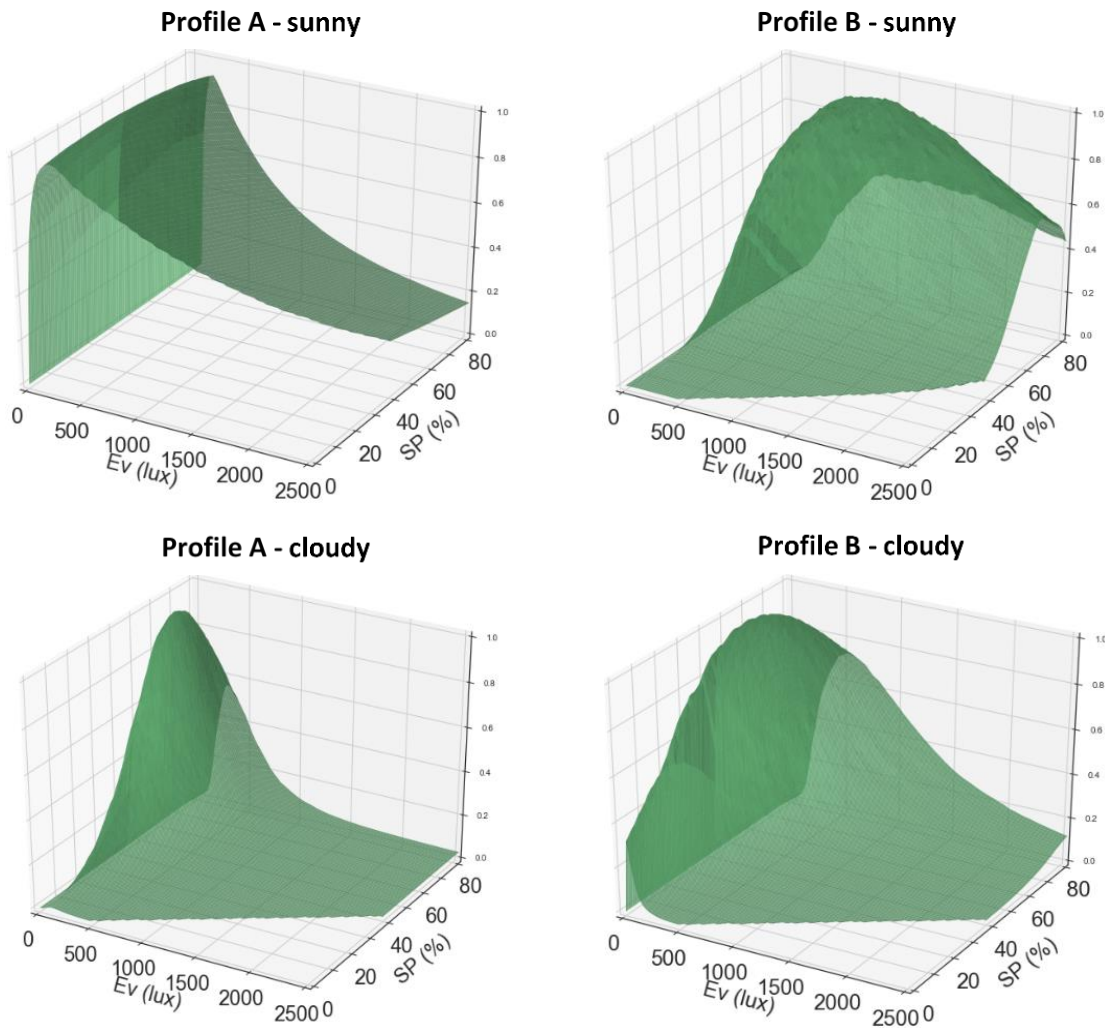


Figure 28 Posterior median of two inferred satisfaction utilities (E_v -SP model).

Under given outside conditions, E_v is determined by the shading position using the predictive lighting model. Therefore, the satisfaction utility eventually is a function of SP:

$$u(E_v, SP) = u(SP) \quad (59)$$

5.2.2 Optimization

The inferred personalized utility functions and the modeling results are used in an optimization framework to maximize visual satisfaction while reducing lighting energy use. Here we present two approaches as outlined in Figure 27. The first approach is to formulate two objectives (occupant satisfaction and lighting energy use) and use them in a multi-objective optimization scheme. The second approach converts one of the objectives (occupant satisfaction) into a constraint with certain tolerance, and formulates a single-objective optimization problem with the other objective (energy). The control variable of the optimization problems is the shading position (SP), ranging from 0 (fully open) to 1 (fully closed).

5.2.2.1 Multi-Objective Optimization (MOO)

The two objective functions (satisfaction utility and lighting power) are derived based on the daylighting/lighting energy model and the inferred satisfaction model at each time step. Figure 29 shows the transfer flowchart of variables between daylighting, lighting and satisfaction models, and the formulation of objectives. Note that E_v is an intermediate shared variable (output from the daylighting-lighting models and input to the satisfaction model), also used to formulate a glare constraint: $E_v \leq 2700$ lux. This value is based on the simplified daylight glare probability (DGPs, Wienold 2007) and it is a valid discomfort glare criterion when the sun is not within the field of view of the occupant (Konstantzos et al. 2016); otherwise, glare is bound to occur, and in the case of roller shades further indices have been proposed (Konstantzos et al. 2017). By controlling SP under specific sky conditions, we can predict light dimming levels and move across the 3-D utility curves.

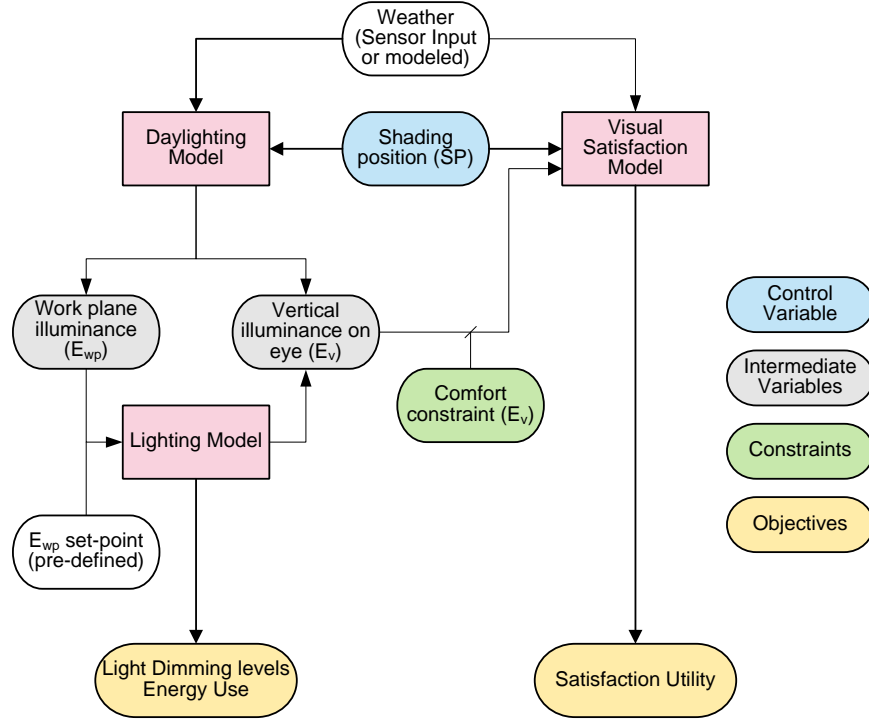


Figure 29 Models and variables transfer flowchart in optimization.

For ease of illustration, the objective of maximizing visual satisfaction is converted to minimizing the negative utility function. Note that the entire process runs as a function of time, to account for changing sky conditions.

$$\min_{SP} \begin{cases} -u(SP) \\ f(SP) \end{cases} \quad (60)$$

5.2.2.2 Single-Objective Optimization (SOO)

In the single-objective optimization scheme, the objective is to minimizing lighting energy (power) while maintaining the occupant satisfaction level near the maximum of the utility function. Therefore the satisfaction objective is converted into a constraint, using the personalized visual preference profiles and a relative tolerance (ε) of the maximum utility value. In addition, the randomness factor σ is considered in the satisfaction constraint in order to investigate the impact of sensitivity of individuals on energy savings potential. In this way, the “true” utility is reflected instead of the “standard” or unit utility, as inferred in the preference learning phase. The objective is then formulated as:

$$\min_{SP} f(SP) \text{ subject to: } \frac{u(SP)}{\sqrt{2}\sigma} \geq \max_{\xi} \frac{u(\xi)}{\sqrt{2}\sigma} - \varepsilon \max_{\xi} u(\xi) \quad (61)$$

The tolerance ε is selected as 0.1 in this study, representing 10% of the unit max utility, which equals to 1 based on the Gaussian bell form structure. The glare constraint is still required for the SOO at every time step.

5.2.2.3 Optimization Algorithm

The integrated lighting and personalized visual satisfaction models, as well as the multi-objective optimization formulation, were implemented in Matlab. Although several toolboxes with different algorithms are available, the optimization objectives in this study are dependent because of the shared variable (E_v): the satisfaction model requires this input from the lighting model as shown in Figure 29, and dependent objectives are not supported by most algorithms. Therefore, a simple enumeration method, fast and efficient, was adopted to solve both optimization problems. As enumeration aims at discrete variable problems, the shade position (our continuous control variable) needs to be approximated by dividing the full range into a specific number of discrete positions, without making a noticeable difference with respect to energy consumption and occupant preference perception.

The controlled variable can be pre-defined with discrete options as a feasible set (e.g., 21 positions with every 5% increments). The discretization depends on the continuity requirement of shading control and efficiency demand of the optimization algorithm. For example, 11 shade positions (10% increments) result in short computational time, while 101 positions (1% increments) simulate the continuous change of roller shade position perfectly. To compromise between computation efficiency and accuracy, 11 shade positions are pre-defined in this study with 10% increments from 0 to 1: $SP \in \{0, 0.1, 0.2 \dots 1\}$.

In the multi-objective optimization process, the two objective models run with all possible shade positions at each time step, and objective values are provided through the discretized feasible region. The optimization solutions are determined by comparing the feasible objectives in the way of Pareto optimality (if there exists no feasible solution that minimizes two objectives simultaneously): at each time step, SP does not belong to a Pareto solution if there is SP* for which:

$$-u(SP^*) \leq -u(SP) \text{ and } f(SP^*) < f(SP) + \tau \quad (62)$$

where $\{SP, SP^*\}$ are values of the controlled variable within the feasible region. Since perimeter offices with large window areas and daylight-linked controls result in low lighting energy use, differences in resulting lighting power between similar shading positions can be quite small. To address this problem, a tolerance (τ) was set to compare power objectives while

searching for the Pareto optimal. In this way, points with negligible differences in power consumption but lower visual satisfaction would be filtered out –as not part of Pareto solutions. In this study we just use a small tolerance of 0.1 W/m² (lighting power per floor area) since such difference is almost insignificant for lighting control and will not affect optimal points for lighting energy use. With these margins, the overall model runs as a function of the control variable (SP) to form real-time optimal solutions on a Pareto front, which describes the dynamic trade-off between the objectives, at each time step.

In the single-objective optimization process, the optimal at each time step is found from the minimum lighting power consumption among all the feasible points, given the visual satisfaction constraint. In rare occasions where no feasible point exists to meet satisfaction and comfort constraints, the visual satisfaction constraint is ensured, since it is a priority in optimal visual environments.

5.3 Results and Discussion

The effectiveness of the developed optimization strategies was studied through annual simulation for both SOO and MOO, using the two personalized satisfaction profiles (for real-time control, the model-based control strategy described in Xiong et al. (2016) can be used in conjunction with the optimization framework). For consistency reasons, the lighting models were applied to the same private offices used to experimentally derive the inferred satisfaction models. The offices information is described in section 3.2.1. The interior surface reflectivities are 80% (ceiling), 50% (walls) and 30% (floor). Light dimming levels are mapped to work plane illuminance levels on a specified grid at the desk height. The offices are located in West Lafayette, Indiana and TMY3 data for that location were used. A 15-minute time step was used for both lighting and the satisfaction models, as well as for the optimization algorithm, from 8:00am to 6:00 pm during weekdays, to consider working hours only. Shorter time steps are not realistic for practical shading control applications. The following section present representative optimization results for specific times, days, as well as annual evaluation.

5.3.1 Representative optimization results – single point in time

Figure 30 shows the MOO feasible points (dashed line) for a single representative time step (winter sunny day at 5:30 pm) with satisfaction Profile A. The units of the satisfaction utility

($-u$, plotted on the y-axis) are relative and not important, since the utility function is personalized and depends on the subject's sensitivity, σ . The lower the value on the plot, the higher the satisfaction utility value. The units of the lighting power (x-axis) are real.

For ease of understanding, the corresponding shading positions (the control variable) are shown next to the feasible points. The feasible points form a v-shaped curve, and theoretically the Pareto front should be the lower-left convex part of the feasible curve (SP=0, 0.1, 0.2, 0.3, 0.4). However, due to the tolerance added in the power objective and the discretization of SP, the actual Pareto optimals limit SP between 0.2 and 0.5, marked with solid dots in the graph.

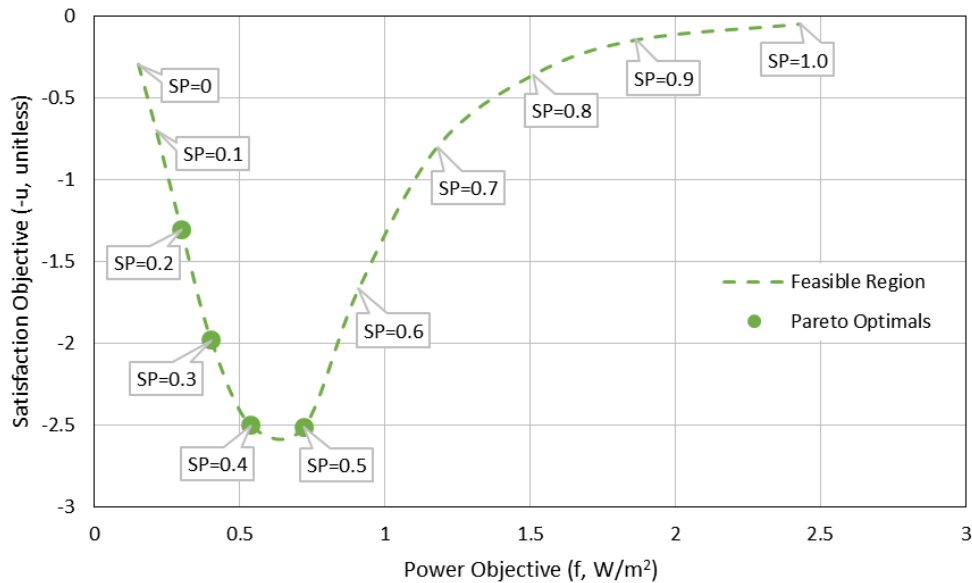


Figure 30 A representative Pareto front with optimal points (satisfaction profile A, single time step).

5.3.2 Time-varying Pareto fronts and optimal points

The optimization is based on dynamic lighting models; therefore, as the outside (sky) and interior (vertical and horizontal illuminance) conditions change, the shape of the feasible region in the objective space, the objectives' values, and the number of Pareto optimals will vary with time (computed every 15-min). Figure 31 shows the transition of the feasible region and the optimal points for two representative days, for both profiles. The solid dots are the Pareto optimals obtained from MOO, while the X marks are the optimal solutions obtained from the SOO at the same time steps.

The graphs show that the solutions are dynamic and depend on both the profile and real-time sky conditions. In both examples, the feasible region becomes narrower from 11:30am-3:30pm, and in some cases only a single Pareto optimal could be achieved with MOO –due to the shape of feasible curve and the tolerance in the power objective. The single optimization results are sometimes one of the Pareto optimals (e.g., at 9:30am and 5:30pm). In other time steps, searching for the maximum energy savings near the maximum satisfaction does not necessarily lead to one of the Pareto solutions, as the tolerance added in the SOO satisfaction constraint relaxes the satisfaction objective compared to the MOO strategy. Also note that transition from cloudy to sunny conditions during the same day (not shown in this graph) could also affect the results, since the satisfaction utility depends on the sky type.

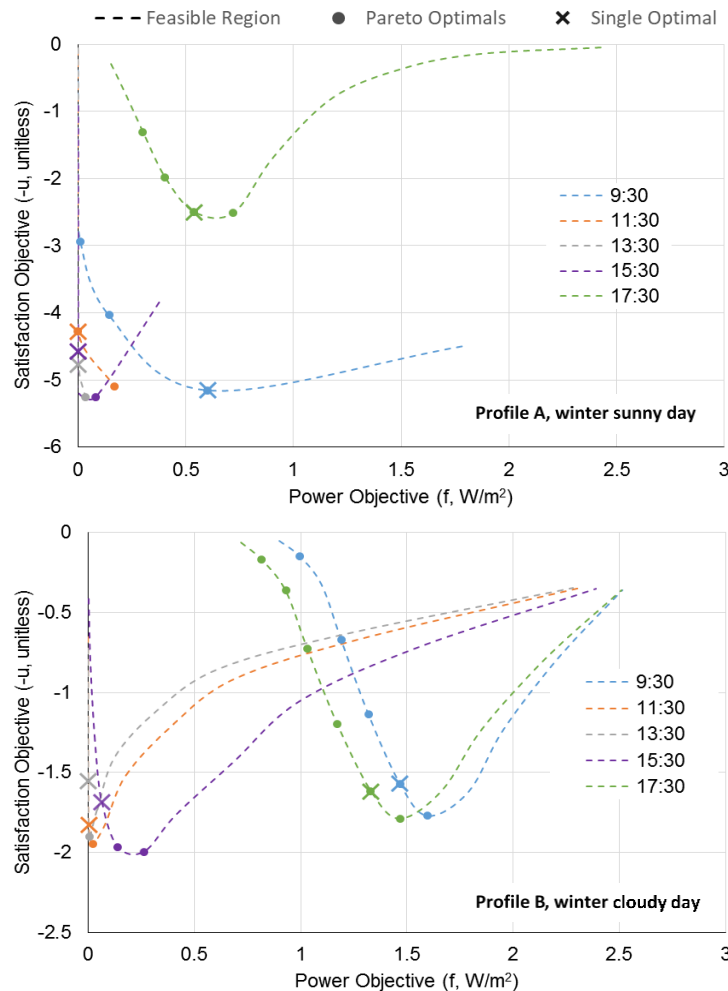


Figure 31 Transition of MOO feasible region (dashed lines) and Pareto optimals (solid dots), as well as single-objective optimals (marked with X) during representative winter days for satisfaction profile A (top) and B (bottom). Different optimal points correspond to different shading positions and interior lighting conditions.

5.3.3 MOO daily and annual results with different visual satisfaction profiles

The impact of weather conditions and different visual preference profiles on the multi-objective optimization results is shown in Figure 32. The optimal SP range is plotted for four days (8am to 6pm) of representative weather types– winter sunny (WS), winter cloudy (WC), summer sunny (SS), summer cloudy (SC) –for the climate of West Lafayette, Indiana. The results show a wider range of optimal SP during cloudy days, especially in winter time. During early morning and late afternoon hours, the glare constraint is more evident due to lower sun positions. Also, the optimal shade positions are seldom fully closed (SP=1), indicating the energy savings potential. The differences between the two visual satisfaction profiles are clear: Profile B, who is satisfied with a wider range of illuminance, allows a broader range of optimal shading positions compared to profile A, especially in the summer. The differences are more evident around the middle of the day, when the sun is higher in the sky and E_v can be modulated through shading control without significant glare constraints. The resulting optimal lighting power density does not exceed 2 W/m^2 , except when it's nearly dark outside.

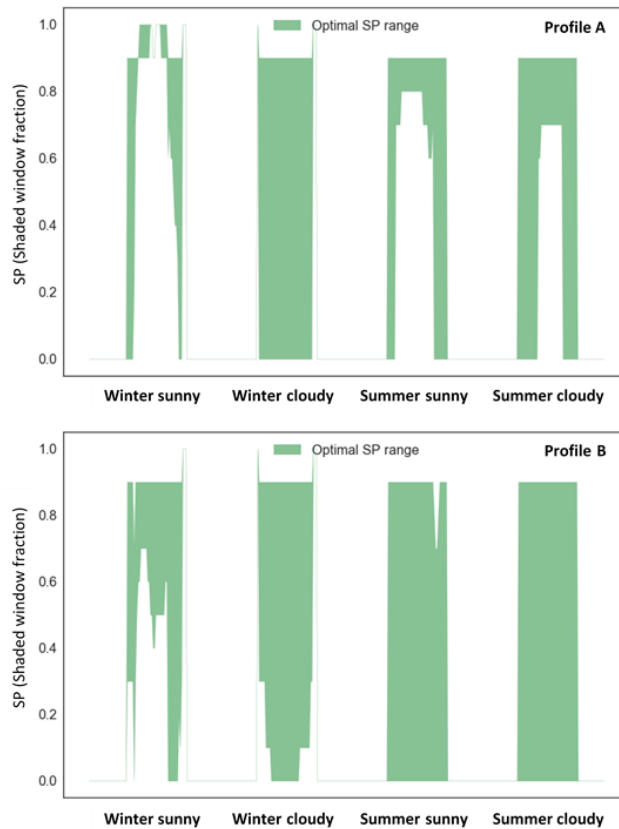


Figure 32 Daily range of optimal SP for the two visual satisfaction profiles under four different weather conditions.

Different preference profiles lead to different Pareto optimal patterns (number of optimal solutions and range of optimal) under various weather conditions through the year as shown in Figure 33. Closed shades appear occasionally in winter for both profiles, due to the glare constraint or due to lower illuminance preference at these times. As a result, lighting power is higher in winter (also because of darker days). The range of annual lighting energy use based on the MOO results is 3.9-29.7 kWh for profile A and 4.0-28.4 kWh for profile B. For reference, the annual lighting energy use for the same office without lighting control is 386 kWh. In the case of smaller or less transparent windows, the differences between the two profiles would be more evident.

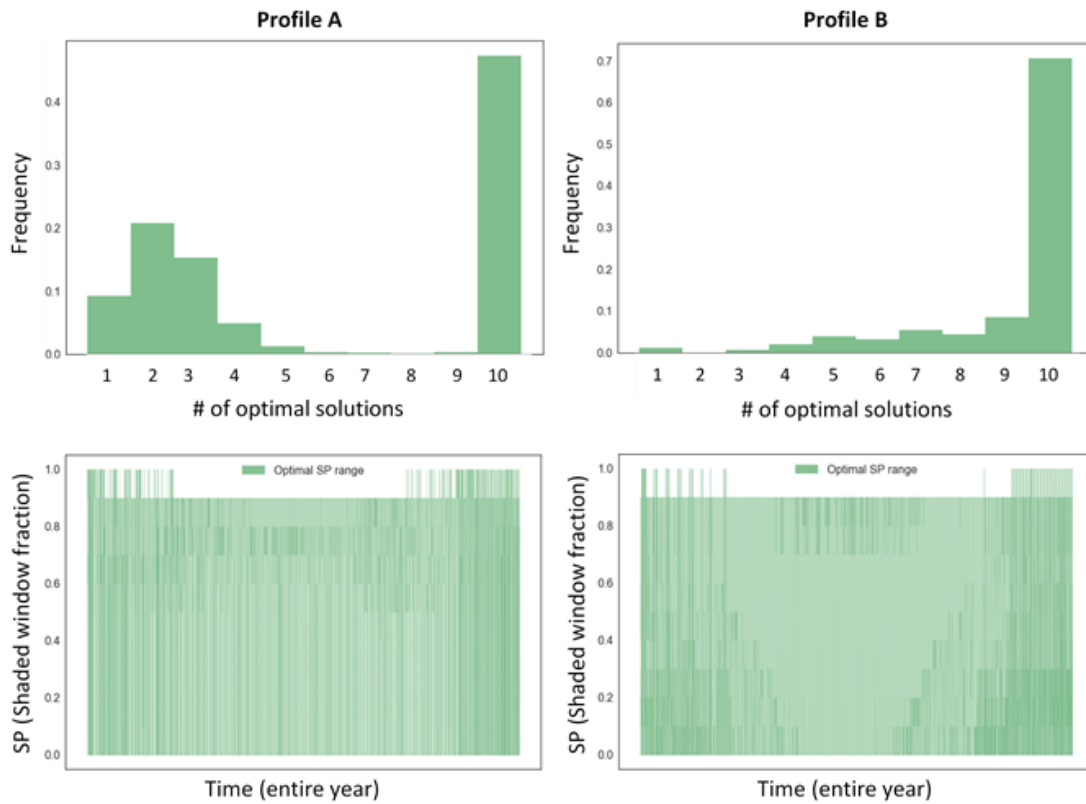


Figure 33 Histogram of optimal solutions (top) and optimal SP range (bottom) during the year with the two visual satisfaction profiles.

5.3.4 SOO daily and annual results with different visual satisfaction profiles

The impact of weather conditions and visual preference profiles on the single-objective optimization results is shown in Figure 34. The same daily weather profiles are used as before, and the optimal SP daily variations are plotted along with optimal lighting power and satisfaction utility. For the last two, the ranges between the optimal values and the values corresponding to

maximum satisfaction are also shown. The range of lighting power illustrates the potential energy savings when following the 10% satisfaction tolerance, while the range of optimal-to-maximum satisfaction level indicates the actual loss of relative satisfaction.

The graphical results are clearer compared to MOO since there are single optimal points in this case: optimal SP is clearly determined by the different personalized satisfaction profiles under the same sky conditions. As a result, the optimal lighting power is different between the two profiles, and allowing a 10% relative tolerance in satisfaction utility can save a noticeable amount of energy during daytime, especially for profile A. For profile B, who prefers brighter conditions, the maximum satisfaction aligns with minimum lighting power, particularly in the summer.

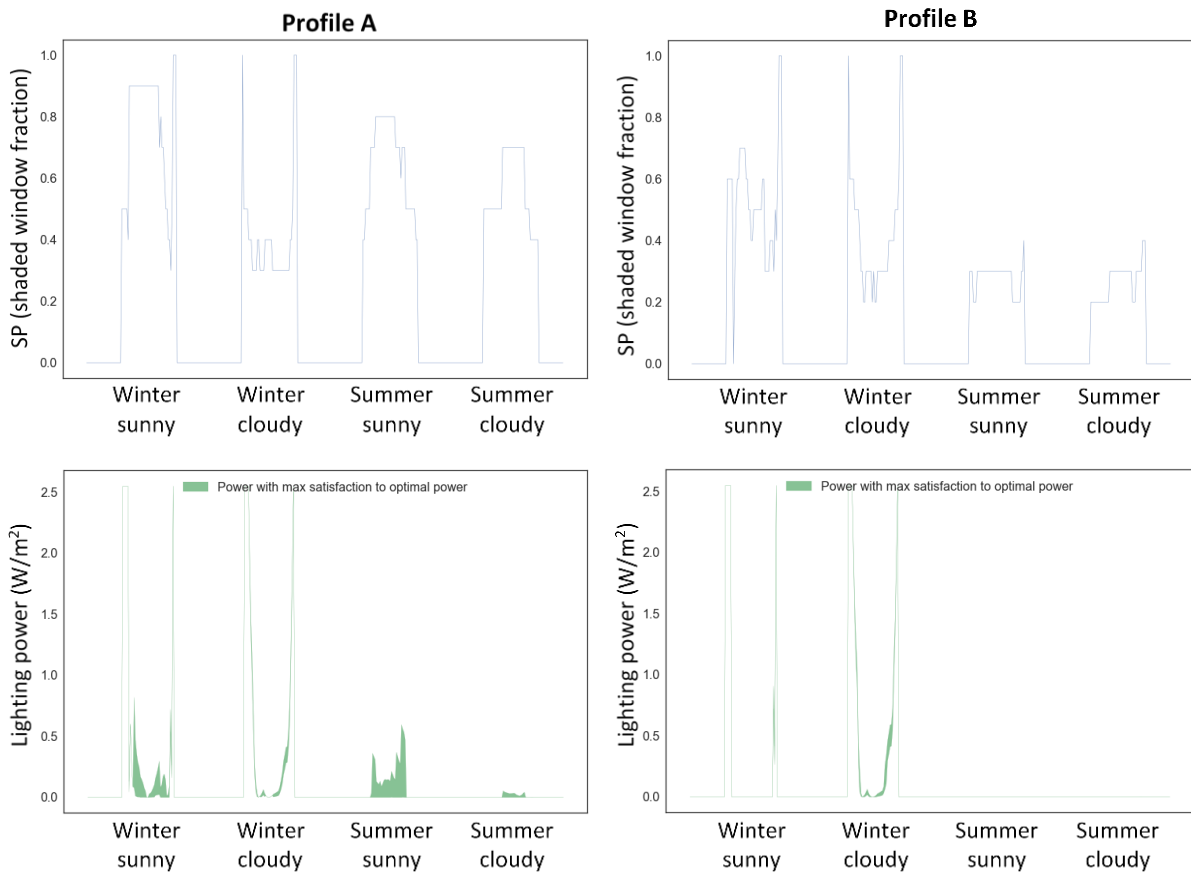


Figure 34 SOO daily results for the two visual satisfaction profiles under four different weather conditions: optimal shading position (top) and range between optimal lighting power and power corresponding to maximum satisfaction (bottom).

The annual SOO results are presented in Figure 35 for each visual satisfaction profile. The optimal SP for profile B allows significantly higher outside view (less shaded window fractions)

compared to profile A as expected, and thus the corresponding optimal vertical illuminance levels are higher and wider. With the glare constraint, optimal E_v values are always maintained below the threshold. The optimal E_v graphs are also useful to evaluate the consistency of optimization results with respect to the personalized profiles. Lighting power consumption is higher in the winter for both profiles, and the optimized annual lighting energy use is 7.6 kWh for profile A and 5.1 kWh for profile B.

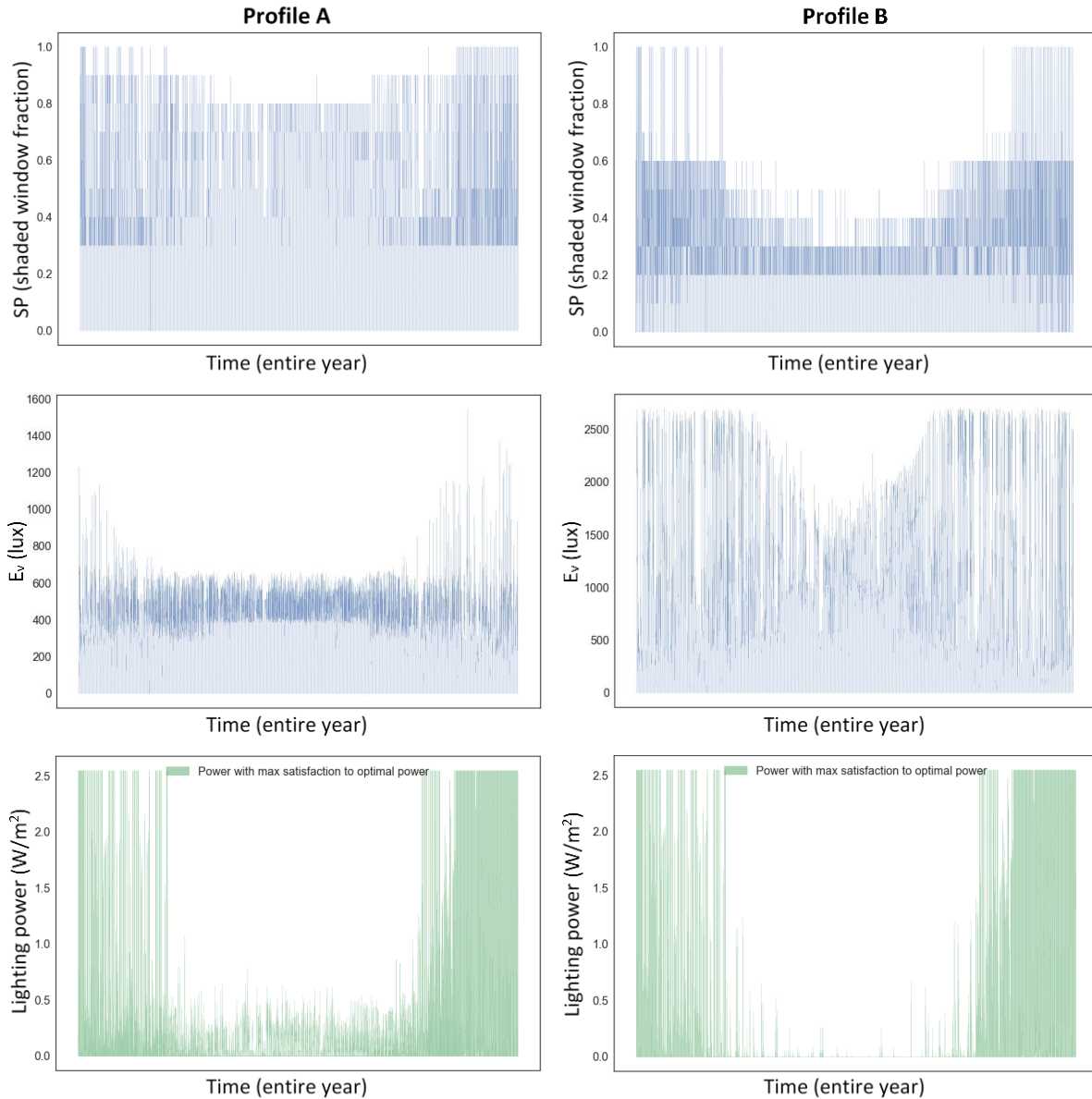


Figure 35 SOO annual results for the two visual satisfaction profiles: optimal shading position (top), optimal vertical illuminance (middle) and range between optimal lighting power and power corresponding to maximum satisfaction (bottom).

5.3.5 Effects of occupant's sensitivity (σ)

The personalized satisfaction utility functions include the parameter σ , which represents how sensitive each individual is to the utility function. This parameter has an effect on the utility curves, which in turn influence the optimal shading position and lighting energy use at every time step. An example of how the sensitivity variable impacts SOO results is shown in Figure 36. A representative satisfaction utility (profile A) is plotted as a function of shading position, for a typical winter sunny day at 5:30 pm. A virtual utility representing an occupant who has a same satisfaction profile but is less sensitive to the utility – with doubled σ – is plotted in the same graph. With smaller sensitivity, the 10% satisfaction constraint results in a wider range of feasible shading positions compared to the original utility. Following the 10% shading position increments, the optimal SP for that time (corresponding to the minimum lighting power), changes from 0.8 to 0.7. Therefore, more daylight is admitted and further lighting energy savings are realized for occupants who are less sensitive to the utility function. The dashed shows the corresponding lighting power consumption (right y-axis) as a function of SP for this specific time step. The additional annual lighting energy savings simulated with the virtual satisfaction utility (2σ) vs actual utility for profile A is 12% for the studied space and climate.

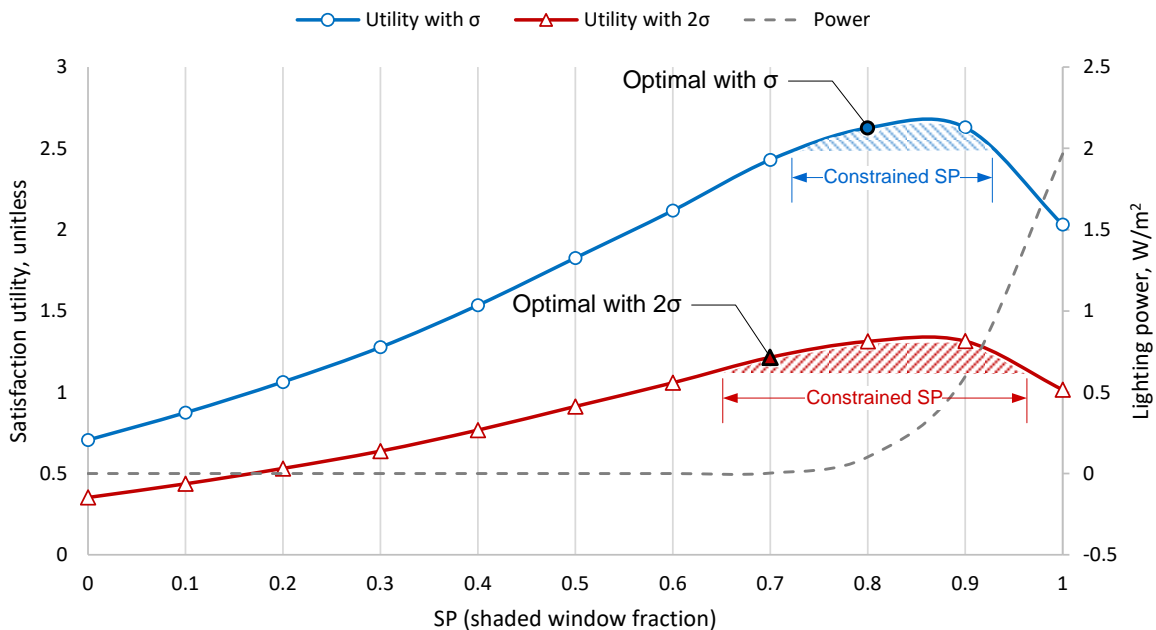


Figure 36 Effect of sensitivity to the satisfaction utility function on optimal shading position and energy savings.

5.4 Potential Application of Multi-Objective Optimization

The multi-objective optimization scheme is designed for application in perimeter offices with personalized shading and lighting controls. As the optimization usually provides a set of Pareto solutions, there are no standard rules for selecting a single “optimal” point for the control system from the solution set. Selecting one of the Pareto front points is equivalent to transforming the problem into a single-objective optimization with assigned weights for the objectives:

$$\min_{SP} \{-\omega \cdot u(SP) + (1 - \omega) \cdot f(SP)\}, \quad (63)$$

where $\omega \in [0,1]$. This approach has been followed in previous studies; however, any ad-hoc weighting of objectives by the control system is questionable when considering the trade-off between energy and comfort. Especially for personalized control, where the level of satisfaction is one of the objectives, and it changes with exterior and interior conditions, fixing arbitrary weights for individuals is meaningless.

To overcome this problem and implement personalized preferences in optimal controls, we propose a solution that comes from the MOO application, where variable weights determined by the occupants themselves are introduced. The optimal points found by the MOO at every time step are used to provide a pool of options to the users, who then become the final decision-makers in the real-time balancing between their personalized visual satisfaction limits and energy use. In this way, the users are able to adjust the trade-off between the two objectives, but always within their dynamic, personalized, optimal satisfaction bounds.

The MOO results provide a set of Pareto front points at each time step. Absolute energy and satisfaction numbers have no practical meaning to the occupants; therefore, the set of non-dominated points could be transformed into a set of sorted options ranging from “most satisfied” (corresponding to maximum satisfaction utility) to “highest energy-savings” (corresponding to minimum lighting energy use). These sorted points need to be provided as possible control options to the occupants using a simple, intuitive user interface.

A slider (Figure 37) can serve that purpose well: different points on the slider can be mapped to each optimal solution; in addition, the two ends of the slider will be mapped to the two extreme values of the Pareto front points (maximum satisfaction and minimum energy), and other intermediate points can be evenly sorted corresponding to their relative locations on the Pareto front between the two ends. In that way, override actions would fit into the optimal conditions range. Communication between the web interface and the building management and control

system is of course required for this application. Sliders “work best when the specific value does not matter to the user” (Aurora Harley) – the trade-off between personalized satisfaction and energy objectives influence the user decision, while the actual values do not. Therefore, the actual values on the bar are hidden to users; by sliding in any direction (changing shading and lighting controls), they will reflect the balance between objectives intuitively, within their personalized satisfaction limits, without being overwhelmed with information about different optimal points.



Figure 37 Example of a slider with hidden mapped optimal points within energy and satisfaction ends.

Since the number of Pareto front points varies with time, the number of options on the slider (possible control options) is variable –changes at every time step. At the extreme, there could even be only one option when there is a single global optimal from the MOO results. For that purpose: (i) the application needs to be updated in real-time, so that new optimal points are calculated and (ii) in each time-step, the new Pareto front points need to be sorted, mapped and evenly distributed on the slider, and (iii) dynamic snapping features should be enabled on the slider to select the Pareto optimal closest to the current bar position every time, always hidden to the users.

An example is shown in Figure 38 for profile A during a winter sunny day. Suppose that we have run the MOO through this day and obtained the Pareto fronts for several time steps (two shown here for ease of illustration). The Pareto points correspond to different shading positions (also marked on the graph), which are “mapped” on the slider at each time step (different positions are mapped each time, and their order and number can change with time). This information is hidden to the user.

At 11:30 am, optimal results can be obtained with two shading positions: 90% and 100%. In this case, the two ends of the bar automatically correspond to these two positions, mapped to the Pareto points corresponding to maximum savings and maximum satisfaction respectively. If the user moves the slider anywhere towards the satisfaction end, the shades will move to fully closed (SP=1); otherwise, they will move to 90% position to minimize energy use. At 5:30 pm,

optimal results can be obtained with four shading positions, from 20% to 50% closed. In this case, the bar will have 4 hidden points mapped to these conditions, evenly distributed on the slider, ranging from minimum energy to maximum satisfaction Pareto point. When the user moves the slider, the shades will move to the position closest to the mapped corresponding optimal on the bar, using a snapping feature. If the user does not change the position of the slider, the shades will still automatically move at each time step to achieve optimal conditions (since these change with outside conditions). In this example, if the user selects to keep the position of the slider as shown from 11:30 am to 5:30 pm, the shades would automatically move to 100% at 11:30am and 40% at 5:30 pm.

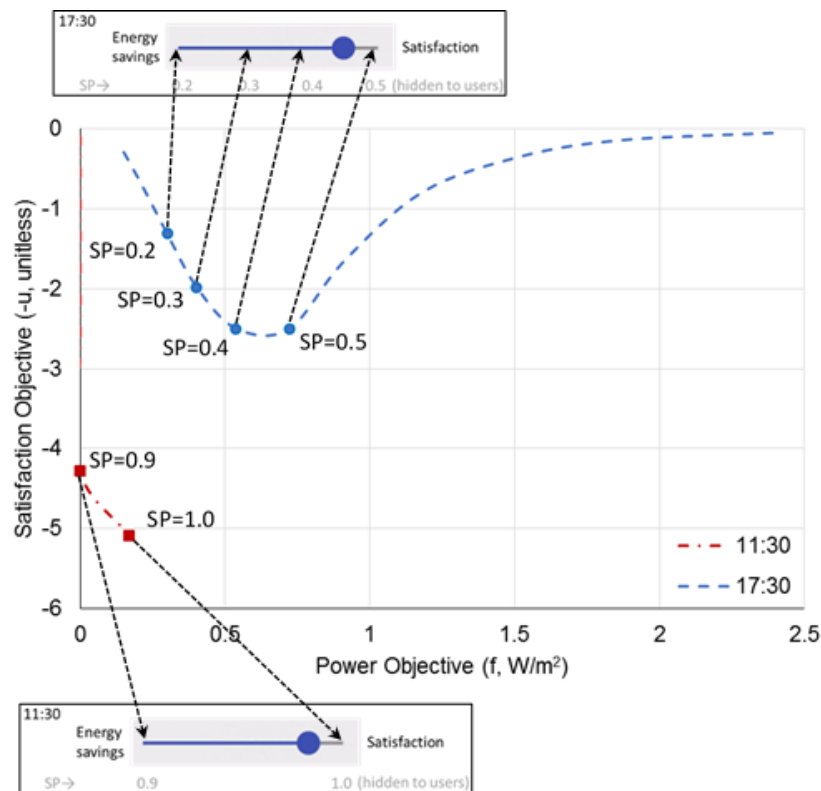


Figure 38 User-enabled application of MOO in personalized shading and lighting control. Example of mapped optimal conditions on the user interface for two different times, with the slider bar ends corresponding to maximum energy savings and maximum satisfaction respectively, at each time step.

This application can also be used for learning user preferences through interactions with the slider interface. Previous studies have shown that personalized feedback can positively affect individuals towards energy savings. Therefore, providing some indicative information, i.e.,

relative “gains” between the two extreme Pareto front points, as illustrated in Figure 39, might help in understanding how occupants are influenced towards energy conservation using this interface that considers their satisfaction. In this case, they would know that all possible positions on the slider still correspond to optimal solutions, and the relative increment for each objective can be provided by comparing the objectives’ values at the slider ends (extreme Pareto points).

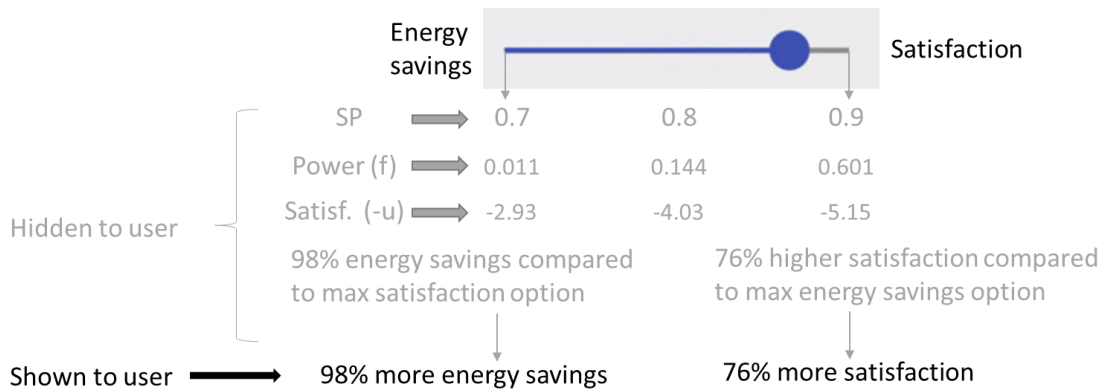


Figure 39 Possible indicative information provided in the optimization application to study the influence of feedback on users.

The implementation of the proposed control framework could be challenging: the real-time learning and actual control intervals should be coordinated. Therefore, adaptive and online learning methods should be applied for updating the personalized models with occupant feedback during the optimization implementation –this is the next phase of this work.

6. FUTURE WORK

6.1 Improving the Personalized Visual Preference and Satisfaction Model

Improving the preference model is a fundamental and long-term work. First, the variables used in the personalized visual preference and satisfaction model in chapter 3 are still limited. More data from different buildings should be collected for training personalized visual preference and satisfaction models, and data with new variables should be measured at the same time with improved sensing networks. New variables will include: 1) luminance distribution measured by HDR camera installed on window that captures the real-time weather conditions (diffuse/direct light components, sky cover), 2) electric lighting variable with two options – electric light dimming level provided by control system and ratio of electric light to day light calculated by daylighting and lighting model, 3) detailed luminance distribution in the field of view (FOV) using a HDR camera with a fisheye lens near subject’s eyes or in other non-intrusive locations.

The model will be improved in several aspects: 1) by using more flexible model structure for the satisfaction utility function such as Gaussian process model; 2) by including the new variables; 2) by introducing auto-selecting techniques for selection of significant variables; 3) by adding hidden variables to account for unmeasurable and/or uncertain variables.

6.2 Integration of Learning and Control

A more prominent question is how to embed the visual preference learning into daylighting and/or lighting control systems, for real-world practical applications. The flowchart in Figure 40 presents a potential implementation of integration of the proposed visual preference learning framework and any optimal daylighting control framework utilizing visual preference model. It’s not realistic to simultaneously run both frameworks as the objectives of learning and control could be conflicting – the iterative exploring-exploiting feature of the proposed learning framework requires achieving unsatisfying visual conditions as satisfying conditions region has lower uncertainty with exploitation, contradicting optimal controls that attempt to satisfy occupant. Therefore, the idea of the integration is to design a “switch” that links the frameworks and is able to (i) turn the system to learning mode, when the preference model is not available or has high uncertainty, and (ii) switch to control mode to satisfy the occupant when the preference model is

adequate. The basic principle is to use the “stop” criterion as a threshold to switch the working framework. In the control framework, an override option should always be provided to the occupant, not only to meet any personal demand, but also to adapt the preference model based on the new preference data translated from the actions. By updating the preference, the control framework could evaluate the performance of the model in the same way of the learning framework, by calculating the entropy (of the PDF of utility maximum). When the calculated entropy is higher than the “stop” criterion – a tolerance is added ($H > 6.4 + \tau$) to reduce the random effects of modeling approach (sampling method), and consecutive steps (e.g. 3 steps) exceeding the criterion are required to avoid the random effects from occupant and learning method – the optimal control is paused and learning framework starts working. In each learning step after model updating, the entropy is compared to the criterion – again with a tolerance and successive violation judgement – and the optimal control takes over visual environment tuning if the criterion is met ($H < 6.4 - \tau$ for 3 consecutive steps), or continues to the next learning step if the entropy is still high or not converging yet.

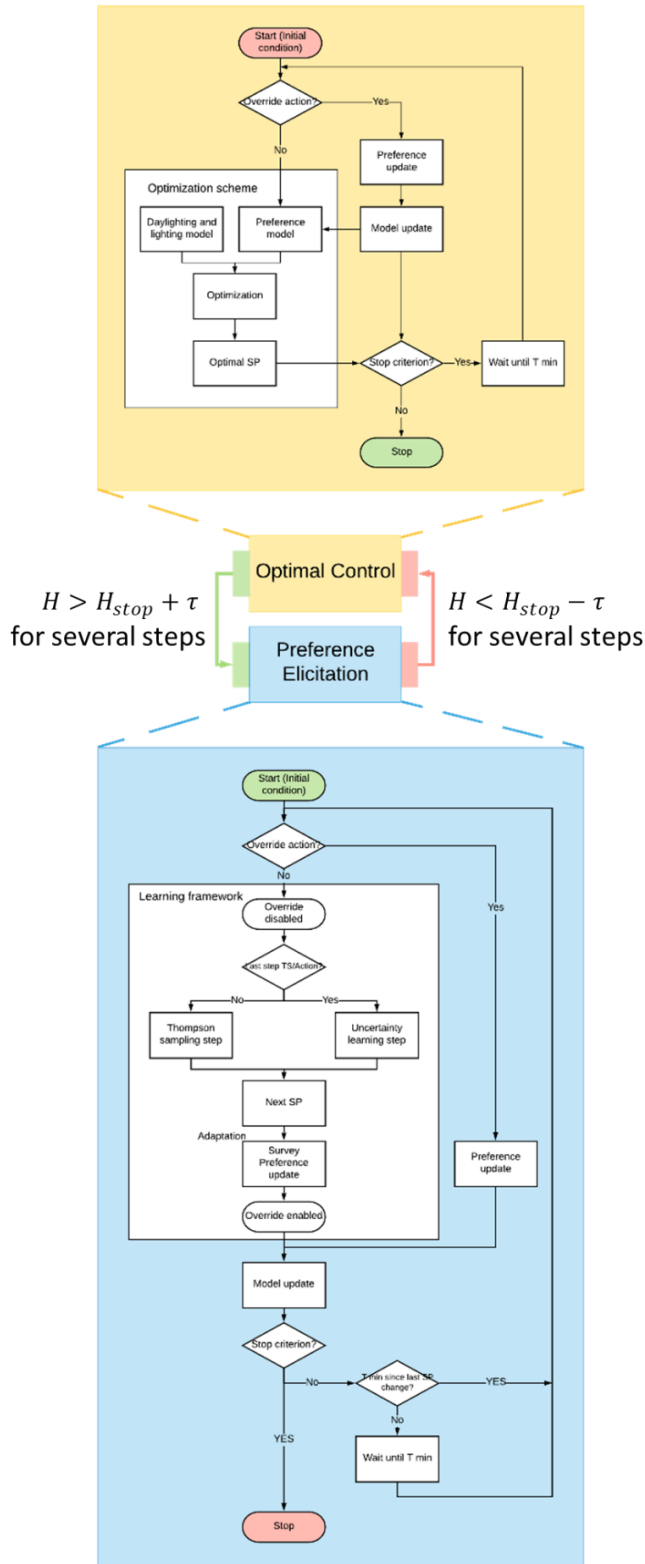


Figure 40 Integration of visual preference learning framework and optimal daylighting control framework.

6.3 Implementation and Evaluation of the Proposed Optimal Personalized Daylighting Controls

Future experiments should be conducted to investigate the feasibility and to evaluate the effectiveness of the proposed control application of MOO introduced in Chapter 5 and its integration with learning framework presented in Chapter 4. The whole system-level framework including a non-intrusive, low-cost sensing network, online learning and updating, optimal control and interface will be carefully designed and integrated, and then implemented in test offices with human subjects. Improved visual preference models will be adopted in the learning framework and the optimization process. Decision of control intervals in sensing, learning, optimization and control will be studied and tested. A friendly and understandable user-interface will be designed and deployed for preference acquisition from subjects, access to override, decision making of personalized optimal by subjects and providing valuable feedback to subjects.

6.4 Integrated Optimal Control for Coordinated Daylighting, Lighting and HVAC Systems Operation Considering Personalized Visual and Thermal Preferences and Energy Use

Although this dissertation focuses on visual preference and satisfaction and lighting energy use, the complete learning, modeling and control framework could be extended to involve thermal preferences and HVAC energy consumption. The integration of different satisfaction models, physical and/or energy models can be challenging when more variables (that might be inter-dependent) are involved. Moreover, the increase of dimensions in both controlled variables and objectives requires more complex optimization algorithms and more comprehensive control decision considerations. For that purpose, simulation studies should be conducted with all the above models plus a building model related to thermal dynamics, HVAC energy use and thermal preference model, using synthetic data, followed by experimental studies and implementation.

APPENDIX A. SURVEYS

Survey for preference modeling experiment

| | |
|--|---|
| 1.1 How do you prefer the overall visual conditions? <ul style="list-style-type: none"><input type="radio"/> I prefer the current visual conditions<input type="radio"/> I prefer the previous visual conditions<input type="radio"/> No preference between these two conditions | 2.1 Do you experience any glare problems? <ul style="list-style-type: none"><input type="radio"/> No glare<input type="radio"/> Slight glare<input type="radio"/> Significant glare<input type="radio"/> Intolerable glare |
| 1.2 How do you prefer the amount of light (light levels) in the room? <ul style="list-style-type: none"><input type="radio"/> I prefer the current light levels<input type="radio"/> I prefer the previous light levels<input type="radio"/> No preference between these two conditions | 2.2 How do you prefer the level of outside view? <ul style="list-style-type: none"><input type="radio"/> I prefer the current amount of outside view<input type="radio"/> I prefer the previous amount of outside view<input type="radio"/> No preference between these two conditions |
| 1.3 How do you prefer the mix of natural and electric lights? <ul style="list-style-type: none"><input type="radio"/> I prefer the current mix<input type="radio"/> I prefer the previous mix<input type="radio"/> No preference between these two conditions | 3.1 What would you do if you could move the shades? <ul style="list-style-type: none"><input type="radio"/> I would raise the shades<input type="radio"/> I would lower the shades<input type="radio"/> I would NOT move the shades |
| 1.4 Do the lighting conditions interfere with your computer work? <ul style="list-style-type: none"><input type="radio"/> They help improve my focus/comfort/efficiency<input type="radio"/> They distract me / make me uncomfortable<input type="radio"/> No interference | 3.2 What would you do if you could adjust the electric light level? <ul style="list-style-type: none"><input type="radio"/> I would increase the electric light level<input type="radio"/> I would decrease the electric light level<input type="radio"/> I would NOT adjust the light level |

Survey for preference learning experiment

Visual comfort Survey

Subject ID:

1. How do you prefer the overall visual environment, comparing the previous and current condition, before and after changing the shade position or lighting level?

- I prefer the current condition.
- I prefer the previous condition.
- No preference between these two conditions.

2. Do you perceive glare now?

- Yes.
- No.

APPENDIX B. PREFERENCES AND UTILITY THEORY

Classical decision theory deals with making optimal decisions taking into account uncertainty in the outcomes. It is based on the assumption that complete user preferences are known to us (Berger, 2013). Therefore, it is essential to understand user preferences in order to make optimal decisions. Due to difficulty in working with human preferences, a utility function is introduced over it. This utility function maps each instance/state or item to a real value and compares different instances/states/items based on their utility function values (Guo, 2011). Von Neumann and Morgenstern (2007) show that if one has preferences defined over outcomes that have uncertain consequences, there is a utility function that assigns a utility to every outcome that represent these preferences. Therefore, utility functions allow us to directly compare arbitrary states/items and reduce the complexity of preference learning framework. In order to formally define preferences and several axioms/theorems related to it, we follow the review examples given in Guo (2011) and Sanders (2015).

Preference Relations

In our problem, preference relations are an intuitive way of thinking about how people rank different visual conditions inside an office. We talk about preferences by mainly using three binary relations: $>$ (strictly preferred to), \sim (indifferent between) and \succcurlyeq (preferred to or indifferent between). Reviewing Von Neumann and Morgenstern's (2007) axioms related to preference relations:

- Completeness: it implies that given two states of visual conditions in the room (p,q) , our preference relation can compare and rank them as either $p \succcurlyeq q$ or $p \preccurlyeq q$.
- Transitivity: If a user prefers p to q , and prefers q to r in the meantime, then it holds that the user prefers p to r , i.e. $p \succcurlyeq r$.
- Continuity: Given strict preferences over any three states, i.e. $p \succ q \succ r$, there exists a linear combination of the most and least preferred states such that $ap+(1-a)r \succ q$ and $r \succ bp+(1-b)q$ where $a,b \in [0,1]$.
- Independence: Preference relation between two states p and q remains unchanged when they are combined in the same way with a third state.

Provided that the preference pairwise comparison dataset satisfies these four axioms, Von Neumann and Morgenstern's (2007) main existence theorem states that there exists a utility function that represents preferences (over different visual states in the room for our problem).

Utility Functions and Monotonic Transformations

As we stated in the previous section, preferences can be easily described with the help of utility functions. A utility function assigns scalar values to all states so that, if we have a preference relation between p and q state as $p \succ q$ then we have $u(p) > u(q)$. For drawing inferences from the utility function values, all that matters is ordinal ranking, and not cardinal ranking. In Economics, an ordinal ranking is a function representing the preferences of a consumer on an ordinal scale. The ordinal utility theory claims that it is only meaningful to ask which option is better than the other but it is meaningless to ask how much better it is (Calhoun, 2002). Put simply, the scalar numerical utility function values we obtain only matter in the context that we can say one utility level is higher than the other, but the actual values do not mean much. For example, if $u(p) = 100$ and $u(q) = 500$, we cannot say that q is five times as good as p (cardinal statement). We can only say that q is preferred to p .

Utility function $u(\cdot)$ is affine i.e. there can be multiple utility functions that describe the same set of preferences. One property of utility functions is that if $u(p)$ is a valid utility and $f(\cdot)$ is a monotonically increasing transformation (e.g. exponential functions), then $f(u(p))$ is also a valid utility function.

In summary, it is useful to operate on preference relations with the use of utility function. It assigns a scalar value to a state as a representation of its utility. Consequently, utility functions allow a mathematical framework for preference learning. In addition, one can handle uncertainty associated with preferences by introducing Bayesian models for practical problems (Guo, 2011).

APPENDIX C. OTHER PREFERENCE ELICITATION METHODS

Based on the relationship between utility function and preference probability, the original PI is equivalent to:

$$PI = p(u(\mathbf{x}_t^*) < u(\mathbf{x})).$$

To account for exploration, previous studies tried to modify the acquisition function by adding a trade-off parameter $\xi \geq 0$:

$$PI = p(u(\mathbf{x}_t^*) + \xi < u(\mathbf{x})).$$

Higher ξ leads to more exploration to help avoiding local maximum. However, the selection of tuning of ξ is arbitrary and sensitive to the objective, which requires expertise and excessive effort to balance between efficacy (finding global maximum) and efficiency.

An alternate acquisition function, the expected improvement (EI). EI, is more promising as it captures both the probability and the magnitude of improvement (Mockus et al. 1978):

$$EI(\mathbf{x}) := \mathbb{E}(\max\{0, u(\mathbf{x}|\theta_t, \mathcal{D}_t) - u(\mathbf{x}_t^*|\theta_t, \mathcal{D}_t)\})$$

However, the formulation of EI does not support bounded utility function with fixed scale, while the adopted utility (Eq. (34)) always has a maximum value of 1 ($u(\mathbf{x}_t^*|\theta_t, \mathcal{D}_t) \equiv 1$), which would trap the exploitation at a fixed \mathbf{x} after the first step.

REFERENCES

- Agha-Hossein, M. M., El-Jouzi, S., Elmualim, A. A., Ellis, J., & Williams, M. (2013). Post-occupancy studies of an office environment: Energy performance and occupants' satisfaction. 2
- Agrawal, S., & Goyal, N. (2012, June). Analysis of thompson sampling for the multi-armed bandit problem. In Conference on Learning Theory (pp. 39-1).
- Aries, M. B., Veitch, J. A., & Newsham, G. R. (2010). Windows, view, and office characteristics predict physical and psychological discomfort. *Journal of Environmental Psychology*, 30(4), 533-541.
- Arsenault, H., Hébert, M., & Dubois, M. C. (2012). Effects of glazing colour type on perception of daylight quality, arousal, and switch-on patterns of electric light in office rooms. *Building and environment*, 56, 223-231.
- Asadi, E., da Silva, M. G., Antunes, C. H., & Dias, L. (2012). A multi-objective optimization model for building retrofit strategies using TRNSYS simulations, GenOpt and MATLAB. *Building and Environment*, 56, 370-378.
- Ascione, F., Bianco, N., De Stasio, C., Mauro, G. M., & Vanoli, G. P. (2016). Simulation-based model predictive control by the multi-objective optimization of building energy performance and thermal comfort. *Energy and Buildings*, 111, 131-144.
- ASHRAE Standard Committee. (2013). *Ashrae handbook: fundamentals 2013*.
- Aston, S. M., & Belichambers, H. E. (1969). Illumination, colour rendering and visual clarity. *Lighting Research & Technology*, 1(4), 259-261.
- Athienitis, A. K., & Tzempelikos, A. (2002). A methodology for simulation of daylight room illuminance distribution and light dimming for a room with a controlled shading device. *Solar Energy*, 72(4), 271-281.

- Bakker, L. G., Hoes-van Oeffelen, E. C. M., Loonen, R. C. G. M., & Hensen, J. L. M. (2014). User satisfaction and interaction with automated dynamic facades: A pilot study. *Building and Environment*, 78, 44-52.
- Bellia, L., Cesarano, A., Iuliano, G. F., & Spada, G. (2008). Daylight glare: a review of discomfort indexes.
- Berger, J. O. (2013). *Statistical decision theory and Bayesian analysis*. Springer Science & Business Media.
- Bergstra, J., & Bengio, Y. (2012). Random search for hyper-parameter optimization. *Journal of Machine Learning Research*, 13(Feb), 281-305.
- Bichiou, Y., & Krarti, M. (2011). Optimization of envelope and HVAC systems selection for residential buildings. *Energy and Buildings*, 43(12), 3373-3382.
- Bijl, H., Schön, T. B., van Wingerden, J. W., & Verhaegen, M. (2016). A sequential Monte Carlo approach to Thompson sampling for Bayesian optimization. arXiv preprint arXiv:1604.00169.
- Bilionis, I., & Koutsourelakis, P. S. (2012). Free energy computations by minimization of Kullback–Leibler divergence: An efficient adaptive biasing potential method for sparse representations. *Journal of Computational Physics*, 231(9), 3849-3870. doi:10.1016/j.jcp.2012.01.033
- Birlutiu, A., Groot, P., & Heskes, T. (2013). Efficiently learning the preferences of people. *Machine Learning*, 90(1), 1-28.
- Bishop, C. M. (2006). *Pattern recognition and machine learning*: springer.
- Bock, R. D., & Jones, J. V. (1968). *The measurement and prediction of judgment and choice*. Oxford, England: Holden-Day.

- Borisuit, A., Scartezzini, J. L., & Thanachareonkit, A. (2010). Visual discomfort and glare rating assessment of integrated daylighting and electric lighting systems using HDR imaging techniques. *Architectural Science Review*, 53(4), 359-373.
- Boutilier, C. (2002, July). A POMDP formulation of preference elicitation problems. In *AAAI/IAAI* (pp. 239-246).
- Boutilier, C. (2003, August). On the foundations of expected utility. In *IJCAI* (Vol. 3, pp. 285-290).
- Boutilier, C., Brafman, R. I., Domshlak, C., Hoos, H. H., & Poole, D. (2004). Preference-Based Constrained Optimization with CP-Nets. *Computational Intelligence*, 20(2), 137-157.
- Boutilier, C., Patrascu, R., Poupart, P., & Schuurmans, D. (2005, July). Regret-based Utility Elicitation in Constraint-based Decision Problems. In *IJCAI* (Vol. 9, pp. 929-934).
- Boyce, P. R. (1977). Investigations of the subjective balance between illuminance and lamp colour properties. *Lighting Research & Technology*, 9(1), 11-24.
- Boyce, P. R., Veitch, J. A., Newsham, G. R., Jones, C. C., Heerwagen, J., Myer, M., & Hunter, C. M. (2006). Lighting quality and office work: two field simulation experiments. *Lighting Research & Technology*, 38(3), 191-223.
- Braziunas, D. (2006). Computational approaches to preference elicitation. Department of Computer Science, University of Toronto, Tech. Rep.
- Brochu, E., Cora, V. M., & De Freitas, N. (2010). A tutorial on Bayesian optimization of expensive cost functions, with application to active user modeling and hierarchical reinforcement learning. arXiv preprint arXiv:1012.2599.
- Brothers Software. Quick Macro 6.6. Last accessed in May 2015. <http://www.qmacro.com/>
- Calhoun, Craig, ed. *Dictionary of the social sciences*. Oxford University Press on Demand, 2002.

- Carlucci, S., Cattarin, G., Causone, F., & Pagliano, L. (2015). Multi-objective optimization of a nearly zero-energy building based on thermal and visual discomfort minimization using a non-dominated sorting genetic algorithm (NSGA-II). *Energy and Buildings*, 104, 378-394.
- Carlucci, S., Causone, F., De Rosa, F., & Pagliano, L. (2015). A review of indices for assessing visual comfort with a view to their use in optimization processes to support building integrated design. *Renewable and sustainable energy reviews*, 47, 1016-1033.
- Carter, D. J., Slater, A. I., & Moore, T. (1999). A study of occupier controlled lighting systems. *Publications-commission internationale de l'eclairage cie*, 133(2), 108-110.
- Cassol, F., Schneider, P. S., França, F. H., & Neto, A. J. S. (2011). Multi-objective optimization as a new approach to illumination design of interior spaces. *Building and Environment*, 46(2), 331-338.
- Chaiwiwatworakul, P., Chirarattananon, S., & Rakkwamsuk, P. (2009). Application of automated blind for daylighting in tropical region. *Energy Conversion and Management*, 50(12), 2927-2943.
- Chajewska, U., Getoor, L., Norman, J., & Shahar, Y. (1998, July). Utility elicitation as a classification problem. In *Proceedings of the Fourteenth conference on Uncertainty in artificial intelligence* (pp. 79-88). Morgan Kaufmann Publishers Inc..
- Chajewska, U., Koller, D., & Parr, R. (2000, July). Making rational decisions using adaptive utility elicitation. In *AAAI/IAAI* (pp. 363-369).
- Chan, Y. C., & Tzempelikos, A. (2012). A hybrid ray-tracing and radiosity method for calculating radiation transport and illuminance distribution in spaces with venetian blinds. *Solar energy*, 86(11), 3109-3124.
- Chan, Y. C., & Tzempelikos, A. (2013a). Analysis of balance between modeling accuracy and computational speed for a hybrid ray-tracing and radiosity method used in lighting simulation. In *AEI 2013: Building Solutions for Architectural Engineering* (pp. 564-573).

- Chan, Y. C., & Tzempelikos, A. (2013b). Efficient venetian blind control strategies considering daylight utilization and glare protection. *Solar Energy*, 98, 241-254.
- Chan, Y. C., Tzempelikos, A., & Konstantzos, I. (2015). A systematic method for selecting roller shade properties for glare protection. *Energy and Buildings*, 92, 81-94.
- Chan, Y. C., Tzempelikos, A., & Protzman, B. (2014). Solar Optical Properties of Roller Shades: Modeling Approaches, Measured Results and Impact on Energy Use and Visual Comfort.
- Chantrelle, F. P., Lahmidi, H., Keilholz, W., El Mankibi, M., & Michel, P. (2011). Development of a multicriteria tool for optimizing the renovation of buildings. *Applied Energy*, 88(4), 1386-1394.
- Chapelle, O., & Li, L. (2011). An empirical evaluation of thompson sampling. In *Advances in neural information processing systems* (pp. 2249-2257).
- Chauvel, P., Collins, J. B., Dogniaux, R., & Longmore, J. (1982). Glare from windows: current views of the problem. *Lighting research and Technology*, 14(1), 31-46.
- Chen, X., Bennett, P. N., Collins-Thompson, K., & Horvitz, E. (2013, February). Pairwise ranking aggregation in a crowdsourced setting. In *Proceedings of the sixth ACM international conference on Web search and data mining* (pp. 193-202). ACM.
- Chraibi, S., Lashina, T., Shrubsole, P., Aries, M., van Loenen, E., & Rosemann, A. (2016). Satisfying light conditions: A field study on perception of consensus light in Dutch open office environments. *Building and Environment*, 105, 116-127.
- Chu, W., & Ghahramani, Z. (2005, August). Preference learning with Gaussian processes. In *Proceedings of the 22nd international conference on Machine learning* (pp. 137-144). ACM.
- CIE (1992). Discomfort Glare in the Interior Lighting. Commission Internationale de l'Éclairage (CIE), Technical committee TC-3.13, Division 4, Interior Environment and Lighting Design, Vienna Austria.

CIE. "CIE e-ILV: 17-330 disability glare".

Claros, S. T., & Soler, A. (2002). Indoor daylight climate—influence of light shelf and model reflectance on light shelf performance in Madrid for hours with unit sunshine fraction. *Building and Environment*, 37(6), 587-598.

Clevenger, C. M., & Haymaker, J. (2006, June). The impact of the building occupant on energy modeling simulations. In *Joint International Conference on Computing and Decision Making in Civil and Building Engineering*, Montreal, Canada (pp. 1-10).

Collins, M., Wright, J. L., & Kotey, N. (2012). Off-normal solar optical property measurements using an integrating sphere. *Measurement*, 45(1), 79-93.

Čongradac, V., Prica, M., Paspalj, M., Bojanić, D., & Čapko, D. (2012). Algorithm for blinds control based on the optimization of blind tilt angle using a genetic algorithm and fuzzy logic. *Solar Energy*, 86(9), 2762-2770.

Conitzer, V. (2009). Eliciting single-peaked preferences using comparison queries. *Journal of Artificial Intelligence Research*, 35, 161-191.

Correia da Silva, P., Leal, V., & Andersen, M. (2015). Occupants' behaviour in energy simulation tools: lessons from a field monitoring campaign regarding lighting and shading control. *Journal of Building Performance Simulation*, 8(5), 338-358.

Craig Boutilier, Relu Patrascu, Pascal Poupart, and Dale Schuurmans. Constraint-based optimization with the minimax decision criterion. In *Ninth International Conference on Principles and Practice of Constraint Programming*, pages 168–182, Kinsale, Ireland, 2003.

Cuttle, C. (1983, June). People and windows in workplaces. In *Proceedings of the people and physical environment research conference*, Wellington, New Zealand (pp. 203-212).

da Silva, P. C., Leal, V., & Andersen, M. (2013). Occupants interaction with electric lighting and shading systems in real single-occupied offices: Results from a monitoring campaign. *Building and Environment*, 64, 152-168.

- Daum, D., Haldi, F., & Morel, N. (2011). A personalized measure of thermal comfort for building controls. *Building and Environment*, 46(1), 3-11.
- Day, J., Theodorson, J., & Van Den Wymelenberg, K. (2012). Understanding controls, behaviors and satisfaction in the daylit perimeter office: a daylight design case study. *Journal of Interior Design*, 37(1), 17-34.
- de Korte, E. M., Spiekman, M., Hoes-van Oeffelen, L., van der Zande, B., Vissenberg, G., Huiskes, G., & Kuijt-Evers, L. F. (2015). Personal environmental control: Effects of pre-set conditions for heating and lighting on personal settings, task performance and comfort experience. *Building and Environment*, 86, 166-176.
- Despenic, M., Chraibi, S., Lashina, T., & Rosemann, A. (2017). Lighting preference profiles of users in an open office environment. *Building and Environment*, 116, 89-107.
- Din, I., & Kim, H. (2014). Joint blind and light control for lighting energy reduction while satisfying light level and anti-glare requirements. *Lighting Research & Technology*, 46(3), 281-292.
- Doucet A., de Freitas N., Gordon N. (2001). *Sequential Monte Carlo Methods in Practice*. Springer-Verlag New York.
- Dyer, J. S. (1972). Interactive goal programming. *Management science*, 19(1), 62-70.
- Eilers, M., Reed, J., & Works, T. (1996). Behavioral aspects of lighting and occupancy sensors in private offices: a case study of a university office building. *ACEEE 1996 Summer Study on Energy Efficiency in Buildings*.
- Einhorn, H. D. (1969). A new method for the assessment of discomfort glare. *Lighting Research and Technology*, 1(4), 235-247.
- Eric, B., Freitas, N. D., & Ghosh, A. (2008). Active preference learning with discrete choice data. Paper presented at the *Advances in neural information processing systems*.

- Escuyer, S., & Fontoynt, M. (2001). Lighting controls: a field study of office workers' reactions. *Lighting Research and Technology*, 33(2), 77-94.
- Fabi, V., Andersen, R. K., & Corgnati, S. (2015). Verification of stochastic behavioural models of occupants' interactions with windows in residential buildings. *Building and Environment*, 94, 371-383.
- Farrugia, V. E., Martínez, H. P., & Yannakakis, G. N. (2015). The preference learning toolbox. arXiv preprint arXiv:1506.01709.
- Ferrara, M., Sirombo, E., & Fabrizio, E. (2018). Automated optimization for the integrated design process: the energy, thermal and visual comfort nexus. *Energy and Buildings*, 168, 413-427.
- Fischer, M., Wu, K., & Agathoklis, P. (2012, June). Intelligent illumination model-based lighting control. In *Distributed Computing Systems Workshops (ICDCSW), 2012 32nd International Conference on* (pp. 245-249). IEEE.
- Fisekis, K., Davies, M., Kolokotroni, M., & Langford, P. (2003). Prediction of discomfort glare from windows. *Lighting Research and Technology*, 35(4), 360-369.
- Fishburn, P. C. (1970). *Utility theory for decision making* (No. RAC-R-105). Research analysis corp McLean VA.
- Foster, M., & Oreszczyn, T. (2001). Occupant control of passive systems: the use of Venetian blinds. *Building and Environment*, 36(2), 149-155.
- Fürnkranz, J., & Hüllermeier, E. (2010). Preference learning (pp. 789-795). Springer US.
- Fürnkranz, J., Hüllermeier, E., Cheng, W., & Park, S. H. (2012). Towards preference-based reinforcement learning. *Machine Learning*.
- Futrell, B. J., Ozelkan, E. C., & Brentrup, D. (2015). Bi-objective optimization of building enclosure design for thermal and lighting performance. *Building and Environment*, 92, 591-602.

- Galasiu, A. D., & Veitch, J. A. (2006). Occupant preferences and satisfaction with the luminous environment and control systems in daylit offices: a literature review. *Energy and Buildings*, 38(7), 728-742.
- Galasiu, A. D., Atif, M. R., & MacDonald, R. A. (2004). Impact of window blinds on daylight-linked dimming and automatic on/off lighting controls. *Solar Energy-Journal of the International Solar Energy Society*, 76(5), 523-544.
- Ghahramani, A., Tang, C., & Becerik-Gerber, B. (2015). An online learning approach for quantifying personalized thermal comfort via adaptive stochastic modeling. *Building and Environment*, 92, 86-96.
- Gilani, S., O'Brien, W., Gunay, H. B., & Carrizo, J. S. (2016). Use of dynamic occupant behavior models in the building design and code compliance processes. *Energy and Buildings*, 117, 260-271.
- Goller, M., Kovach-Hebling, A., Herkel, S., Sørensen, H., Nielsen, L. T., Nielsen, L. H., & Larsen, H. V. (1998). Integration of daylighting technologies in demand side management programmes: Estimation of the energetical and peak load potential. Final report. Fraunhofer IRB Verlag.
- Gonzalez, J., Dai, Z., Damianou, A., & Lawrence, N. D. (2017). Preferential Bayesian Optimization. arXiv preprint arXiv:1704.03651.
- Goral, C. M., Torrance, K. E., Greenberg, D. P., & Battaile, B. (1984, January). Modeling the interaction of light between diffuse surfaces. In *ACM SIGGRAPH Computer Graphics* (Vol. 18, No. 3, pp. 213-222). ACM.
- Goyal, S., Ingle, H. A., & Barooah, P. (2013). Occupancy-based zone-climate control for energy-efficient buildings: Complexity vs. performance. *Applied Energy*, 106, 209-221.
- Graepel, T., Candela, J. Q., Borchert, T., & Herbrich, R. (2010). Web-scale bayesian click-through rate prediction for sponsored search advertising in microsoft's bing search engine. Omnipress.

- Granmo, O. C. (2010). Solving two-armed bernoulli bandit problems using a bayesian learning automaton. *International Journal of Intelligent Computing and Cybernetics*, 3(2), 207-234.
- Greenhill, B., Ward, M. D., & Sacks, A. (2011). The Separation Plot: A New Visual Method for Evaluating the Fit of Binary Models. *American Journal of Political Science*, 55(4), 991-1002. doi:10.1111/j.1540-5907.2011.00525.x
- Gruber, M., Trüschel, A., & Dalenbäck, J. O. (2014a). Combining performance and implementability of model-based controllers for indoor climate control in office environments. *Building and Environment*, 82, 228-236.
- Gruber, M., Trüschel, A., & Dalenbäck, J. O. (2014b). Model-based controllers for indoor climate control in office buildings—complexity and performance evaluation. *Energy and Buildings*, 68, 213-222.
- Grünewälder, S., Audibert, J. Y., Opper, M., & Shawe-Taylor, J. (2010, March). Regret bounds for Gaussian process bandit problems. In *Proceedings of the Thirteenth International Conference on Artificial Intelligence and Statistics* (pp. 273-280).
- Grynning, S., Time, B., & Matusiak, B. (2014). Solar shading control strategies in cold climates—Heating, cooling demand and daylight availability in office spaces. *Solar Energy*, 107, 182-194.
- Guillemin, A., & Molteni, S. (2002). An energy-efficient controller for shading devices self-adapting to the user wishes. *Building and Environment*, 37(11), 1091-1097.
- Guillemin, A., & Morel, N. (2001). An innovative lighting controller integrated in a self-adaptive building control system. *Energy and buildings*, 33(5), 477-487.
- Gunay, H. B., O'Brien, W., Beausoleil-Morrison, I., & Gilani, S. (2017). Development and implementation of an adaptive lighting and blinds control algorithm. *Building and Environment*, 113, 185-199.

- Gunay, H. B., O'Brien, W., Beausoleil-Morrison, I., & Huchuk, B. (2014a). On adaptive occupant-learning window blind and lighting controls. *Building Research & Information*, 42(6), 739-756.
- Gunay, H. B., O'Brien, W., Beausoleil-Morrison, I., Goldstein, R., Breslav, S., & Khan, A. (2014b). Coupling stochastic occupant models to building performance simulation using the discrete event system specification formalism. *Journal of Building Performance Simulation*, 7(6), 457-478. doi:10.1080/19401493.2013.866695
- Guo, S. (2011). *Bayesian recommender systems: Models and Algorithms*. Australian National University.
- Guo, S., Sanner, S., & Bonilla, E. V. (2010). Gaussian process preference elicitation. In *Advances in neural information processing systems* (pp. 262-270).
- Guo, X., Tiller, D. K., Henze, G. P., & Waters, C. E. (2010). The performance of occupancy-based lighting control systems: A review. *Lighting Research & Technology*, 42(4), 415-431. doi:10.1177/1477153510376225
- Guth, S. K. (1963). A method for the evaluation of discomfort glare. *Illuminating Engineering*, 58(5), 351-364.
- Guth, S. K. (1966). Computing visual comfort ratings for a specific interior lighting installation. *Illuminating Engineering*, 61(10), 634.
- Haldi, F., & Robinson, D. (2008). On the behaviour and adaptation of office occupants. *Building and environment*, 43(12), 2163-2177.
- Haldi, F., & Robinson, D. (2009). Interactions with window openings by office occupants. *Building and Environment*, 44(12), 2378-2395.
- Haldi, F., & Robinson, D. (2010a). Adaptive actions on shading devices in response to local visual stimuli. *Journal of Building Performance Simulation*, 3(2), 135-153.

- Haldi, F., & Robinson, D. (2010b). On the unification of thermal perception and adaptive actions. *Building and Environment*, 45(11), 2440-2457.
- Haldi, F., Cal`ı D., Andersen, R. K., Wesseling, M., & Mller, D. (2017). Modelling diversity in building occupant behaviour: a novel statistical approach. *Journal of Building Performance Simulation*, 10(5-6), 527-544.
- Hanley, J. A., & McNeil, B. J. (1982). The meaning and use of the area under a receiver operating characteristic (ROC) curve. *Radiology*, 143(1), 29-36.
- Hazyuk, I., Ghiaus, C., & Penhouet, D. (2012a). Optimal temperature control of intermittently heated buildings using Model Predictive Control: Part I–Building modeling. *Building and Environment*, 51, 379-387.
- Hazyuk, I., Ghiaus, C., & Penhouet, D. (2012b). Optimal temperature control of intermittently heated buildings using Model Predictive Control: Part II–Control algorithm. *Building and Environment*, 51, 388-394.
- Hedge, A., & Dorsey, J. A. (2013). Green buildings need good ergonomics. *Ergonomics*, 56(3), 492-506.
- Hedge, A., Sims Jr, W. R., & Becker, F. D. (1995). Effects of lensed-indirect and parabolic lighting on the satisfaction, visual health, and productivity of office workers. *Ergonomics*, 38(2), 260-290.
- Heerwagen, J. (2000). Green buildings, organizational success and occupant productivity. *Building Research & Information*, 28(5-6), 353-367.
- Heerwagen, J. H., & Heerwagen, D. R. (1986). Lighting and psychological comfort. *Lighting Design and Application*, 16(4), 47-51.
- Heerwagen, J., & Diamond, R. (1992). Adaptations and Copng: Occupant Response tn Discomfort in Energy Efficient Buildings. ACEEE.

- Hernández-Lobato, J. M., Hoffman, M. W., & Ghahramani, Z. (2014). Predictive entropy search for efficient global optimization of black-box functions. In *Advances in neural information processing systems* (pp. 918-926).
- Hirning, M. B., Isoardi, G. L., & Cowling, I. (2014). Discomfort glare in open plan green buildings. *Energy and Buildings*, 70, 427-440.
- Hirning, M. B., Isoardi, G. L., & Garcia-Hansen, V. R. (2017). Prediction of discomfort glare from windows under tropical skies. *Building and Environment*, 113, 107-120.
- Hopkinson, R. G. (1972). Glare from daylighting in buildings. *Applied Ergonomics*, 3(4), 206-215.
- Hu, J., & Olbina, S. (2011). Illuminance-based slat angle selection model for automated control of split blinds. *Building and Environment*, 46(3), 786-796.
- Hu, M., & Cho, H. (2014). A probability constrained multi-objective optimization model for CCHP system operation decision support. *Applied Energy*, 116, 230-242.
- Hua, Y., Oswald, A., & Yang, X. (2011). Effectiveness of daylighting design and occupant visual satisfaction in a LEED Gold laboratory building. *Building and Environment*, 46(1), 54-64.
- Hunt, D. R. G. (1979). The use of artificial lighting in relation to daylight levels and occupancy. *Building and environment*, 14(1), 21-33.
- IESNA, L. H. (2000). Reference and application volume. New York: Illuminating Engineering Society of North America.
- IES-The Daylight Metrics Committee. (2012). Approved Method: IES Spatial Daylight Autonomy (sDA) and Annual Sunlight Exposure (ASE). Illuminating Engineering Society of North America: IES, New York, USA.
- Inkarojrit, V. (2005). Balancing comfort: occupants' control of window blinds in private offices.
- Inkarojrit, V. (2008). Monitoring and modelling of manually-controlled Venetian blinds in private offices: a pilot study. *Journal of Building Performance Simulation*, 1(2), 75-89.

- Inkarojrit, V., & Paliaga, G. (2004, September). Indoor climatic influences on the operation of windows in a naturally ventilated building. In Proceedings of the 21st international conference on passive and low energy architecture (pp. 19-22).
- Inoue, T. (1988). Development of an Optimal Control System for Window Shading Devices based on Investigation in Office Buildings. *ASHRAE transactions*, 94, 1034-1049.
- Inoue, T., Kawase, T., Ibamoto, T., Takakusa, S., & Matsuo, Y. (1988). The development of an optimal control system for window shading devices based on investigations in office buildings. *ASHRAE transactions*, 94, 1034-1049.
- Iwata, T., Kimura, K. I., Shukuya, M., & Takano, K. (1991). Discomfort caused by wide-source glare. *Energy and Buildings*, 15(3), 391-398.
- Jain, S., & Garg, V. (2018). A review of open loop control strategies for shades, blinds and integrated lighting by use of real-time daylight prediction methods. *Building and Environment*.
- Jakubiec, J. A., & Reinhart, C. F. (2012). The ‘adaptive zone’—A concept for assessing discomfort glare throughout daylit spaces. *Lighting Research & Technology*, 44(2), 149-170.
- Jakubiec, J. A., & Reinhart, C. F. (2016). A concept for predicting occupants’ long-term visual comfort within daylit spaces. *Leukos*, 12(4), 185-202.
- Jaynes, E. T. (2003). *Probability theory: The logic of science*: Cambridge university press.
- Jazizadeh, F., Ghahramani, A., Becerik-Gerber, B., Kichkaylo, T., & Orosz, M. (2013). Human-building interaction framework for personalized thermal comfort-driven systems in office buildings. *Journal of Computing in Civil Engineering*, 28(1), 2-16.
- Jazizadeh, F., Ghahramani, A., Becerik-Gerber, B., Kichkaylo, T., & Orosz, M. (2014). User-led decentralized thermal comfort driven HVAC operations for improved efficiency in office buildings. *Energy and Buildings*, 70, 398-410.

- Karlsen, L., Heiselberg, P., Bryn, I., & Johra, H. (2015). Verification of simple illuminance based measures for indication of discomfort glare from windows. *Building and Environment*, 92, 615-626.
- Kass, R. E., & Natarajan, R. (2006). A default conjugate prior for variance components in generalized linear mixed models (comment on article by Browne and Draper). *Bayesian Analysis*, 1(3), 535-542.
- Keeney, R. L. (1974). Multiplicative utility functions. *Operations Research*, 22(1), 22-34.
- Kent, M. G., Altomonte, S., Wilson, R., & Tregenza, P. R. (2017). Temporal effects on glare response from daylight. *Building and Environment*, 113, 49-64.
- Kim, D. W., & Park, C. S. (2012). Comparative control strategies of exterior and interior blind systems. *Lighting Research and Technology*, 1477153511433996.
- Kim, G. Y. (2009). Performance Analysis and Design Guidelines for Lightshelves (Doctoral dissertation, Architectural Engineering).
- Kim, J. H., Park, Y. J., Yeo, M. S., & Kim, K. W. (2009). An experimental study on the environmental performance of the automated blind in summer. *Building and Environment*, 44(7), 1517-1527.
- Kingsley, D. C. (2006). Preference uncertainty, preference refinement and paired comparison choice experiments. Dept. of Economics. University of Colorado.
- Kolokotsa, D., Niachou, K., Geros, V., Kalaitzakis, K., Stavrakakis, G. S., & Santamouris, M. (2005). Implementation of an integrated indoor environment and energy management system. *Energy and Buildings*, 37(1), 93-99.
- Konis K., Annavaram M. (2017). The Occupant Mobile Gateway: A participatory sensing and machine learning approach for occupant-aware energy management. *Building and Environment*, 118, 1-13.

- Konis, K. (2013). Evaluating daylighting effectiveness and occupant visual comfort in a side-lit open-plan office building in San Francisco, California. *Building and Environment*, 59, 662-677.
- Konis, K. (2014). Predicting visual comfort in side-lit open-plan core zones: results of a field study pairing high dynamic range images with subjective responses. *Energy and Buildings*, 77, 67-79.
- Konis, K., & Annavaram, M. (2017). The occupant mobile gateway: a participatory sensing and machine-learning approach for occupant-aware energy management. *Building and Environment*, 118, 1-13.
- Konstantzos, I., & Tzempelikos, A. (2017). Daylight glare evaluation with the sun in the field of view through window shades. *Building and Environment*, 113, 65-77.
- Konstantzos, I., Tzempelikos, A., & Chan, Y. C. (2015). Experimental and simulation analysis of daylight glare probability in offices with dynamic window shades. *Building and Environment*, 87, 244-254.
- Koo, S. Y., Yeo, M. S., & Kim, K. W. (2010). Automated blind control to maximize the benefits of daylight in buildings. *Building and Environment*, 45(6), 1508-1520.
- Kotey, N. A., Wright, J. L., & Collins, M. R. (2009). Determining off-normal solar optical properties of roller blinds. *ASHRAE Transactions*, 117(1).
- Kushner, H. J. (1964). A new method of locating the maximum point of an arbitrary multipeak curve in the presence of noise. *Journal of Basic Engineering*, 86(1), 97-106.
- Lafortune, E. P., & Willems, Y. D. (1996). Rendering participating media with bidirectional path tracing. In *Rendering Techniques '96* (pp. 91-100). Springer Vienna.
- Lah, M. T., Zupančič, B., Peternelj, J., & Krainer, A. (2006). Daylight illuminance control with fuzzy logic. *Solar energy*, 80(3), 307-321.

- Langevin, J., Wen, J., & Gurian, P. L. (2012). Relating occupant perceived control and thermal comfort: statistical analysis on the ASHRAE RP-884 database. *HVAC&R Research*, 18(1-2), 179-194.
- Lawrence Berkeley National Lab. WINDOW 7 program and manual. Last accessed in May 2015. <http://windows.lbl.gov/software/window/window.html>
- Le, K., Bourdais, R., & Guéguen, H. (2014). From hybrid model predictive control to logical control for shading system: A support vector machine approach. *Energy and Buildings*, 84, 352-359.
- Leather, P., Pyrgas, M., Beale, D., & Lawrence, C. (1998). Windows in the workplace: Sunlight, view, and occupational stress. *Environment and behavior*, 30(6), 739-762.
- Lee, E. S., & Selkowitz, S. E. (1994). The design and evaluation of integrated envelope and lighting control strategies for commercial buildings (No. LBL--34638; CONF-950104--3). Lawrence Berkeley Lab., CA (United States).
- Lee, E. S., & Selkowitz, S. E. (2006). The New York Times Headquarters daylighting mockup: Monitored performance of the daylighting control system. *Energy and buildings*, 38(7), 914-929.
- Lee, M., Carswell, C. M., Seidelman, W., & Sublette, M. (2013, September). Green expectations: The story of a customizable lighting control panel designed to reduce energy use. In *Proceedings of the Human Factors and Ergonomics Society Annual Meeting* (Vol. 57, No. 1, pp. 1353-1357). Sage CA: Los Angeles, CA: SAGE Publications.
- Lee, S., Bilonis, I., Karava, P., & Tzempelikos, A. (2017). A Bayesian approach for probabilistic classification and inference of occupant thermal preferences in office buildings. *Building and Environment*, 118, 323-343. doi:<https://doi.org/10.1016/j.buildenv.2017.03.009>
- Lepird, J. R., Owen, M. P., & Kochenderfer, M. J. (2015). Bayesian Preference Elicitation for Multiobjective Engineering Design Optimization. *Journal of Aerospace Information Systems*, 12(10), 634-645. doi:10.2514/1.i010363

- Li, D., Menassa, C. C., & Kamat, V. R. (2017). Personalized human comfort in indoor building environments under diverse conditioning modes. *Building and Environment*, 126, 304-317.
- Lindelöf, D., & Morel, N. (2008). Bayesian estimation of visual discomfort. *Building Research & Information*, 36(1), 83-96.
- Lindsay, C. R. T., & Littlefair, P. J. (1993). Occupant use of venetian blinds in offices (PD 233/92). Watford: Building Research Establishment.
- Lindsay, C. T. R., & Littlefair, P. J. (1992). Occupant Use of Venetian Blinds in Offices. Building Research Establishment (BRE), Contract PD233/92. Garston Library, Watford, UK.
- Lockhead, G. R. (2004). Absolute Judgments Are Relative: A Reinterpretation of Some Psychophysical Ideas. *Review of General Psychology*, 8(4), 265-272. doi:10.1037/1089-2680.8.4.265
- Love, J. A. (1998). Manual switching patterns in private offices. *International journal of lighting research and technology*, 30(1), 45-50.
- Lu, T., Lü X., & Viljanen, M. (2011). A novel and dynamic demand-controlled ventilation strategy for CO₂ control and energy saving in buildings. *Energy and buildings*, 43(9), 2499-2508.
- Mahdavi, A. (2008, March). Predictive simulation-based lighting and shading systems control in buildings. In *Building Simulation* (Vol. 1, No. 1, pp. 25-35). Springer-Verlag.
- Mahdavi, A., Mohammadi, A., Kabir, E., & Lambeva, L. (2008). Occupants' operation of lighting and shading systems in office buildings. *Journal of Building Performance Simulation*, 1(1), 57-65.
- Manzan, M., & Padovan, R. (2015). Multi-criteria energy and daylighting optimization for an office with fixed and moveable shading devices. *Advances in Building Energy Research*, 9(2), 238-252.

- Marler, R. T., & Arora, J. S. (2004). Survey of multi-objective optimization methods for engineering. *Structural and Multidisciplinary Optimization*, 26(6), 369-395. doi:10.1007/s00158-003-0368-6
- May, B. C., & Leslie, D. S. (2011). Simulation studies in optimistic Bayesian sampling in contextual-bandit problems. *Statistics Group, Department of Mathematics, University of Bristol*, 11, 02.
- May, B. C., Korda, N., Lee, A., & Leslie, D. S. (2012). Optimistic Bayesian sampling in contextual-bandit problems. *Journal of Machine Learning Research*, 13(Jun), 2069-2106.
- Meerbeek, B. W., de Bakker, C., De Kort, Y. A. W., Van Loenen, E. J., & Bergman, T. (2016). Automated blinds with light feedback to increase occupant satisfaction and energy saving. *Building and Environment*, 103, 70-85.
- Meerbeek, B., te Kulve, M., Gritti, T., Aarts, M., van Loenen, E., & Aarts, E. (2014). Building automation and perceived control: a field study on motorized exterior blinds in Dutch offices. *Building and Environment*, 79, 66-77.
- Mockus, J., Tiesis, V., & Zilinskas, A. (1978). The application of Bayesian methods for seeking the extremum. *Towards global optimization*, 2(117-129), 2.
- Moore, T., Carter, D. J., & Slater, A. I. (2002). A field study of occupant controlled lighting in offices. *Lighting Research & Technology*, 34(3), 191-202.
- Moore, T., Carter, D. J., & Slater, A. I. (2003). Long-term patterns of use of occupant controlled office lighting. *Lighting Research & Technology*, 35(1), 43-57.
- Morgenstern, O., & Von Neumann, J. (1953). *Theory of games and economic behavior*. Princeton university press.
- Moroşan, P. D., Bourdais, R., Dumur, D., & Buisson, J. (2010). Building temperature regulation using a distributed model predictive control. *Energy and Buildings*, 42(9), 1445-1452.

- Mosteller, F. (2006). Remarks on the method of paired comparisons: I. The least squares solution assuming equal standard deviations and equal correlations. In *Selected Papers of Frederick Mosteller* (pp. 157-162): Springer.
- Nabil, A., & Mardaljevic, J. (2006). Useful daylight illuminances: A replacement for daylight factors. *Energy and buildings*, 38(7), 905-913.
- Nagy, Z., Yong, F. Y., Frei, M., & Schlueter, A. (2015). Occupant centered lighting control for comfort and energy efficient building operation. *Energy and Buildings*, 94, 100-108.
- Nazzal, A. A. (2001). A new daylight glare evaluation method: Introduction of the monitoring protocol and calculation method. *Energy and Buildings*, 33(3), 257-265.
- Newsham, G. R. (1994). Manual control of window blinds and electric lighting: implications for comfort and energy consumption. *Indoor Environment*, 3(3), 135-144.
- Nguyen, A. T., Reiter, S., & Rigo, P. (2014). A review on simulation-based optimization methods applied to building performance analysis. *Applied Energy*, 113, 1043-1058.
- Nicholas J Sanders (2015) Preferences and Utility – Basic Review and Exmaples. Cornell University's Lecture Handouts.
- Nicol, F., Wilson, M., & Chiancarella, C. (2006). Using field measurements of desktop illuminance in European offices to investigate its dependence on outdoor conditions and its effect on occupant satisfaction, and the use of lights and blinds. *Energy and Buildings*, 38(7), 802-813.
- Nicol, J. F. (2001, August). Characterising occupant behaviour in buildings: towards a stochastic model of occupant use of windows, lights, blinds, heaters and fans. In *Proceedings of the seventh international IBPSA conference, Rio* (Vol. 2, pp. 1073-1078).
- Nicol, J. F., & Humphreys, M. A. (2004). A Stochastic Approach to Thermal Comfort--Occupant Behavior and Energy Use in Buildings. *ASHRAE transactions*, 110(2).

- Nielsen, M. V., Svendsen, S., & Jensen, L. B. (2011). Quantifying the potential of automated dynamic solar shading in office buildings through integrated simulations of energy and daylight. *Solar Energy*, 85(5), 757-768.
- O'Brien, W., Gunay, H. B., Tahmasebi, F., & Mahdavi, A. (2017). A preliminary study of representing the inter-occupant diversity in occupant modelling. *Journal of Building Performance Simulation*, 10(5-6), 509-526.
- O'Brien, W., & Gunay, H. B. (2014). The contextual factors contributing to occupants' adaptive comfort behaviors in offices—A review and proposed modeling framework. *Building and Environment*, 77, 77-87.
- O'Brien, W., Kapsis, K., & Athienitis, A. K. (2013). Manually-operated window shade patterns in office buildings: A critical review. *Building and Environment*, 60, 319-338.
- Ochoa, C. E., Aries, M. B., van Loenen, E. J., & Hensen, J. L. (2012). Considerations on design optimization criteria for windows providing low energy consumption and high visual comfort. *Applied Energy*, 95, 238-245.
- Oh, M. H., Lee, K. H., & Yoon, J. H. (2012). Automated control strategies of inside slat-type blind considering visual comfort and building energy performance. *Energy and Buildings*, 55, 728-737.
- Oldewurtel, F., Sturzenegger, D., & Morari, M. (2013). Importance of occupancy information for building climate control. *Applied Energy*, 101, 521-532.
- Osterhaus, W. (2009, September). Design guidelines for glare-free daylight work environments. In 11th European Conference on Lighting-Lux Europe.
- Osterhaus, W. K. (2005). Discomfort glare assessment and prevention for daylight applications in office environments. *Solar Energy*, 79(2), 140-158.
- Osterhaus, W. K. E. (1996, November). Discomfort glare from large area glare sources at computer workstations. In Proceedings for the 1996 International Daylight Workshop, Building with Daylight: Energy-Efficient Design, Perth. Western Australia (pp. 103-110).

- Ouarghi, R., & Krarti, M. (2006). Building Shape Optimization Using Neural Network and Genetic Algorithm Approach. *Ashrae transactions*, 112(1).
- Park, B. C., Choi, A. S., Jeong, J. W., & Lee, E. S. (2011). Performance of integrated systems of automated roller shade systems and daylight responsive dimming systems. *Building and Environment*, 46(3), 747-757.
- Payne, J. W., Bettman, J. R., & Johnson, E. J. (1993). *The adaptive decision maker*: Cambridge University Press.
- Payne, J. W., Payne, J. W., Bettman, J. R., & Johnson, E. J. (1993). *The adaptive decision maker*. Cambridge university press.
- Peters, M., & Ketter, W. (2013). Towards autonomous decision-making: A probabilistic model for learning multi-user preferences.
- Petherbridge, P., & Hopkinson, R. G. (1950). Discomfort glare and the lighting of buildings. *Lighting Research and Technology*, 15(2 IEStrans), 39-79.
- Prívarva, S., Široký, J., Ferkl, L., & Cigler, J. (2011). Model predictive control of a building heating system: The first experience. *Energy and Buildings*, 43(2), 564-572.
- Raanaas, R. K., Patil, G. G., & Hartig, T. (2012). Health benefits of a view of nature through the window: a quasi-experimental study of patients in a residential rehabilitation center. *Clinical rehabilitation*, 26(1), 21-32.
- Radlinski, F., & Joachims, T. (2005, August). Query chains: learning to rank from implicit feedback. In *Proceedings of the eleventh ACM SIGKDD international conference on Knowledge discovery in data mining* (pp. 239-248). ACM.
- Rakha, T., & Nassar, K. (2011). Genetic algorithms for ceiling form optimization in response to daylight levels. *Renewable energy*, 36(9), 2348-2356.
- Rao, S. (2011). Thermal and daylighting analysis of building perimeter zones equipped with combined dynamic shading systems (Doctoral dissertation, PURDUE UNIVERSITY).

- Rapone, G., & Saro, O. (2012). Optimisation of curtain wall facades for office buildings by means of PSO algorithm. *Energy and Buildings*, 45, 189-196.
- Rea, M. S. (1984). Window blind occlusion: a pilot study. *Building and Environment*, 19(2), 133-37.
- Reinhart, C. F. (2004). Lightswitch-2002: a model for manual and automated control of electric lighting and blinds. *Solar energy*, 77(1), 15-28.
- Reinhart, C. F., & Voss, K. (2003). Monitoring manual control of electric lighting and blinds. *Lighting research & technology*, 35(3), 243-258.
- Reinhart, C. F., & Wienold, J. (2011). The daylighting dashboard—A simulation-based design analysis for daylit spaces. *Building and environment*, 46(2), 386-396.
- Robbins, H. (1952). Some aspects of the sequential design of experiments. *Bulletin of the American Mathematical Society*, 58(5), 527-535.
- Rubin, A. I., Collins, B. L., & Tibbott, R. L. (1978). Window blinds as a potential energy saver: A case study. US Department of Commerce, National Bureau of Standards.
- S. Siegel, N.J. Castellan, JR. (1988): *Nonparametric Statistics for the Behavioral Sciences*, McGraw-Hill Book Company, New York, 1981.
- Sadeghi, S. A., Awalgaonkar, N. M., Karava, P., & Bilonis, I. (2017). A Bayesian modeling approach of human interactions with shading and electric lighting systems in private offices. *Energy and Buildings*, 134, 185-201.
- Sadeghi, S. A., Karava, P., Konstantzos, I., & Tzempelikos, A. (2016). Occupant interactions with shading and lighting systems using different control interfaces: a pilot field study. *Building and Environment*, 97, 177-195.
- Sadeghi, S. A., Lee, S., Karava, P., Bilonis, I., & Tzempelikos, A. (2018). Bayesian classification and inference of occupant visual preferences in daylit perimeter private offices. *Energy and Buildings*, 166, 505-524.

- Salo, A. A., & Hamalainen, R. P. (2001). Preference ratios in multiattribute evaluation (PRIME)-elicitation and decision procedures under incomplete information. *IEEE Transactions on Systems, Man, and Cybernetics-Part A: Systems and Humans*, 31(6), 533-545.
- Sarkar, C., Nambi, S. A. U., & Prasad, R. V. (2016, February). iLTC: Achieving Individual Comfort in Shared Spaces. In *EWSN* (pp. 65-76).
- Scott, S. L. (2010). A modern Bayesian look at the multi-armed bandit. *Applied Stochastic Models in Business and Industry*, 26(6), 639-658.
- Shannon, C. E. (1948). A mathematical theory of communication. *Bell system technical journal*, 27(3), 379-423.
- Shen, E., Hu, J., & Patel, M. (2014). Energy and visual comfort analysis of lighting and daylight control strategies. *Building and Environment*, 78, 155-170.
- Shen, H., & Tzempelikos, A. (2012). Daylighting and energy analysis of private offices with automated interior roller shades. *Solar energy*, 86(2), 681-704.
- Shen, H., & Tzempelikos, A. (2017). Daylight-linked synchronized shading operation using simplified model-based control. *Energy and Buildings*, 145, 200-212.
- Shin, J. Y., Yun, G. Y., & Kim, J. T. (2012). View types and luminance effects on discomfort glare assessment from windows. *Energy and Buildings*, 46, 139-145.
- Siegel, S., & Castellan, N. J. (1981). *JR.(1988): Nonparametric Statistics for the Behavioral Sciences*. McGraw-Hill Book Company, New York.
- Slider Design: Rules of Thumb by Aurora Harley: <https://www.nngroup.com/articles/gui-slider-controls>
- Sorensen, K. (1987). Comparison of glare index definitions. Research Note of the Danish Illuminating Engineering Laboratory, Lyngby.

- Suga, K., Kato, S., & Hiyama, K. (2010). Structural analysis of Pareto-optimal solution sets for multi-objective optimization: An application to outer window design problems using Multiple Objective Genetic Algorithms. *Building and Environment*, 45(5), 1144-1152.
- Suk, J. Y., Schiler, M., & Kensek, K. (2013). Development of new daylight glare analysis methodology using absolute glare factor and relative glare factor. *Energy and Buildings*, 64, 113-122.
- Suk, J. Y., Schiler, M., & Kensek, K. (2017). Investigation of existing discomfort glare indices using human subject study data. *Building and Environment*, 113, 121-130.
- Sutter, Y., Dumortier, D., & Fontoynt, M. (2006). The use of shading systems in VDU task offices: A pilot study. *Energy and Buildings*, 38(7), 780-789.
- Tahmasebi, F., & Mahdavi, A. (2017). The sensitivity of building performance simulation results to the choice of occupants' presence models: a case study. *Journal of Building Performance Simulation*, 10(5-6), 625-635.
- Takahashi, R., & Morimura, T. (2015, February). Predicting preference reversals via Gaussian process uncertainty aversion. In *Artificial Intelligence and Statistics* (pp. 958-967).
- Technoteam Bildverarbeitung GmbH, LMK Labsoft 14.3.6.
http://www.technoteam.de/product_overview/lmk/software/lmk_labsoft/index_eng.html
- Tee, K., McCourt, M., Martinez-Cantin, R., Dewancker, I., & Liu, F. (2017). Active Preference Learning for Personalized Portfolio Construction. arXiv preprint arXiv:1708.07567.
- Thompson, W. R. (1933). On the likelihood that one unknown probability exceeds another in view of the evidence of two samples. *Biometrika*, 25(3/4), 285-294.
- Thornton, W. A., & Chen, E. (1978). What is visual clarity?. *Journal of the Illuminating Engineering Society*, 7(2), 85-94.
- Thurstone, L. L. (1927). A law of comparative judgment. *Psychological Review*, 34(4), 273-286.
 doi:10.1037/h0070288

- Tregenza, P. R. (1983). The Monte Carlo method in lighting calculations. *Lighting Research and Technology*, 15(4), 163-170.
- Tsangrassoulis, A., Niachou, K., Papakostantinou, N., Pavlou, C., & Santamouris, M. (2002). A numerical method to estimate time-varying values of diffuse irradiance on surfaces in complex geometrical environments. *Renewable energy*, 27(3), 427-439.
- Tuaycharoen, N., & Tregenza, P. R. (2007). View and discomfort glare from windows. *Lighting Research & Technology*, 39(2), 185-200.
- Tuhus-Dubrow, D., & Krarti, M. (2010). Genetic-algorithm based approach to optimize building envelope design for residential buildings. *Building and environment*, 45(7), 1574-1581.
- Tzempelikos, A. (2008). The impact of venetian blind geometry and tilt angle on view, direct light transmission and interior illuminance. *Solar Energy*, 82(12), 1172-1191.
- Tzempelikos, A. (2010). The impact of manual light switching on lighting energy consumption for a typical office building.
- Tzempelikos, A., & Athienitis, A. K. (2005). Integrated Thermal and Daylighting Analysis for Design of Office Buildings. *ASHRAE transactions*, 111(1).
- Tzempelikos, A., & Athienitis, A. K. (2007). The impact of shading design and control on building cooling and lighting demand. *Solar Energy*, 81(3), 369-382.
- Tzempelikos, A., & Chan, Y. C. (2016). Estimating detailed optical properties of window shades from basic available data and modeling implications on daylighting and visual comfort. *Energy and Buildings*, 126, 396-407.
- Tzempelikos, A., & Shen, H. (2013). Comparative control strategies for roller shades with respect to daylighting and energy performance. *Building and Environment*, 67, 179-192.
- USGBC, L. (2009). *New Construction and Major Renovations*. USGBC–United States Green Building Council, Washington, DC (2011) (updated November 2011).

- Van Den Wymelenberg, K. (2012). Patterns of occupant interaction with window blinds: A literature review. *Energy and Buildings*, 51, 165-176.
- Van Den Wymelenberg, K. G. (2014). Visual comfort, discomfort glare, and occupant fenestration control: developing a research agenda. *Leukos*, 10(4), 207-221.
- Van Den Wymelenberg, K., & Inanici, M. (2014). A critical investigation of common lighting design metrics for predicting human visual comfort in offices with daylight. *Leukos*, 10(3), 145-164.
- Van Den Wymelenberg, K., Inanici, M., & Johnson, P. (2010). The effect of luminance distribution patterns on occupant preference in a daylit office environment. *Leukos*, 7(2), 103-122.
- Van Moeseke, G., Bruyère, I., & De Herde, A. (2007). Impact of control rules on the efficiency of shading devices and free cooling for office buildings. *Building and environment*, 42(2), 784-793.
- Vartiainen, E. (2001). Electricity benefits of daylighting and photovoltaics for various solar facade layouts in office buildings. *Energy and Buildings*, 33(2), 113-120.
- Veitch, J. A., & Gifford, R. (1996). Assessing beliefs about lighting effects on health, performance, mood, and social behavior. *Environment and Behavior*, 28(4), 446-470.
- Veitch, J. A., & Newsham, G. R. (2000). Preferred luminous conditions in open-plan offices: Research and practice recommendations. *International Journal of Lighting Research and Technology*, 32(4), 199-212.
- Veitch, J. A., Hine, D. W., & Gifford, R. (1993). End Users 'Knowledge, Beliefs, and Preferences for Lighting. *Journal of Interior Design*, 19(2), 15-26.
- Versluis, R. (2005). Ray-Tracing Vs. Radiosity Modeling of Venetian and Pleated Blinds and the Influence of the Energetic Properties of Windows. IBPSA-NVL Conference. Delft, Netherlands

- Villa, C., & Labayrade, R. (2013). Multi-objective optimisation of lighting installations taking into account user preferences—a pilot study. *Lighting Research & Technology*, 45(2), 176-196.
- Volkovs, M. N., & Zemel, R. S. (2012, April). A flexible generative model for preference aggregation. In *Proceedings of the 21st international conference on World Wide Web* (pp. 479-488). ACM.
- Wang, C., Yan, D., Sun, H., & Jiang, Y. (2016). A generalized probabilistic formula relating occupant behavior to environmental conditions. *Building and Environment*, 95, 53-62.
- Wang, T., & Boutilier, C. (2003, August). Incremental utility elicitation with the minimax regret decision criterion. In *Ijcai* (Vol. 3, pp. 309-316).
- Wang, W., Rivard, H., & Zmeureanu, R. (2006). Floor shape optimization for green building design. *Advanced Engineering Informatics*, 20(4), 363-378.
- Wang, W., Zmeureanu, R., & Rivard, H. (2005). Applying multi-objective genetic algorithms in green building design optimization. *Building and environment*, 40(11), 1512-1525.
- Wang, Z., & Jegelka, S. (2017). Max-value entropy search for efficient Bayesian optimization. *arXiv preprint arXiv:1703.01968*.
- Wankanapona, P., & Mistrickb, R. G. (2011). Roller shades and automatic lighting control with solar radiation control strategies. *BUILT*, 1(1), 2011.
- Wells, B. W. P. (1965). Subjective responses to the lighting installation in a modern office building and their design implications. *Building Science*, 1(1), 57-68.
- White, C. C., Sage, A. P., & Dozono, S. (1984). A model of multiattribute decisionmaking and trade-off weight determination under uncertainty. *IEEE Transactions on Systems, Man, and Cybernetics*, (2), 223-229.
- Wienold, J. (2007, September). Dynamic simulation of blind control strategies for visual comfort and energy balance analysis. In *Building Simulation* (pp. 1197-1204).

- Wienold, J. (2009, July). Dynamic daylight glare evaluation. In Proceedings of Building Simulation (pp. 27-30).
- Wienold, J. (2012). EvalGlare Version 1.0. Fraunhofer Institute for Solar Energy Systems, Freiburg.
- Wienold, J., & Christoffersen, J. (2006). Evaluation methods and development of a new glare prediction model for daylight environments with the use of CCD cameras. *Energy and buildings*, 38(7), 743-757.
- Wienold, J., Frontini, F., Herkel, S., & Mende, S. (2011, November). Climate based simulation of different shading device systems for comfort and energy demand. In 12th Conference of International Building Performance Simulation Association (pp. 14-16).
- Wilson, H. R., GEORG, A., & NITZ, P. (2000). Switchable glazing with a large dynamic range in total solar energy transmittance (g value). In World renewable energy congress (pp. 195-200).
- Wright, J. A., Loosemore, H. A., & Farmani, R. (2002). Optimization of building thermal design and control by multi-criterion genetic algorithm. *Energy and buildings*, 34(9), 959-972.
- Xiong, J., & Tzempelikos, A. (2016). Model-based shading and lighting controls considering visual comfort and energy use. *Solar Energy*, 134, 416-428.
- Xiong, J., Tzempelikos, A., Bilonis, I., Awalgaonkar, N. M., Lee, S., Konstantzos, I., ... & Karava, P. (2018). Inferring personalized visual satisfaction profiles in daylit offices from comparative preferences using a Bayesian approach. *Building and Environment*, 138, 74-88.
- Yan, D., O'Brien, W., Hong, T., Feng, X., Gunay, H. B., Tahmasebi, F., & Mahdavi, A. (2015). Occupant behavior modeling for building performance simulation: Current state and future challenges. *Energy and Buildings*, 107, 264-278.
- Yao, J. (2014). An investigation into the impact of movable solar shades on energy, indoor thermal and visual comfort improvements. *Building and Environment*, 71, 24-32.

- Yılmaz, F. S., Ticleanu, C., Howlett, G., King, S., & Littlefair, P. J. (2016). People-friendly lighting controls—User performance and feedback on different interfaces. *Lighting Research & Technology*, 48(4), 449-472.
- Yonemura, G., & Kohayakawa, Y. (1976). A new look at the research basis for lighting level recommendations (No. 82). US Dept. of Commerce, National Bureau of Standards: for sale by the Supt. of Docs., US Govt. Print. Off..
- Yun, G., Yoon, K. C., & Kim, K. S. (2014). The influence of shading control strategies on the visual comfort and energy demand of office buildings. *Energy and Buildings*, 84, 70-85.
- Zarkadis, N., Morel, N., & Scartezzini, J. L. (2015). A novel occupant-adapted and fuzzy logic-ready visual comfort modelling approach using machine learning algorithms. In *Proceedings of International Conference CISBAT 2015 Future Buildings and Districts Sustainability from Nano to Urban Scale* (No. EPFL-CONF-213360, pp. 419-424). LESO-PB, EPFL.
- Zhang, R., & Lam, K. P. (2011, June). Comparison of building load performance between first principle based and implementable shading control algorithms. In *Building Simulation* (Vol. 4, No. 2, pp. 135-148). Tsinghua Press.
- Zhang, S., & Birru, D. (2012). An open-loop venetian blind control to avoid direct sunlight and enhance daylight utilization. *Solar Energy*, 86(3), 860-866.
- Zhang, Y., & Barrett, P. (2012). Factors influencing occupants' blind-control behaviour in a naturally ventilated office building. *Building and Environment*, 54, 137-147.
- Zhao, N., Reinhart, C. F., & Paradiso, J. A. (2018). Image-based perceptual analysis of lit environments. *Lighting Research & Technology*, 1477153518786768.
- Zhao, Q., Zhao, Y., Wang, F., Wang, J., Jiang, Y., & Zhang, F. (2014). A data-driven method to describe the personalized dynamic thermal comfort in ordinary office environment: From model to application. *Building and Environment*, 72, 309-318.

VITA

Jie Xiong

Ph.D., Lyles School of Civil Engineering, Purdue University (2015 – 2019)

M.S., Lyles School of Civil Engineering, Purdue University (2015)

B.S., Department of Electrical Engineering, Xi'an Jiaotong University (2013)

PUBLICATIONS

Journal papers:

1. **Xiong, J.**, & Tzempelikos, A. (2016). Model-based shading and lighting controls considering visual comfort and energy use. *Solar Energy*, 134, 416-428.
2. **Xiong, J.**, Tzempelikos, A., Bilionis, I., Awalgaonkar, N. M., Lee, S., Konstantzos, I., ... & Karava, P. (2018). Inferring personalized visual satisfaction profiles in daylit offices from comparative preferences using a Bayesian approach. *Building and Environment*, 138, 74-88.
3. **Xiong, J.**, Tzempelikos, A., Bilionis, I., & Karava, P. (2019). A personalized daylighting control approach to dynamically optimize visual satisfaction and lighting energy use. *Energy and Buildings*, 193, 111-126.

Conference papers:

1. **Xiong, J.**, Chan, Y-C. & Tzempelikos, A. (2015). Model-based control algorithms for optimized shading and lighting operation considering visual comfort and energy use. Proceedings of CISBAT15 Conference, Lausanne, Switzerland, September 2015.
2. **Xiong, J.**, Lee, S., Tzempelikos, A., & Karava, P. (2016). Adaptive personalized shading control strategies to maximize occupant satisfaction while reducing lighting energy use In buildings. Proceedings of 4th High Performance Buildings conference at Purdue, July 2016, 12 pages.
3. **Xiong, J.**, Lee, S., Karava, P., & Tzempelikos, A. (2017). Personalized visual satisfaction profiles from comparative preferences using Bayesian inference. *Energy Procedia*, 122, 547-552.
4. **Xiong, J.**, Lee, S., Karava, P. & Tzempelikos, A. (2018). The influence of lighting conditions, shading patterns and weather on occupant visual preferences in perimeter building zones. Proceedings of ASHRAE Winter Conference, Chicago, January 2018.
5. Awalgaonkar, N., **Xiong, J.**, Bilionis, I., Tzempelikos, A. & Karava, P. (2018). Design of Experiments for Learning Personalized Visual Preferences of Occupants In Private Offices. Proceedings of 5th High Performance Buildings conference at Purdue, July 2018.